Author response to Referee #1

The authors thank the reviewer for interest in our work and for the helpful comments to improve the manuscript. We have addressed each of comments as outlined below.
Please note that all page and line numbers refer to the revised manuscript and the revised supplementary material with track changes. If the text is significantly changed only the number of section is given. Author's responses are in italics and text coloured in red refers to the added text in the manuscript.

Comment: This manuscript studied the biomass burning organic aerosol in Australia by using a c-ToF-AMS. The heavy biomass burning causes that 90% of NR-PM1 is organics. Five intense BB events with different burning conditions are analyzed. The enhancement of ozone and SOA in biomass burning plumes in examined. PMF analysis on background OA resolved three factors, BBOA, OOA, and IEPOX-SOA. The IEPOX-SOA is identified for the first time in Australia. The manuscript is well structured and the content is appropriate for ACP. However, most of the work presented here has been done before. The manuscript in its current form does not add significantly to the literature. Thus, I recommend major revisions. More in depth analysis and conclusions are required.

Response: We agree that this kind of work has been done previously, however it is the first time that this has been done within the Australian continent. The Australian continent is globally an important source of BB emissions, particularly the tropical savannah region. However, data related to BB emissions are remarkably lacking for this region. Therefore, we think that the results from this work provide valuable information to enhance the understanding of the loading and composition of fresh and aged organic aerosols from biomass burning in Australia, Southern Hemisphere and in general.

The following has been modified or added to the manuscript:

- *The title of the manuscript is modified.*
- *Separation on "close BB" and "distant BB" periods is clarified.*
- *More analysis and discussion are added for BB events, including backtrajectories and Sentinel hot spot locations.*
- *The suggestions regarding isoprene-derived OA are incorporated in the manuscript.*
- *Discussion regarding the sea salt-chlorides and f44-resolved size distribution is modified and clarified.*

Major comments

Comment 1: Whether this study is suitable/capable to study the aging of biomass burning OA.
Previous field studies on this topic usually used aircraft to follow the biomass burning plumes, which ensures investigating the same air mass (Cubison et al., 2011; Yokelson et al., 2009; Forrister et al., 2015; May et al., 2015). However, this is not the case in this study as the air mass is changing. In fact, many observations in this study can be explained by changes in air mass or physical changes, instead of aging of biomass burning OA. For example, an increase in f44 and a decrease in f60 (Figure 4b) could be simply due to an BBOA-rich air mass mixing with OOA-rich background air or physical changes during dilution (May et al., 2015). This could be potentially revealed in Figure 4a (close BB) if the authors color the data

points by OA concentration. The data points with higher f60 and lower f44 would have higher OA concentration.

The authors may use MODIS sensor and backtrajectory analysis (section 2.1.7) to pinpoint fire position and calculate transport time. Then, the oxidation rate of BBOA or its tracers (such as f60) can be calculated, which is highly uncertain now. The aging time may also be estimated by using the photochemical clock, such as NOx/NOy ratio.

The OA in the five biomass burning events (section 3.2.4) is dominantly from fresh biomass burning, which provides a good opportunity to study the properties of fresh BBOA. The study would benefit from expanding related discussions. For example, "different burning conditions" are vaguely mentioned multiple times to explain the difference between the five biomass burning events. However, can the authors be more explicit about the relationship between specific burning conditions/burning materials with OA concentration, f44, f60, ΔO3, etc? It is helpful to bring Table S2 to the main text.

Response 1: The authors are aware that more conclusions about the BB aging can be drawn when tracking the plume is available. However, the limitation of the stationary measurements made it extremely difficult to track any plume with certainty. We agree that process of aging is not covered by this study. However, results for aged BB emissions, including SOA and ozone formation and change in particle size, are presented in this study. Therefore, the title of the manuscript is changed from: "Aging of aerosols emitted from biomass burning in northern Australia" to "Fresh and aged aerosols emitted from biomass burning in northern Australia". The sentence at Page 3, lines 14-16 is also modified: "This publication presents insights into fresh and aged aerosols emitted during the SAFIRED, while a detailed description of the campaign can be found in Mallet et al. (2016)".

Considering the number of fires that occurred across the area during the campaign, ground-based (stationary) measurements and the limitations of satellite detection (once per day) it was difficult to identify the exact source of fires. The backtrajectories analysis was done for all days and all elevated signals, and while the path of trajectories can indicate the sources it is a challenge to apportion the signals to a specific event. In the case of all close fires, according to backtrajectories air masses could reach the ATARS within less than half an hour. The approximate time for air masses to reach the sampling location from the particular fire was included into the "Biomass burning events" section (Sect. 3.2.4) at Page 12.

The "biomass burning events" section (Sect. 3.2.4) is expanded as suggested. The Sentinel hotpots and the backtrajectories for BB events are presented. More discussion about differences in BB events is given. Text was changed through the "Biomass burning events" section (Sect. 3.2.4) at Page 12. Table S2 is now in the main text (Table 1).

Comment 2: IEPOX-SOA related.
Firstly, it is not appropriate to label the PMF factor as IEPOX-OA. While the majority of this factor is from the reactive uptake of IEPOX, this factor also likely includes contribution from isoprene OA formed via other pathways. For example, a recent study by Schwantes et al. (2015) showed clearly that SOA formed via the reactive uptake of isoprene nitrooxy hydroxyepoxide could also produce fragment m/z 82. In addition, the mass concentration of this PMF factor cannot be fully explained by the total IEPOX SOA tracers (Hu et al., 2015;

Budisulistiorini et al., 2015). Thus, it is more appropriate the name the factor as isoprene-derived OA (Xu et al., 2016; Pye et al., 2016).

Secondly, since the isoprene-OA factor is identified for the first time in Australia, more analysis could be done related to this factor. For example, does this factor correlate with sulfate, which has been shown in previous studies (Xu et al., 2015a; Budisulistiorini et al., 2015)? What's the NO concentration at the measurement site? Is IEPOX formed locally or from transport? What's the particle pH? As shown in Figure 9f, in general, IEPOX-OA correlates well with Org 82. However, some data are scattered (i.e., Org 82 0.004 to 0.008 µg m-3 range). What happens for these data? Is it due to sources other than IEPOX uptake contributing to Org 82?

Response 2: Thank you for the comment. The PMF factor "IEPOX-SOA" is changed for "isoprene-derived OA" throughout the manuscript and supplementary material. Moreover, the following sentence is added to Page 15, lines 24-26: "In order to consider other possible pathways in isoprene-derived OA formation (Schwantes et al., 2015), the PMF factor has been named as isoprene-derived OA (Pye et al.; Xu et al., 2016)".

According to calculations for the composition depended collection efficiency, 22% of the aerosol were acidic. Furthermore, the correlation of IEPOX-SOA and sulfate is found to be weak (R of 0.3) (Fig. S18). However, two periods (period before 5th of June and after 15th of June) could be clearly separated on the plot. While there is no correlation between sulfate and isoprene-derived OA factor for the first period, when plotting only data collected from the 15th of June, correlation is found to be slightly higher (R of 0.4). The following is added to the manuscript at Page 16 line 6-14: "The main path for isoprene-derived OA formation is proposed to be acid catalysed IEPOX uptake (Lambe et al., 2015; Lin et al., 2011). According to calculations for the composition depended collection efficiency, 22% of the aerosol were acidic. In order to estimate whether the acidity of the particles had an influence on isoprene-derived OA generation in ATARS, the correlation between sulfate (taken as proxy of aerosol acidity) and isoprene-derived OA factor was examined. The correlation between the factor and sulfate can be considered as weak (R of 0.3) (Fig S18). However, two periods can be clearly distinguished from the graph: the period before 5th of June and the period after 15th of June. While there is no correlation between sulfate and isoprene-derived OA factor for the first period, when plotting only data collected from 15th of June, correlation is found to be slightly higher than correlation for all background data (R of 0.4)".

The concentration of NO at the measurement site is not available. Unfortunately due to the issue with instrumentation, NOx data are unreliable and thus not used in analysis.

As isoprene-derived OA was found to be prominent over the night period, one of the suggestions was detection of distant masses as suggested at Page 16, line 27.

After further investigation of the scattered data (i.e., Org 82 0.004 to 0.008 µg m-3 range) we couldn't tell what other source contributed. Further analysis of the biogenic loadings and sources for this region are needed in order to make more detailed conclusions regarding the isoprene-derived OA.

Minor comments

Comment 1: Page 2, line 6: Elemental carbon (EC) is not the same as black carbon (BC). EC is defined by thermal properties and BC is defined by optical properties (Andreae and Gelencsér, 2006).

Response 1: Elemental carbon (EC) is used throughout the manuscript. "Black" is removed from the sentence at Page 2, line 6.

Comment 2: Page 4, line 4. It is stated that sampled air mass had mainly passed over land. However, this seems to contradict with the conclusion in Page 8 Line 18-20, that a significant portion of chlorides could be sea salt.

Response 2: The sampled air masses mainly passed over the land according to a dominant wind direction (southeast) and backtrajectories, as illustrated in the Figure 1 in Mallet et al. (2016). The high chloride concentration was detected (by the AMS, Figure 1c and by the BAM Figure S3a) during the close BB periods when air masses were passing over the land affected by fires (as stated in the manuscript at Page 8 line 27), meaning that they originated from fires. This is especially the case of close fires on the 25th and 26th of June (Fig. 1c). However, oceanic influence cannot be excluded as on some days (e.g. period between 3rd and 6th of June) in the afternoons northeast winds were dominant (Figure 4c in Mallet et al. (2016)). More precisely on the way to the sampling station air masses were passing over the land and then turning over the ocean before reaching the ATARS. Furthermore, the measurement period between 19th and 22nd of June was characterised by air masses coming mostly along the Australian east coast and passing over some of the land before reaching the station (Mallet et al., 2016). The oceanic influence through high chloride concentration that has a sea salt origin can be clearly seen from the Fig S3a. Chlorides from BAM were detected during the influence of close BBs, but also during the oceanic influenced days. Therefore the Mg^{2+}/Na^{+} ratio for oceanic-influenced days was close to the see salt ratio (Figure S3b) and the sea salt-related chlorides were collected on filters (BAM) (Figure S3a). The least terrestrial fetch (indicated by low radon concentration) was also observed during the days with the high ocean breeze (Mallet et al., 2016).

To clarify this in the manuscript the following is added at Page 4, lines 4-7: "However, on some days (e.g. between 3rd and 6th of June) in the afternoon hours northeast wind direction was dominant, directing the air masses from land to pass over the ocean before being detected at ATARS. Moreover, an oceanic influence was observed between 19th and 22nd of June (Mallet et al., 2016)".

The following sentences are modified on the Page 9, line 3 – Page 9 line 8: "Mg^{2+}/Na^{+} ratio values for the filters collected during the high oceanic influence (between 3rd and 6th and 19th and 22nd of June) were close to the sea salt Mg^{2+}/Na^{+} ratio of 0.12 (Fig. S3b). At the same time low terrestrial fetch (low radon concentration) was observed (Mallet et al., 2016). Moreover, the chlorides collected on filters were prominent during the period of oceanic influence (Fig. S3a). This suggests that a significant portion of chlorides detected on the BAM filters was of a sea salt origin, which is refractory and therefore not well measured by the AMS, thereby explaining the poor chloride correlation" and at Page 8, line 27: "Increased chloride concentration during the close BB periods was also indicated by the BAM data (Fig S3a)".

A new Figure, Fig S3a that shows the BAM chloride time series is added to the supplementary material and Fig. S3 is now Fig. 3b. Figure 3b is also modified: z-axis (date) was added to the graph.

Comment 3: Page 4 Line 19-20. It is not clear if the CE is determined by using the UMR data or the HR data. Or HR data are used in the squirrel panel? Also, sulfate fragments should not have interference from organic fragments in HR data. Thus, HR data should be used throughout the analysis.

Response 3: CE was determined using the HR data in PIKA and these data are used through the analysis as stated now at Page 4, lines 21 and 22: The AMS collection efficiency was determined using the calculations provided within the PIKA Toolkit" and Page 4, lines 25-27: "Significant improvement was made in distinguishing sulfate fragments from organic fragments at the same m/z by performing HR peak fits in PIKA (Sect. S1 in supplementary material). Therefore, HR peak fitting fata (PIKA) *were chosen for further analysis".*

Comment 4: Page 7, line 31: It is not clear how the "close BB" and "distant BB" periods are separated. The criteria for separation should be clearly stated?

Response 4: The authors agree that more specific definitions should be given for "close" and "distant" BB periods and clear presentation of data separation should be given.

The measurement period was separated into "close BB" and "distant BB" periods based on organics, carbon monoxide and particle number concentration and their correlation, as well based on the distance of known fires (Sentinel hot spots) from the ATARS.

Firstly, we were looking at the time series of organics, carbon monoxide and particle number concentration (Figure 2, Page 25) in order to identify the periods of significant BB influences, e.g. their high signals (e.g. on 9th and 26th of June) gave us a guide on which days intense/close BB took place. The increases in BB markers (levoglucosan, soluble non-sea salt potassium and Org 60) also showed the same trend (Figure 3, Page 26). After identifying these periods, the next step was to relate these signals to the possible BB events. Therefore, we have mapped all fires (Sentinel hot spots) that have happened during these periods and have confidence level of 50% and more. To make sure that everything is included (e.g. close fires with low intensity) we have gone through every measurement day and mapped all the events that have occurred.

Hot spots detected within 20 km occurred on 30th of May, between 7th and 11th and 25th and 26th of June (Figure 2, Page 25). Taken the distance of 20 km and increased concentrations of organics, carbon monoxide and particle number, these days were taken as "close BB" periods. Knowing that ATARS was constantly affected by the BB air masses the remaining measurement days were taken as "distant BB" periods. In summary, "close BB" periods refer to periods where close fires (within 20 km) have taken the place and correlated increases in carbon monoxide, organics and particle number concentration were observed (Fig. 2), while the rest of the measurement is defined as "distant BB" periods.

In order to clarify the close and distant BB periods the paragraph at Page 8, line 3- Page 8 Line 16 is modified: "The sampling site was constantly impacted by fire emissions with periods of heavy BBs characterized by high aerosol and gas phase concentrations, for instance CO reaching up to ~10^4 ppb and organics up to 350 µg m^{-3} (Fig. 2). The most *intense BB episodes were on the 30th of May, between the 7th and 11th of June, and on the 25th and 26th of June (Fig. 1c) (Mallet et al., 2016). During intense fire periods, organics, CO and particle number concentration showed correlated increases (Fig. 2). Moreover, looking at Sentinel Hot spots during these periods, hot spots were detected within 20 km from the ATARS. Based on this, the dataset was separated into periods of "close BB" (corresponding to high organics, CO and particle number concentration signals and close events (< 20 km)) and "distant BB" (corresponding to less intense organics, CO and particle number concentration signals and distant events (> 20 km)). It is important to emphasize that all periods during the measurement that have not been included in close BB periods have been assigned to distant BB periods, as ATARS was constantly influenced by BBs. The selection does not mean that emissions from distant fires were not present during the close BB periods but that the influence of fires near the measurement station during these periods was dominant. Nine intense BB events were identified from close BB periods as single source emissions (Desservettaz et al., 2016). Five of the nine BB events (Fig. 2) were analysed here (Sect. 3.2.4), due to the instrument not sampling during the remaining events. Most of the events occurred in the afternoon/night time (Table 1)".*

In order to indicate distant BB periods the following is added to Fig. 2 caption at Page 25: "The distant BB periods cover all days of the measurement other than days included in close BB periods".

Comment 5: Page 8, line 14: The authors can use the NO+/NO2+ ratio to infer if the nitrate functionality originates from inorganic or organic nitrate (Xu et al., 2015b; Farmer et al., 2010).

Response 5: According to the NO^+/NO_2^+ ratio in our study, close BB period between 7th and 11th of June is characterised by nitrate that originates from the ammonium nitrate rather than from organic nitrate (NO^+/NO_2^+ ratio is higher for organic nitrates than ammonium nitrate (Farmer et al., 2010)) (see Figure below). Other two close BB periods (on 30th and between 25th and 26th) produced inorganic as well as organic nitrates. Periods influenced with ocean breezes (between 3rd and 5th and 19th and 22nd of June) seem to have higher portion of organic than inorganic nitrates.

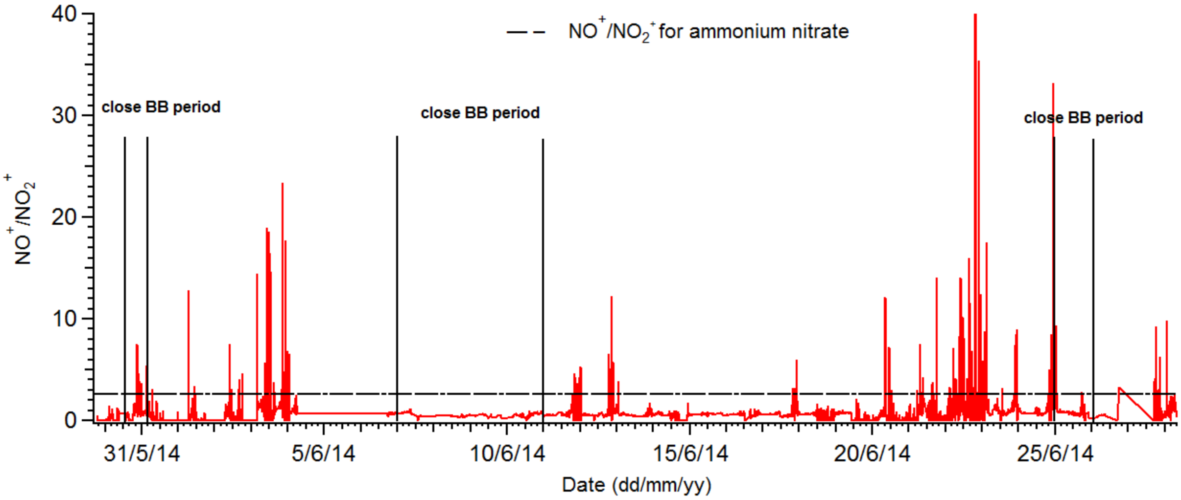

Time series of NO^+/NO_2^+ ratio throughout the campaign. Solid lines indicate close BB periods. Dashed line indicates NO^+/NO_2^+ ratio for ammonium nitrate.

Comment 6: Page 10, line 22-23: This sentence is really confusing and should be re-written.

Response 6: The diurnal trends of the f44, $\Delta O_3/\Delta CO$ and $\Delta OA/\Delta CO$ ratios for close BB periods and diurnal trend of $\Delta O_3/\Delta CO$ ratio for distant BB periods are added to the Fig. 5 and therefore apart from the sentence that was mentioned in the comment, the changes are made throughout the "Secondary organic aerosol (SOA) formation" section (Sect. 3.2.2 at Page 11).

Comment 7: Page 11, line 22. Is the OA mass loading related to wind speed or wind direction?

Response 7: The wind direction was highly variable influencing detected signals related to the event F. This is incorporated into the manuscript at Page 13, lines 22-26: "However, the f44 value was highly variable during the event F, ranging from 0.07 to 0.18. Other parameters including f60 and organics varied as well. On that time, the wind direction significantly varied between 140° and 80° and likely influenced changes in detected air mass. One of the explanations can be detection of fresh plume and aged masses coming from the distant fires with the change in wind. The low correlation between f60 and f73 might also be an indicator for detection of different BB air masses (Fig. S8)".

Comment 8: Page 12, line 14. The authors may check if the relationship between f60 and f73 changes with burning conditions or burning materials.

Response 8: We have observed changes in f60/f73ratio for different events (varying between 1.2 and 2.5) (Fig. S8), however there was no trend in relationship of f60/f73 ratio and burning conditions/material (using the MCE value). Low correlation between f60 and f73 for the event F (r^2=0.16) was likely due to the changes in masses that were detected during this time period (due to high variability in wind direction).

The sentence at Page 12, lines 16 and 17 is modified: "Different factors were considered including f44, time of day, $\Delta O_3/\Delta CO$, f60, f60/f73, organic concentration and MCE". The following is added to the manuscript at Page 13 lines 25 and 26: "The low correlation between f60 and f73 might also be an indicator for detection of different BB air masses (Fig. S8)" and at Page 14, lines 19-21: "Events were characterised with different f60/f73 ratios (varying between 1.2 and 2.5), but there was no trend in the relationship of f60/f73 ratio and burning material/conditions (MCE values) (Fig. S8)".

Figure illustrating f60/f73 ratio changes for different events and relationship between this ratio and MCE (Fig. S8) is added to supplementary material.

Comment 9: Page 12, line 31. Is there any study to show that fresh emissions from biomass burning contain OOA?

Response 9: Contribution of primary (fresh emissions) from biomass burning to OOA portion of emitted OA cannot be excluded as shown in wood burning studies, Heringa et al. (2012) and Weimer et al. (2008). The references are added at Page 15, lines 12 and 13.

Comment 10: Page 13, line 10. Cite Xu et al. (2015a).

Response 10: The citation is added to the new version of the manuscript at Page 15, line 23.

Comment 11: Page 14, lines 8-11: The low correlation between IEPOX-OA and BBOA could be simply due to that these two factors are from completely different sources and a correlation is not expected. The discussion in this sentence is not supported and should be removed.

Response 11: The sentence was removed from the manuscript (Page 17, lines 11-14) and figure S15 (supplementary material) that corresponds to the statement was removed as well.

References

Heringa M, DeCarlo P, Chirico R, Lauber A, Doberer A, Good J, et al. Time-resolved characterization of primary emissions from residential wood combustion appliances. Environmental science & technology 2012; 46: 11418-11425.

Mallet MD, Desservettaz MJ, Miljevic B, Milic A, Ristovski ZD, Alroe J, et al. Biomass burning emissions in north Australia during the early dry season: an overview of the 2014 SAFIRED campaign. Phys. Discuss., doi:10.5194/acp-2016-866, in review, 2016 2016.

Pye HO, Murphy BN, Xu L, Ng NL, Carlton AG, Guo H, et al. On the implications of aerosol liquid water and phase separation for organic aerosol mass.

Schwantes RH, Teng AP, Nguyen TB, Coggon MM, Crounse JD, St. Clair JM, et al. Isoprene NO3 Oxidation Products from the RO2+ HO2 Pathway. The Journal of Physical Chemistry A 2015; 119: 10158-10171.

Weimer S, Alfarra M, Schreiber D, Mohr M, Prévôt A, Baltensperger U. Organic aerosol mass spectral signatures from wood-burning emissions: Influence of burning conditions and wood type. Journal of Geophysical Research: Atmospheres (1984–2012) 2008; 113.

Xu L, Middlebrook AM, Liao J, Gouw JA, Guo H, Weber RJ, et al. Enhanced formation of isoprene-derived organic aerosol in sulfur-rich power plant plumes during Southeast Nexus. Journal of Geophysical Research: Atmospheres 2016; 121.

Author response to Referee #2

The authors appreciate the reviewer's comments that helped us to improve the manuscript. We have addressed each of comments as outlined below.
Please note that all page and line numbers refer to the revised manuscript and the revised supplementary material with track changes. If the text is significantly changed only the number of section is given. Author's responses are in italics and text coloured in red refers to the added text in the manuscript.

Comment: This paper discussed the aging of biomass burning (BB) aerosols from Northern territory of Australia based on aerosol mass spectrometer (AMS) at a ground observation site. The entire field study (29 May to 20 June, 2014) was divided to be "close BB" and "distant BB" periods. The BB aerosols were investigated by comparing aerosol chemical composition, aging process, ozone formation, size distribution and SOA formation between those two periods. PMF analysis was performed on the background OA period. Ambient Isoprene Epoxydiols-Derived SOA (IEPOX-SOA) factor from three PMF-factors solution was discussed and showed similar performances to the same factor reported in the previous studies. This paper showed a good dataset for investigating the biomass burning influences on aerosols. However, the analysis in this paper is not clear and is not presented in a quite logic way. Thus I recommend a major revision for this paper before considering its publication in ACP.

Response: Number of changes is made throughout the manuscript in order to present data in more clear way. The following has been modified or added to the manuscript:

- *The title of the manuscript is modified.*
- *Separation on "close BB" and "distant BB" periods is clarified.*
- *More analysis and discussion are added for BB events, including backtrajectories and Sentinel hot spot locations.*
- *The suggestions regarding isoprene-derived OA are incorporated in the manuscript.*
- *Discussion regarding the sea salt-chlorides and f44-resolved size distribution is modified and clarified.*

Comment 1: The authors analysed the data in section 3.2 based on dividing the entire study to be "distant BB" and "close BB" periods in section 3.1. However, it is not clear that how the "close BB" and "distant BB" periods were defined. Was it based on distance or the emission intensity, or the correlation between organic, CO and particle number concentration? The authors only labelled "close BB" period in Figs.1-2, "distant BB" period and background OA period are unknown.

Response 1: The authors agree that more specific definitions should be given for "close" and "distant" BB periods and clear presentation of data separation should be given.

The measurement period was separated into "close BB" and "distant BB" periods based on organics, carbon monoxide and particle number concentration and their correlation, as well based on the distance of known fires (Sentinel hot spots) from the ATARS.

Firstly, we were looking at the time series of organics, carbon monoxide and particle number concentration (Figure 2, Page 25) in order to identify the periods of significant BB influences, e.g. their high signals (e.g. on 9th and 26th of June) gave us a guide on which days *intense/close BB took place. The increases in BB markers (levoglucosan, soluble non-sea salt potassium and Org 60) also showed the same trend (Figure 3, Page 26). After identifying these periods, the next step was to relate these signals to the possible BB events. Therefore, we have mapped all fires (Sentinel hot spots) that have happened during these periods and have confidence level of 50% and more. To make sure that everything is included (e.g. close fires with low intensity) we have gone through every measurement day and mapped all the events that have occurred.*

Hot spots detected within 20 km occurred on 30th of May, between 7th and 11th and 25th and 26th of June (Figure 2, Page 25). Taken the distance of 20 km and increased concentrations of organics, carbon monoxide and particle number, these days were taken as "close BB" periods. Knowing that ATARS was constantly affected by the BB air masses the remaining measurement days were taken as "distant BB" periods. In summary, "close BB" periods refer to periods where close fires (within 20 km) have taken the place and correlated increases in carbon monoxide, organics and particle number concentration were observed (Fig. 2), while the rest of the measurement is defined as "distant BB" periods.

In order to clarify the close and distant BB periods the paragraph at Page 8, line 3- Page 8 Line 16 is modified: "The sampling site was constantly impacted by fire emissions with periods of heavy BBs characterized by high aerosol and gas phase concentrations, for instance CO reaching up to ~10^4 ppb and organics up to 350 µg m^{-3} (Fig. 2). The most intense BB episodes were on the 30th of May, between the 7th and 11th of June, and on the 25th and 26th of June (Fig. 1c) (Mallet et al., 2016). During intense fire periods, organics, CO and particle number concentration showed correlated increases (Fig. 2). Moreover, looking at Sentinel Hot spots during these periods, hot spots were detected within 20 km from the ATARS. Based on this, the dataset was separated into periods of "close BB" (corresponding to high organics, CO and particle number concentration signals and close events (< 20 km)) and "distant BB" (corresponding to less intense organics, CO and particle number concentration signals and distant events (> 20 km)). It is important to emphasize that all periods during the measurement that have not been included in close BB periods have been assigned to distant BB periods, as ATARS was constantly influenced by BBs. The selection does not mean that emissions from distant fires were not present during the close BB periods but that the influence of fires near the measurement station during these periods was dominant. Nine intense BB events were identified from close BB periods as single source emissions (Desservettaz et al., 2016). Five of the nine BB events (Fig. 2) were analysed here (Sect. 3.2.4), due to the instrument not sampling during the remaining events. Most of the events occurred in the afternoon/night time (Table 1)".

In order to indicate distant BB periods the following is added to Fig. 2 caption at Page 25: "The distant BB periods cover all days of the measurement other than days included in close BB periods".

Background period is related just to the PMF analysis and therefore it was not introduced in the 3.1 chapter, but it is clearly defined at Page 15, lines 1 – 4 and illustrated in Figures S13 and S14.

Comment 2: Suggest revising the structure of the results and discussion part. After all comparisons between the "close BB" and "distant BB" being discussed in section 3.2.1-3.2.3, the paper started to describe the details about the "close BB" period in section 3.2.4, which is very confusing. I do not quite understand what the relationship between the 5 BB events in section 3.2.4 with the "close BB" period analysed in section 3.2.1-3.2.3 is. I suggest the authors introduce the details on “close BB” and “distant BB” period first, and then discuss the general comparison results. In this way, the readers can get a rough idea on what “close BB” and “distant BB” are then understand later comparison better. I also suggest the authors add a separate figure for readers to see the details of those “close BB” and “distant BB” periods. In this way, the good correlation addressed in page 7 Line 30 can also be understood.

Response 2: As suggested (previous comment) the “close BB” and “distant BB” periods were clearly defined and introduced before the comparison of the results. Moreover the following is added to the manuscript at Page 8, lines 14-16: “Nine intense BB events were identified from close BB periods as single source emissions (Desservettaz et al., 2016). Five of the nine events (Fig. 2) were analysed here (Sect. 3.2.4), due to the instrument not sampling during the remaining events”. This is repeated at the beginning of the “Biomass burning events” section (Sect.3.2.4) at Page 12, lines 10-12: “Five single source BB events were analysed here (Fig. 2). These episodes were within previously defined close BB periods“. This clearly explains that nine events were identified as a single source events (coming just from the one fire source) and that these events are within the close BB periods. The AMS was not sampling during all events, therefore, five events labelled on Fig. 2 are addressed in this paper. As discussed in the previous comment, distant BB periods were clarified in the main text and in the figure caption (Fig. 2, Page 25).

Comment 3: Page 8, line 10-20:

1) The authors mentioned there were high chloride (KCl or NH_4Cl) mass concentrations from the biomass burning, then said a significant portion of chlorides from BAM measurement came from sea salt. Those two statements are conflictive.

2) If the signals are strong, KCl+ and NaCl+ ions can be resolved in the OA spectra in the HR fitting of PIKA.

3) The chloride with high concentrations in Fig.1 was not shown in the comparison plot of Fig. S2. Were some periods missed in Fig. S2? The authors should point out which periods were used for comparison in Fig.S2.

4) Line 10, “This can be explained by the depletion of chloride with transport and aging of BB plumes (Li et al., 2003; Li et al., 2010;Liu et al., 2000).” There is no proof for this sentence. Since the author has the K+ and Na+ measurement, the authors can calculate the chloride depletion fraction to show the evidence for this sentence. See equation (A1) and Fig. (A2) in (Hayes et al., 2013) for reference.

Response 3:

1) High AMS-resolved chloride concentrations during the close BB periods can be clearly seen from the AMS (Fig.1(c)) and BAM (Fig. S3a) time series and also high correlation of AMS-resolved chlorides and organics during the close BB periods indicates BB-related origin. The high contribution of chlorides originating from fires has been also emphasised in the campaign overview publication (Mallet et al., 2016). However, apart from the fire-related chloride signals, BAM filters collected the sea salt chlorides during the periods of oceanic influence (period between 3rd and 6th and 19th and 22nd of June, as it can be seen in the Fig S3a. Moreover, the Mg^{2+}/Na^{+} ratio (ions measured by BAM) for the filters collected during the oceanic-influenced periods was close to the ratio for the sea salt (Fig. S3b). Therefore we *concluded that significant portion of chlorides from BAM filters were from the sea salt. For more details please see the response to the minor comment number 2, from Referee 1.*

To clarify this in the manuscript the following is modified to the Page 9, line 3- Page 9, line 8: “Mg^{2+}*/*Na^{+} *ratio values for the filters collected during the high oceanic influence (between 3rd and 6th and 19th and 22nd of June) were close to the sea salt* Mg^{2+}*/*Na^{+} *ratio of 0.12 (Fig. S3b). At the same time low terrestrial fetch (low radon concentration) was observed (Mallet et al., 2016). Moreover, the chlorides concentration collected on filters was prominent during the period of oceanic influence (Fig. S3a). This suggests that a significant portion of chlorides detected on the BAM filters was of a sea salt origin, which is refractory and therefore not well measured by the AMS, thereby explaining the poor chloride correlation”. Moreover, the sentence was added at Page 8, line 27: “Increased chloride concentration during the close BB periods was also indicated by the BAM data (Fig S3a)”.*

In order to present the BAM chloride time series a new Figure, Fig S3a is added to the supplementary material and Fig. 3 is now to Fig. 3b. Figure 3b is also modified: z-axis (date) was added to the graph.

2) After HR analysis of KCl^{+} *and* $NaCl^{+}$ *ions, further analysis couldn’t be done as resolving the ions was not possible due to their low contribution (see in Figure below).*

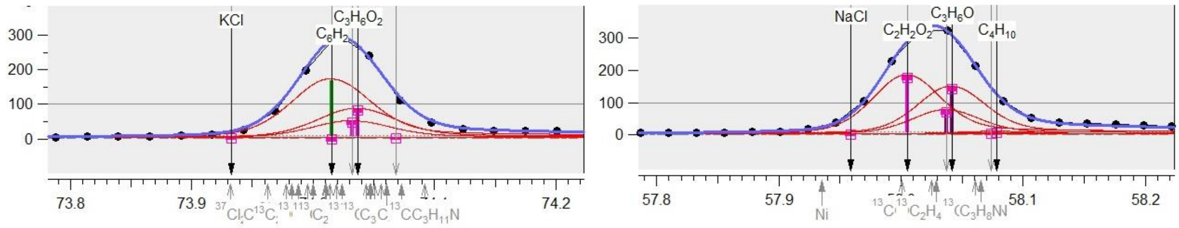

3) All AMS data were averaged to BAM 12h data, therefore the AMS concentrations at Fig.1 and Fig. S2 are not the same. To emphasise this, the following sentence is added to the Fig. S2 caption: “The AMS data were averaged to BAM 12h data”.

4) Unfortunately, we were not able to track the plumes and it was a challenge to separate the plumes and investigate their aging and thus chlorides depletion. Therefore, further analysis could not be performed.

Comment 4: Page 9, line 7: “The variability observed in f44 vs. f60 for close BB events (Fig. 4a) probably reflect BB plumes generated during different burning conditions rather than different atmospheric processing of BB masses.” There is no evidence to support this sentence. In Fig. 5a, higher ΔO3/ΔCO was observed for the high f44. The authors explained this figure as (page 9 line 31): “On average, the ΔO3/ΔCO ratio increases with f44 and decreases with f60, indicating increased photochemical processing of OA in plumes with atmospheric aging and ozone production”. Two statements are contradicting with each other.

Response 4: The authors have changed the sentences at Page 9, lines 25-27 as following: “The variability observed in f44 vs. f60 for close BB events (Fig. 4a) can reflect BB plumes generated during different burning conditions but also different atmospheric processing of BB masses” Ozone enrichments were observed in close as well as in distant plumes, therefore this statement is kept as it is and in addition sentence is added at Page 10, lines 28 *and 29: "The $\Delta O_3/\Delta CO$ enrichments for close BB period indicate that aging of close emissions cannot be excluded".*

Comment 5: Page 9, line 14: "This confirms that levoglucosan-like species carried by the BB plume did not degrade to background levels even as oxidized species were formed. Thus, f60 is a reasonable marker of distant BB in this study." This expression is not quite true; lots of points in Fig 4b are around background level when the f44 is very high. Mixing BB plumes with other aged plumes also can degrade the f60.

Response 5: Most of the points in Fig. 4b are higher than the f60 background level when f44 is high (from 0.2 to 0.25). Mixing of BB plumes can result in lower f60, but even then most of the points are higher than the background. So the overall conclusion is that levoglucosan can be used as a reliable marker for distant BBs in this study.

Comment 6: Page 9 line 23 "The wide range in f44 can be attributed to difference in burning conditions for close BB". What the author missing in this entire section is dilution or mixing BB plumes with other plumes. Not only different burning condition or aging, but also the dilution and mixing will also lead the similar evolution trend of f44 vs f60 in the triangle plot (Fig. 4).

Response 6:
Dilution effect: The authors agree that dilution effect should be included in the text, as a factor influencing f44 vs f60 trend. This is added to the manuscript at Page 10, lines 11 and 12: "One more factor that can influence f44 vs f60 trend for both close and distant fire is dilution effect".

Mixing between plumes: The backtrajectories clearly show that during the close BB periods, apart from the close fires all other hot spots are located on 60km or more from the ATARS (Fig S7 in the supplementary material). The authors thus suggest that the mixing of fresh plumes with the plumes coming from the distant fires in most of the cases won't influence the f44/f60 changes due to the fact that both m/z 44 (60) and total organics for distant diluted masses are likely much smaller than m/z 44 (60) and total organics for close plume masses. This is simplified through the equation below.

$$f44 = \frac{Org\ 44\ (fresh\ plume\ masses) + Org\ 44\ (diluted\ distant\ plume\ masses)}{Org\ (fresh\ plume\ masses) + Org\ (diluted\ distant\ plume\ masses)}$$

As same implies for f44 and f60, it is assumed that the mixing of fresh plumes with the distant diluted plumes coming from the distant fires won't affect the f44/f60 trend.

As not the same can be concluded in case for the distant BB periods the following is added to the manuscript at Page 10, line 7 and 8: "The observed evolution trend in f44 vs f43 for distant fires can be also influenced by mixing between the plumes" and sentence at Page 14, lines 26-28 is modified: "The thousands of fires that occurred during the SAFIRED campaign contributed to a wide range of OA composition that reflect different burning materials, conditions, mixed fresh and aged emissions and processing in the atmosphere".

Comment 7: Page 10, line 2: Suggest the authors use Ox (=NO2+O3) instead of O3, or use both, then the O3 loss by NO can be accounted for (Herndon et al., 2008).

Response 7: This comment unfortunately cannot be addressed due to the unreliable NOx data.

Comment 8: Page 10, lines 6 and 7: How did the authors calculate the average ΔO3/ΔCO from different fires? How did the authors obtain ΔO3/ΔCO from "distant BB" fire plumes since the plume spikes are not obvious as those in "close BB" period?

Response 8: The average $\Delta O_3/\Delta CO$ ratio for particular BB event (5 events that were singled out) was calculated by averaging all values for the time of the fire. The average $\Delta O_3/\Delta CO$ ratio for distant BB periods is the average of all $\Delta O_3/\Delta CO$ values for the whole distant BB periods, not for the fires in periods separately.

Comment 9: Page 10, line 14: The authors should calculate ΔOA/ΔCO vs Δf44 (not f44), because it is not clear if high f44 can really reflect the SOA aging since different BB plumes may have different f44 due to burning condition and mixing or dilution. I suggest the authors check the photochemical age calculated from VOCs (de Gouw et al., 2005), which can be another parameter for indicating oxidation/aging process of plumes. And also the authors have a great dataset to see emission ratio of BB emitted aerosols (e.g. ΔSO4/ΔCO, ΔNH4/ΔCO and ΔCl/ΔCO).

Response 9: The authors think that considering Δf44 (the change in f44 for different burning conditions) would only be beneficial for individual plumes, but not for the whole data set as we have presented here. Furthermore, for individual plumes, this is only possible if the plume can be tracked and the initial value of f44 is known. That is not the case for this study (stationary measurement site).

Unfortunately, due to the numerous fires which occurred across the area and the limitations of satellite (passing the region once per day) and ground-based measurements, we were not able to single out individual plumes that could be used for the suggested analysis.

Comment 10: Page 10, 3.2.3 section: Suggest adding size distributions of m/z 44 and m/z 60, which can be used to compare with the size distributions from SMPS. This comparison can help to interpret the comparison between "low f44" and "high f44" periods. In addition, the comparison of size distributions between "close BB" and "distant BB" can be added. This can help to characterize those two periods and see if the "distant BB" are really more aged or mixed with aged aerosols.

Response 10: In order to further analyse changes in size distribution with aging, size distributions for organics (sampled by the AMS) were examined for both close and distant BB periods. Data were categorised based on different f44 ranges, same as for the SMPS data (Fig 6).

More conclusions were made and paragraph for the Sect. 3.2.3 at Page 11 is modified: "Atmospheric aging of plume particles increases particle diameter due to gas to particle transfer of organic and inorganic gaseous species (Martins et al., 1998). In order to estimate whether the aging of BB masses during SAFIRED influenced particle size, average SMPS size distributions and AMS size distributions for organics, both categorised based on different f44 ranges, were examined (Fig. 6). It is important to emphasise that SMPS uses electrical mobility diameter, while AMS uses vacuum aerodynamic diameter. The close and distant BB periods were analysed separately. The f44 values were classified into four groups *that represent different aging stages (0.05<f44<0.1, 0.1<f44<0.15, 0.15<f44<0.2, 0.2<f44<0.25). The first f44 bin (0.05<f44<0.1) was not considered in case of the distant BB periods, as only a few data points were in this range (Fig. 4). The same was done for the highest f44 bin (0.2<f44<0.25) for close BB periods. According to SMPS data, the average particle mode varied between 101 - 113 nm and 104 - 106 nm for close and distant BB periods, respectively. The average mode for organics showed larger sizes and varied between 259 - 293 nm and 293 - 305 nm for close and distant BB periods, respectively. Increased f44 was accompanied by a reduction in SMPS particle size for close plumes, going from 113 nm (0.05<f44<0.1) to 101 nm (0.1<f44<0.15). The same trend was observed for the organic aerosols. Considering both AMS and SMPS data for distant fires, there was no considerable change in diameter with aging from less aged BB plumes to more aged BB air masses. The particle modes show only slight differences between different f44 bins. This is not consistent with the observed increase in OA for distant fires. Changes in size distribution will be discussed further in the Sect. 3.2.4 where results related to specific BB events are presented".*

Please note that after further analyses we realised that only a few points were in the f44 range 0.05-0.1 for distant fires, therefore this was removed from the manuscript and new graph was added (Fig. 6).

Comment 11: Page 14, lines 1-2: What is the monoterpene concentration in this study? Monoterpene-derived SOA also can influence the background level of C5H6O+ (Hu et al., 2015). Isoprene concentration was not reported in this study, which is important for discussing IEPOX-SOA.

Response 11: The average monoterpenes concentration was found to be 0.22 ± 0.41 ppb. The average isoprene concentration was 0.49 ± 0.78 ppb. The following is added to the manuscript at Page 16, line 2-5: "The average isoprene concentration measured during the campaign was 0.49 ± 0.78 ppb. However, it should be emphasised that monoterpene-derived OA can also influence the background level of $C_5H_6O^+$ *(Hu et al., 2015). The average monoterpenes concentration for this study was found to be 0.22 ± 0.41 ppb".*

Comment 12: Page 14, lines 8-9: Low correlation between the IEPOX-SOA time series with both OOA and BBOA was observed (Fig. S15) suggesting that during BB influenced periods either higher NOX concentrations suppressed IEPOX and consequently IEPOX-SOA generation or the dominant BB aerosol during these periods inhibited measurement of isoprene oxidation products." This sentence does not have evidences to support. In theory, the high OM concentration from BBOA can facilitate the oxidation product to partition into the aerosol phase (Kroll and Seinfeld, 2008). To investigate the BB influence to IEPOX-SOA: 1) suggest the authors start to see if the BBOA plumes can increase the acidity of aerosol, which can promote the IEPOX uptake (Gaston et al., 2014). 2) the NOx concentration can influence the oxidation product of isoprene (Surratt et al., 2010; Bates et al., 2014). At the absent of IEPOX measurement, the authors can investigate the IEPOX-SOA concentration level or the fC5H6O abundance based on different categories of NOx concentrations by checking if there is systematic differences of IEPOX- SOA mass concentrations at high NOx and low NOx. This analysis presumably assumed the isoprene emissions in the large areas were relatively constant within the field study period.

Response 12: Due to the lack of supporting evidence for either of proposed reasons, this sentence is deleted from the manuscript (Page 17, lines 11-14).
1) According to calculations for the composition depended collection efficiency, 22% of the aerosol were acidic. Furthermore, the correlation of IEPOX-SOA and sulfate is found to be weak (R of 0.3) (Fig. S18). However, two periods (period before 5th of June and after 15th of June) could be clearly separated on the plot. While there is no correlation between sulfate and isoprene-derived OA factor for the first period, when plotting only data collected from the 15th of June, correlation is found to be slightly higher (R of 0.4). The following is added to the manuscript at Page 16 line 6-14: "The main path for isoprene-derived OA formation is proposed to be acid-catalysed IEPOX uptake (Lambe et al., 2015; Lin et al., 2011). According to calculations for the composition depended collection efficiency, 22% of the aerosol were acidic. In order to estimate whether the acidity of the particles had an influence on isoprene-derived OA generation in ATARS, the correlation between sulfate (taken as proxy of aerosol acidity) and the isoprene-derived OA factor was examined. The correlation between the factor and sulfate can be considered as weak (R of 0.3) (Fig S18). However, two periods can be clearly distinguished from the graph: the period before 5th of June and the period after 15th of June. While there is no correlation between sulfate and the isoprene-derived OA factor for the first period, when plotting only data collected from 15th of June, correlation is found to be slightly higher than the correlation for all background data (R of 0.4)".

2) The comment unfortunately cannot be addressed due to the unreliable NOx data.

Minor comments

Comment 1: Page 4 lines 1-2: Please give the standard deviations of those reported average values.

Response 1: The standard deviation values for all reported average values are given in the revised manuscript. Sentence at Page 4, lines 1-3 has been modified: " The early dry season was characterized by dry weather conditions (average relative humidity of 67 ± 23 %) and warm days with an average daily and nightly temperatures of 27 ± 5 °C (up to 34 °C) and 19 ± 4 °C (with a minimum of 10 °C), respectively".

Comment 2: Page 4, line 27: How can the authors separate aged POA and SOA? To what extent, the authors will define the aerosol is aged POA since SOA can be from aged POA (Robinson et al., 2007).

Response 2: The authors agree that aged POA and SOA cannot be separated using the fragment analysis that was stated by this sentence. Therefore, "aged POA" was excluded from the sentence (Page 4, line 30): "Organic aerosols measured by the AMS encompassed aerosols that were processed in the atmosphere for different periods of time and included both POA and SOA. As such, a tool was needed to distinguish BB aerosol from other sources and fresh from processed BB aerosol".

Comment 3: Page 5, line 20: Have the authors offset the background of BAM measurement e.g. the background concentration can refer to the mass concentrations of different species on blank filters?

Response 3: Yes, all of the species measured on the BAM PM_1 filters were blank corrected. This is added to the manuscript at Page 5, lines 26 and 27: "All of the species measured on BAM filters were blank corrected".

Comment 4: Page 5 line 21: Suggest changing "PM1" to be "PM_1", which is more commonly used.

Response 4: "PM1" has been changed in "PM_1" throughout the manuscript.

Comment 5: Page 6, line 17: Is the PTR-MS data UMR or HR? How did the authors separate the contributions of isoprene and furan to the m/z 69.

Response 5: An unit mass resolution PTR-MS (quadrupole mass spectrometer) has been used and this is added to the manuscript at Page 6, lines 22-24: "A high sensitivity Proton Transfer Reaction-Mass Spectrometer (PTR-MS, Ionicon Analytik) with a quadrupole mass spectrometer and an H_3O^+ ion source was employed to measure non-methane organic compounds (NMOCs) that include non-methane hydrocarbons and oxygenated volatile organic compounds".

The authors used the PTR-MS-resolved m/z 69 as a signal related to isoprene. Furan concentrations were significant only at the time of close BB periods (as it can be seen from Fig S17). These have been removed from the data for the PMF (background data) where isoprene-derived OA were examined.

The following is added to the manuscript at Page 7, lines 1 and 2: "In order to distinguish furan and isoprene contribution over the sampling period, a gas chromatography-mass spectrometry method was used" and at Page16, lines 15-18: "The isoprene/furan concentrations at m/z 69 (PTR-MS) were treated as an isoprene contribution due to the dominance of isoprene signal compared to furan, according to the samples analysed by gas chromatography-mass spectrometry (Fig. S17). The furan contribution was more significant in BB plumes, during the close BB period, as suggested previously (Warneke et al., 2011)".

Figure (Fig. S17) illustrating the furan and isoprene data analysed by the gas chromatography-mass spectrometry is presented in the supplementary material.

Comment 6: Page 7, line 14: Suggest adding the OM/OC values.

Response 6: The average OM/OC value of 1.4 is stated at Page 7, line 23.

Comment 7: Page 7, line 20: Please change "organic mass" to be OM. Since the authors start to use OM as an abbreviation, it should be consistent in the following text.

Response 7: "OM" has been used as an abbreviation through the manuscript (Page 7, line 23; Page 7, line 24). "Organic mass" is used just at the beginning of the sentence (Page 7, line 27).

Comment 8: Page 7, line 25: Please give the standard deviations to those reported average concentrations.

Response 8: The standard deviation values for all reported average values are given in the new manuscript version at Page 7, line 29 – Page 8, line 2: "In this study, the remaining submicron non-refractory mass was made up of inorganics including sulfates (4.2 %), ammonium (2.8 %), nitrates (1.5 %) and chlorides (1.3 %), with average concentrations of 0.51 ± 0.32 µg m^{-3}*, 0.35 ± 0.68 µg m*$^{-3}$*, 0.19 ± 0.45 µg m*$^{-3}$ *and 0.17 ± 1.28 µg m*$^{-3}$*, respectively."*

Comment 9: Page 8 line 25: It is not clear that Org 60 is UMR or HR. The authors already use m/z 60 refers to UMR and $C_2H_4O_2^+$ refers to HR. Please be consistent. F60 (HR or UMR) has a similar problem e.g., in page 9 line 1.

Response 9: HR peak fitting data (PIKA) were used through the analysis as stated in Page 4, line 27: "Therefore, HR peak fitting data (PIKA) were chosen for further analysis". Since these are UMR data fitted in PIKA, Org60 and f60 are used in the manuscript instead of $C_2H_4O_2^+$ *and f*$C_2H_4O_2^+$*. The same is done with other fragments.*

To make it clear the following is modified to Page 5 lines 1 and 2: "An extensively employed fragments analysis using the AMS-extracted parameters f43 (ions $C_3H_7^+$ *and* $C_2H_3O^+$*), f44 (*CO_2^+*) and f60 (*$C_2H_4O_2^+$*) was applied here' and at Page 4 lines 7-9: "The AMS parameter f60 and accompanying f73 (*$C_3H_5O_2^+$*) are widely used as BB emission signatures as they are directly related to levoglucosan-like species, which are a substantial fraction of organics emitted in pyrolysis of cellulose (Alfarra et al., 2007; Simoneit et al., 1999)".*

Comment 10: Page 9, line 23: What does "atmospheric processing" refer to?

Response 10: Atmospheric processing refer to aging process which is defined at Page 2, lines 21 and 22 as: fresh particle or gaseous species transformed in the atmosphere through photochemical processing.

Comment 11: Page 11, line 4: Repeated sentence, which was already said in page 7 line 29.

Response 11: This sentence (Page 12, lines 10 and 11) is changed for : "Five single source BB events were analysed here (Fig.2)".

Comment 12: Page 11, line 27: OOA should be SOA, OOA PMF factor has not been introduced here yet.

Response 12: OOA was used here as an oxygenated fraction of OA, as defined in Page 2, line 28 and not as a PMF-resolved factor. Therefore OOA is kept as it is.

Comment 13: Page 11, line 8: "As these plumes were mostly related to sources close to the sampling site (within 2 to 10 km), differences in m/z 44 and 43 can be mostly related to different burning conditions." No evidence was shown to support this sentence.

Response 13: The sentence was removed from the revised manuscript at Page 12, lines 14-16.

For figures

Comment 1: Figure 1. Suggest adding EC fraction in Fig. 1(a) to the total AMS fraction measured in Fig. 1(b), then a full chemical composition of PM1 can be obtained.

Response 1: Mass fractions for inorganic species collected by BAM are added to Figure 1 (a) bar so full chemical composition of PM1 is obtained. Manuscript text is modified, Page 7, lines 19 and 20: "Organic carbon made up 72 % and EC 15 % of the measured PM_1 *on the BAM filters (Fig. 1a)." Fig. 1 at Page 25 and its caption are also updated.*

Comment 2: Figure 3. Has the background of org 60 been subtracted (0.003). If the answer is negative, please offset the background.

Response 2: The background value of 0.003 is related to f60, not to Org 60. The authors did not offset the background value for Org 60. This is not done in other studies as well.

Comment 3: Figure 4. Empirical triangle area was reported in Cubison et al. (2011). Suggest adding right guide line here as well, which can help to compare this study with other studies.

Response 3: We agree that adding the empirical BBOA-related triangle plot in f44 vs. f60 space, introduced by Cubison et al. (2011) will facilitate comparison with other BB studies. The triangle plot is added to plots in Figure 4 but also to Figure 5 and Figure 6 plots, for the same reason. As Figure 4, 5 and 6 are combined in one panel figure (please see the next comment), the new Figure 4 caption is modified: "f44 vs. f60 coloured by date for (a) close and (b) distant BB periods, by ΔO3/ΔCO ratio for (c) close and (d) distant BB periods, and by ΔOA/ΔCO ratio for (e) close and (f) distant BB periods. Vertical black lines refer to the f60 background level of 0.003. Red dashed lines refer to the ambient BBOA-related data introduced by Cubison et al. (2011). Note: ozone data from 29th of May until the 1st of June were not available".

Comment 4: Figure 5-6. They are all identical plots. It will be easier to see by combining them together as one panel figure.

Response 4: We agree that combining all f44 vs. f60 plots into the one panel figure gives better insight into the plots. Figure 4 (Page 27) now represents combined figures (previously Figure 4, Figure 5 and Figure 6).

Comment 5: Figure 9 (b): What is the correlation between BBOA with levoglucosan and K+? what is the correlation between IEPOX-SOA with sulfate and isoprene? Does any compound correlate with OOA? Those external tracers should be added on the diurnal variation plot as well. Figure 9 (c): It is better to add the exact fraction values on the bar.

Response 5: The authors have already examined all correlations that have been suggested in this comment. In overall, the correlation of PMF factors was difficult to access due to the "chopped" background dataset that resulted in limited dot points for correlation. The BBOA had a weak correlation with the levoglucosan and nnsK. Moreover, levoglucosan and nssK data are given every 12h, which is the reason why diurnal trend couldn't give useful information.
The correlation of isoprene-derived OA and sulfate has found to be weak (R of 0.3) (Please see an answer on the major comment number 12 from Referee 1). There is no correlation between isoprene and isoprene-derived OA, as it was stated and presented in Figure S14. None of parameters have strong trend with the OOA.
The exact fraction values for PMF factor contribution are added to the Figure 7 (c).

Comment 6: Figure 10. There are more f44 vs f82 points from IEPOX-SOA factors in Hu et al. (Hu et al., 2015). The authors should add the range of those data, which is more meaningful than showing only two points.

Response 6: The two points present the position of two IEPOX-SOA profiles from two specific studies, Budisulistiorini et al. (2013) and Robinson et al. (2011) in f44 vs. f82 plot.

References

Alfarra MR, Prevot AS, Szidat S, Sandradewi J, Weimer S, Lanz VA, et al. Identification of the mass spectral signature of organic aerosols from wood burning emissions. Environmental science & technology 2007; 41: 5770-5777.

Budisulistiorini SH, Canagaratna MR, Croteau PL, Marth WJ, Baumann K, Edgerton ES, et al. Real-time continuous characterization of secondary organic aerosol derived from isoprene epoxydiols in downtown Atlanta, Georgia, using the Aerodyne Aerosol Chemical Speciation Monitor. Environmental science & technology 2013; 47: 5686-5694.

Desservettaz M, Paton-Walsh C, Griffith D, Kettlewell G, Keywood M, Schoot MV, et al. Emission factors of trace gases and particles from tropical savanna fires in Australia. submitted to Journal of Geophysical Research 2016.

Mallet MD, Desservettaz MJ, Miljevic B, Milic A, Ristovski ZD, Alroe J, et al. Biomass burning emissions in north Australia during the early dry season: an overview of the 2014 SAFIRED campaign. Phys. Discuss., doi:10.5194/acp-2016-866, in review, 2016 2016.

Martins JV, Dunlap MR, Liousse C. Physical, chemical, and optical properties of regional hazes dominated by smoke in Brazil. Journal of Geophysical Research 1998; 103: 32,059-32,080.

Robinson N, Hamilton J, Allan J, Langford B, Oram D, Chen Q, et al. Evidence for a significant proportion of Secondary Organic Aerosol from isoprene above a maritime tropical forest. Atmospheric Chemistry and Physics 2011; 11: 1039-1050.

Simoneit BR, Schauer JJ, Nolte C, Oros DR, Elias VO, Fraser M, et al. Levoglucosan, a tracer for cellulose in biomass burning and atmospheric particles. Atmospheric Environment 1999; 33: 173-182.

Warneke C, Roberts J, Veres P, Gilman J, Kuster W, Burling I, et al. VOC identification and inter-comparison from laboratory biomass burning using PTR-MS and PIT-MS. International Journal of Mass Spectrometry 2011; 303: 6-14.

Author response to Referee #3

The authors thank the reviewer for comments and suggestions to improve the manuscript. We have addressed each of comments as outlined below.
Please note that all page and line numbers refer to the revised manuscript and the revised supplementary material with track changes. If the text is significantly changed only the number of section is given. Author's responses are in italics and text coloured in red refers to the added text in the manuscript.

Comment: This paper presents an analysis of atmospheric data from northern Australia, mainly AMS data impacted by biomass burning. A range of analyses is performed on the data, which gives some insight into the behaviour of the aerosol regarding the biomass burning plumes, ageing and also the formation of SOA from isoprene through the IEPOX route.

None of the results are particularly earth shattering or unexpected, given the pre-existing literature, and there is nothing really new on a process level compared to previous publications. However, there is currently a lack of in situ characterisation work like this in the tropics, so should probably be publishable on that basis. However, the paper is a little rambling and unfocused in paces, with discussions like isoprene SOA detracting from the supposed subject of the paper (ageing of biomass burning emissions), so the general theme of the paper should maybe be better defined.

Response: Significant changes have been made throughout the manuscript and subject of the paper is better defined. The following has been modified or added to the manuscript:

- *The title of the manuscript is modified.*
- *Separation on "close BB" and "distant BB" periods is clarified.*
- *More analysis and discussion are added for BB events, including backtrajectories and Sentinel hot spot locations.*
- *The suggestions regarding isoprene-derived OA are incorporated in the manuscript.*
- *Discussion regarding the sea salt-chlorides and f44-resolved size distribution is modified and clarified.*

Comment 1: Title: The title is probably not appropriate, given that many other scientific phenomena other than the aging of BB plumes (e.g. IEPOX-SOA) are discussed.

*Response 1: Beside the "Biomass burning events" and "isoprene-derived OA" sections (Sect 3.2.4 and Sect. 3.3.1, respectively), the accent of the manuscript is on the investigation of the aerosol changes influenced by the aging processes. The limitation of the stationary measurements made extremely difficult to track any plume with certainty, therefore, we removed the "aging" from the title. A new title is: "*Fresh and aged aerosol emitted from *biomass burning in northern Australia".*

Comment 2: Page 8: "close BB" and "distant BB" should be given more specific definitions. "Prominent" is not very descriptive.

Response 2: The authors agree that more specific definitions should be given for "close" and "distant" BB periods and clear presentation of data separation should be given.

The measurement period was separated into "close BB" and "distant BB" periods based on organics, carbon monoxide and particle number concentration and their correlation, as well based on the distance of known fires (Sentinel hot spots) from the ATARS.

Firstly, we were looking at the time series of organics, carbon monoxide and particle number concentration (Figure 2, Page 25) in order to identify the periods of significant BB influences, e.g. their high signals (e.g. on 9th and 26th of June) gave us a guide on which days intense/close BB took place. The increases in BB markers (levoglucosan, soluble non-sea salt potassium and Org 60) also showed the same trend (Figure 3, Page 26). After identifying these periods, the next step was to relate these signals to the possible BB events. Therefore, we have mapped all fires (Sentinel hot spots) that have happened during these periods and have confidence level of 50% and more. To make sure that everything is included (e.g. close fires with low intensity) we have gone through every measurement day and mapped all the events that have occurred.

Hot spots detected within 20 km occurred on 30th of May, between 7th and 11th and 25th and 26th of June (Figure 2, Page 25). Taken the distance of 20 km and increased concentrations of organics, carbon monoxide and particle number, these days were taken as "close BB" periods. Knowing that ATARS was constantly affected by the BB air masses the remaining measurement days were taken as "distant BB" periods. In summary, "close BB" periods refer to periods where close fires (within 20 km) have taken the place and correlated increases in carbon monoxide, organics and particle number concentration were observed (Fig. 2), while the rest of the measurement is defined as "distant BB" periods.

In order to clarify the close and distant BB periods the paragraph at Page 8, line 3- Page 8 Line 16 is modified: "The sampling site was constantly impacted by fire emissions with periods of heavy BBs characterized by high aerosol and gas phase concentrations, for instance CO reaching up to ~10^4 ppb and organics up to 350 µg m^{-3} (Fig. 2). The most intense BB episodes were on the 30th of May, between the 7th and 11th of June, and on the 25th and 26th of June (Fig. 1c) (Mallet et al., 2016). During intense fire periods, organics, CO and particle number concentration showed correlated increases (Fig. 2). Moreover, looking at Sentinel Hot spots during these periods, hot spots were detected within 20 km from the ATARS. Based on this, the dataset was separated into periods of "close BB" (corresponding to high organics, CO and particle number concentration signals and close events (< 20 km)) and "distant BB" (corresponding to less intense organics, CO and particle number concentration signals and distant events (> 20 km)). It is important to emphasize that all periods during the measurement that have not been included in close BB periods have been assigned to distant BB periods, as ATARS was constantly influenced by BBs. The selection does not mean that emissions from distant fires were not present during the close BB periods but that the influence of fires near the measurement station during these periods was dominant. Nine intense BB events were identified from close BB periods as single source emissions (Desservettaz et al., 2016). Five of the nine BB events (Fig. 2) were analysed here (Sect. 3.2.4), due to the instrument not sampling during the remaining events. Most of the events occurred in the afternoon/night time (Table 1)".

In order to indicate distant BB periods the following is added to Fig. 2 caption at Page 25: "The distant BB periods cover all days of the measurement other than days included in close BB periods".

Comment 3: Page 10: Given the dynamic relationship between NOx and Ozone, it might be sensible to look at perturbations in ‘potential ozone’ (Ox = $NO_2 + O_3$) as well. This would remove the NO titration effect.

Response 3: Unfortunately this comment cannot be addressed as the NOx data were unreliable due to the issue with the instrumentation.

Comment 4: Page 10: The discussion of OA/CO vs time of day is problematic because the total amount of OA in a plume is the product of the total photochemical history of the air mass, not just the time of day that it was measured at. Without a more detailed treatment of the full air mass history, I do not see how any conclusions regarding things like fragmentation can be made.

Response 4: The authors agree that the photochemical history of an air mass is important when discussing the changes in OA in the plume. To emphasize this the following sentence is added to the manuscript at Page 11, lines 9-11: “It must be noted that simply examining ΔOA/ΔCO vs time of day is a simplified approach which does not fully take into account the total photochemical history of the air mass”. We have added the diurnal trend of $\Delta O_3/\Delta CO$ *ratio (Figure 7) as a support for the increased photochemical activity of these masses at the time when OA/CO ratio is increased. In addition, diurnal trend of mentioned parameters is examined also for close fires.*

Comment 5: Page 10: How is the change in SMPS size distributions consistent with SOA formation? Have you compared the particulate volume concentrations? Care should be exercised because an increase in mode diameter can occur simply through coagulation processes, which require no additional particulate mass formation.

Response 5: The authors agree that coagulation process is another pathway leading to increase in particle size which cannot be excluded. However, coagulation would not result in OA mass increase. The “f44-resolved size distribution” section (Sect. 3.2.3) is however modified and the sentence “SMPS size distributions consistent with SOA formation” is changed.

Comment 6: Page 11: The assumption that f44 corresponds to photochemical activity is problematic. Biomass burning can produce a large amount of primary HULIS, which has a very high f44. Furthermore, while it has been shown that a plume’s f44 will increase with time, it is not proven that photochemistry is necessarily responsible, particularly in the very early stages after emission where repartitioning or ‘dark’ chemical processes may occur. I would be more guarded and state that the high f44 implies a high level of oxygenation that could be caused by photochemistry.

Response 6: The authors agree with the referee’s comment.
The following has been modified: Page 13, lines 17-18: “The detected plumes included a considerable portion of oxygenated OA (average f44 value of 0.13, up to 0.18) that could be caused by high daytime photochemical activity”.

Comment 7: Page 13: A lower boundary layer height can increase concentrations of primary emissions, but how would it increase IEPOX-SOA?

Response 7: The authors suggest the following: during the night when the boundary level lowers the increase in concentration of gaseous compounds (including low volatility gas-phase isoprene-derived OA) in the volume of air can induce partitioning of gases onto the particles. Therefore, lower boundary layer during the night might create conditions for low volatility isoprene-derived OA partitioning and increase in isoprene-derived OA. This was added to the manuscript at Page 16, lines 27-30 as following: "During the night, the boundary level lowers which increases the concentration of gaseous compounds and can induce partitioning of gases onto the particles. Therefore, the lower night-time boundary layer might create conditions for low volatility isoprene-derived OA partitioning and an increase in isoprene-derived OA".

Comment 8: Page 14: There may be other explanations for a different f82, such as the formation of isoprene SOA through other routes (e.g. MPAN).

Response 8: The authors agree that other pathways for isoprene-derived SOA formation exist and can contribute to f82 signal. Therefore the "IEPOX-SOA" factor has been renamed to "isoprene-derived OA" (throughout the manuscript), to include the possibility of other pathways in OA formation from isoprene and contribution to f82 through these pathways.

~~Aging of~~Fresh and aged aerosols emitted from biomass burning in northern Australia

Andelija Milic[1], Marc D. Mallet[1], Luke T. Cravigan[1], Joel Alroe[1], Zoran D. Ristovski[1], Paul Selleck[2], Sarah J. Lawson[2], Jason Ward[2], Maximilien J. Desservettaz[3], Clare Paton-Walsh[3], Leah R. Williams[4], Melita D. Keywood[2], Branka Miljevic[1]

[1]International Laboratory for Air Quality and Health, Queensland University of Technology, Brisbane, Queensland, 4000, Australia
[2]CSIRO Oceans and Atmosphere, Aspendale, Victoria, 3195, Australia
[3]Centre for Atmospheric Chemistry, University of Wollongong, Wollongong, New South Wales, 2522, Australia
[4]Aerodyne Research, Inc., Billerica, Massachusetts, 01821, USA

Correspondence to: Branka Miljevic (b.miljevic@qut.edu.au)

Abstract. There is a lack of knowledge of how biomass burning aerosols in the tropics age, including those in the fire-prone Northern Territory in Australia. This paper reports chemical characterization ~~and aging~~ of fresh and aged aerosols monitored during the one month long SAFIRED (Savannah Fires in the Early Dry Season) field study, with an emphasis on chemical signature and aging of organic aerosols. The campaign took place in June 2014 during the early dry season when the surface measurement site, the Australian Tropical Atmospheric Research Station (ATARS), located in the Northern Territory, was heavily influenced by thousands of wild and prescribed bushfires. ATARS was equipped with a wide suite of instrumentation for gaseous and aerosol characterization. A compact time-of-flight aerosol mass spectrometer was deployed to monitor aerosol chemical composition. Approximately ~~80 % of submicron carbonaceous mass and~~ 90 % of submicron non-refractory mass was composed of organic material. Ozone enhancement in biomass burning plumes indicated increased air mass photochemistry and increased organic aerosol ~~and particle diameter~~ with the aging parameter (f44) suggested secondary organic aerosol formation. Diversity of biomass burning emissions was illustrated through variability in chemical signature (e.g. wide range in f44, from 0.06 to 0.18~~3~~) for five intense fire events. The background particulate loading was characterized using Positive Matrix Factorization (PMF). A PMF-resolved BBOA (biomass burning organic aerosol) factor comprised 24 % of the submicron non-refractory organic aerosol mass, confirming the significance of fire sources. A dominant PMF factor, OOA (oxygenated organic aerosol), made up 47 % of sampled aerosol fraction, illustrating the importance of aerosol aging in the Northern Territory. Biogenic ~~IEPOX SOA~~isoprene-derived organic aerosol factor ~~(isoprene epoxydiols-related secondary organic aerosol)~~ was the third significant fraction of the background aerosol (28 %).

Keywords. Biomass burning, savannah fires, organic aerosol, aerosol aging

1 Introduction

Tropical regions are some of the most fire-prone areas in the world (Crutzen and Andreae, 1990). As one of them, Northern Australia is observed to be a significant contributor to the global biomass burning (BB) budget (Russell-Smith et al., 2007). Fire emissions are made up of a variety of gaseous and particle-phase species, with the particle-phase consisting primarily of carbonaceous particles, including organic carbon (OC) and elemental ~~(black)~~ carbon (EC) (Bond et al., 2004;Hallquist et al., 2009;Formenti et al., 2003;Crutzen and Andreae, 1990). Open fires are the largest contributors to carbonaceous emissions; approximately 70 % and 40 % of the global annual emissions of OC and EC are formed in open fire events, respectively (Bond et al., 2004). Annually, 60-75 % of Australia's carbon emissions are attributed to BB emissions in tropical savannahs (Hurst et al., 1994). Organic carbon and EC affect the Earth's radiation balance by scattering and absorbing solar radiation, respectively (Penner et al., 1998;Haywood and Boucher, 2000). O'Brien and Mitchell (2003) suggested that atmospheric heating caused by UV absorbing carbonaceous aerosol, related to BB events in the Northern Territory during a dry season, can be significant and will likely have an influence on local (and possibly even global) climate. Carbonaceous species can also serve as condensation nuclei in cloud formation processes (Roberts et al., 2002). It is therefore important to build a comprehensive knowledge of BB emissions as they play a key role in the climate.

The characterization, processing and estimation of impact of BB emissions is a complex and challenging issue due to a wide range of burning material and combustion conditions (flaming/smouldering), as well as complex atmospheric physics and chemistry that BB plumes undergo once emitted (Reid et al., 2005;Weimer et al., 2008). Besides the characterization of fresh BB emissions, it is important to address their evolution in the atmosphere since aging of the BB emissions will alter their properties and thus how they interact with the climate system. Fresh BB emissions are those released directly from BB sources, while processed emissions refer to fresh particle or gaseous species transformed in the atmosphere through photochemical processing (aging). Organic aerosols (OA) can be differentiated as directly emitted primary organic aerosols (POA), aged primary organic aerosols (aged POA) and secondary organic aerosols (SOA) that form via condensation of lower volatility photo-oxidation products. A large fraction of BB-related POA is observed to be semivolatile (Grieshop et al., 2009) and can therefore change upon dilution with background air by evaporation of its content into the gas phase and be exposed to further transformations in the atmosphere.

Processing of BB emissions in the ambient atmosphere and in laboratory experiments is characterized by increases in the oxygenated fraction of OA (OOA) and degradation of species that are indicators of BB origin (Cubison et al., 2011;DeCarlo et al., 2008;Capes et al., 2008). However, there is no agreement on whether the aging of BB emissions leads to additional OA production. Some recent field and laboratory studies investigating the evolution of BB plumes have shown that OA mass increases with aging (DeCarlo et al., 2008;Yokelson et al., 2009;Heringa et al., 2011), while others have found no significant change or a decrease in OA with atmospheric processing (Akagi et al., 2012;Brito et al., 2014;Cubison et al., 2011;Capes et al., 2008). In addition to SOA formation, BB plumes promote the production of another important secondary pollutant, tropospheric ozone (Real et al., 2007). An excess of nitrogen oxides (NO_X), non-methane organic compounds (NMOCs) and carbon monoxide (CO) in the atmosphere from fire emissions promote additional pathways for ozone production (Parrington et al., 2013). Ozone enhancement in BB emissions has been extensively used as a proxy for air mass photochemical activity (Hobbs et al., 2003;Jaffe and Wigder, 2012;Yokelson et al., 2009;Akagi et al., 2012).

An extensive area of the Northern Territory of Australia is burned each year during the dry season (May-October) and the region is strongly affected by BB emissions. Considering that this area is a globally significant source of BB aerosol emissions (Mitchell et al., 2013), and that there have been a limited number of studies on aerosol characterization and aging, there is a need for more research. Information about the composition and degree of aging of OA that makes up the majority of emitted species generated in these fires will facilitate the estimate of the influence of BB in the Northern Territory. This will also contribute to a better understanding of fire emissions in tropical regions. In order to address these issues, the one month long SAFIRED (Savannah Fires in the Early Dry Season) field study was conducted at the Australian Tropical Atmospheric Research Station (ATARS) during a frequent burning period (late May/June 2014). This publication presents insights into fresh and aged aerosol~~s aging~~ emitted during the SAFIRED, while a detailed description of the campaign can be found in Mallet et al. (2016).

2 Measurement site and period

The Australian Tropical Atmospheric Research Station (ATARS) is situated on the Gunn Point peninsula in the Northern Territory (12°14'56.6" S, 131°02'40.8" E). The northern Australian tropical land mass is mostly covered by savannah biomes including scattered eucalypt trees, shrubs and grasses (Lacey et al., 1982). The sampling site can be described as rural background due to its remote location, with the closest populated centre, the city of Darwin, approximately 80 km south west of the ATARS. During the measurement period, the dominant sources of gaseous and aerosol species were wild and prescribed fires. Apart from planned burns, anthropogenic inputs to this region can be considered negligible (Bowman et al., 2007) and observations have highlighted the importance of biogenic sources for this area (Allen et al., 2008). The sampling site can also be impacted by marine aerosols (Bouya et al., 2010); however, fires are the major source of aerosols during the dry season.

The SAFIRED campaign was conducted from the 29th of May until the 30th of June, 2014 at the beginning of the dry season. The early dry period is characterized by natural fires as well as prescribed burns conducted to reduce the extent, intensity and frequency of wildfires in the late dry season (October-November). Thousands of fires in the Northern Territory during the campaign were detected by MODIS and VIIRS satellite sensors (Mallet et al., 2016). Fire emissions sources ranged from approximately two to up to hundreds of kilometres distant from the sampling station.

The early dry season was characterized by dry weather conditions (average relative humidity of 67 ~~%~~ ± 23 %) and warm days with an average daily and nightly temperatures of 27 ± 5 °C (up to 34 °C) and 19 ± 4 °C (with a minimum of 10 °C), respectively. There were no days of rainfall. Wind direction was predominantly southeast, suggesting that the sampled air masses had mainly passed over land affected by fire emissions ~~(Mallet et al., 2016)~~. However, on some days (e.g. between 3rd and 6th of June) in the afternoon hours northeast wind direction was dominant, directing the air masses from land to pass over the ocean before being detected at ATARS. Moreover, an oceanic influence was observed between 19th and 22nd of June (Mallet et al., 2016).

2.1 Instrumentation and method

Ground level characterization was performed using a wide range of instrumentation for gas- and particle-phase measurements. Detailed description of all instruments used in SAFIRED is given in Mallet et al. (2016). The focus of this study was on the aerosol chemical composition and aging using the instrumentation listed in the following paragraphs.

2.1.1 Compact Time-of-Flight Aerosol Mass Spectrometer (cToF-AMS)

A compact time-of-flight aerosol mass spectrometer (cToF-AMS or AMS, Aerodyne Research, Inc.) was deployed to monitor the chemical composition of non-refractory submicron (PM_1) aerosol. Monitored species were submicron particulate organic and inorganic compounds (sulfate, ammonium, nitrates and chlorides). Details about instrument operation during this campaign can be found in Mallet et al. (2016).

Unit mass resolution (UMR) and high resolution (HR) AMS data analysis was performed in Wavemetrics Igor Pro software (version 6.36) using the standard AMS Analysis Toolkits, Squirrel (Version 1.56D) and PIKA (Version 1.16), respectively. Data collection with a filter at the instrument inlet was used to correct for contributions from air in the fragmentation table (Aiken et al., 2008). Measured time-resolved gas-phase CO_2 concentrations were applied instead of the fragmentation table default value. The AMS collection efficiency was determined using the calculations provided within the ~~Squirrel~~ PIKA Toolkit. The ~~Squirrel~~ composition dependent collection efficiency panel enables an estimate of the collection efficiency based on ammonium nitrate, organic content, aerosol acidity and relative humidity (Middlebrook et al., 2012). The time-resolved collection efficiency (with an average value of 0.61) was applied to the entire dataset. High OA loadings during the campaign caused interferences in the detection of sulfate in the UMR analysis. Significant improvement was made in distinguishing sulfate fragments from organic fragments at the same m/z by performing HR peak fits in PIKA (Sect. S1 in supplementary information). Therefore, HR peak fitting data (PIKA) ~~results~~ were chosen for further ~~data~~ analysis.

AMS fragments analysis

~~Considering that OA~~Organic aerosols measured by the AMS encompassed aerosols that were processed in the atmosphere for different periods of time and included both POA~~, aged POA~~ and SOA. As such, a tool was needed to distinguish BB

Formatted: Subscript

aerosol from other sources and fresh from processed BB aerosol. An extensively employed fragments analysis using the AMS-extracted parameters f43 (ions $C_3H_7^+$ and $C_2H_3O^+$), f44 (CO_2^+) and f60 ($C_2H_4O_2^+$) was applied here. The ratio of an integrated organic signal, e.g. m/z 43, to total organic signal is referred to as f43. Parameters f43 and f44 were used to estimate the level of OA processing, as they illustrate OA fractions of different aging degree. While f43 is mainly associated with hydrocarbon-like and semivolatile OA fractions (fragments $C_3H_7^+$ and $C_2H_3O^+$, respectively) (Jimenez et al., 2009;Lanz et al., 2007;Zhang et al., 2007;Heringa et al., 2011), f44 is assigned to highly oxygenated OA species (fragment CO_2^+) (Aiken et al., 2007;DeCarlo et al., 2010;Alfarra et al., 2007). The AMS parameter f60 and accompanying f73 ($C_3H_5O_2^+$) are widely used as BB emission signatures as they are directly related to levoglucosan-like species, which are a substantial fraction of organics emitted in pyrolysis of cellulose (Alfarra et al., 2007;Simoneit et al., 1999). The f60 can be applied as a valuable BB marker for time periods of up to one day (Cubison et al., 2011;Bougiatioti et al., 2014). Ambient aerosols characterized by an f60 value higher than 0.003 are considered to be influenced by BB emissions (Cubison et al., 2011). A graphical approach of comparing f44 vs. f60 introduced by Cubison et al. (2011) was used in this study to estimate the degree of aging of BB emissions.

Formatted: Subscript

Formatted: Subscript

Formatted: Subscript

Formatted: Superscript

Positive Matrix Factorization (PMF)

Positive Matrix Factorization (PMF) analysis (Paatero and Tapper, 1994) using the PMF evaluation tool (Ulbrich et al., 2009) was used in source apportionment of the AMS OA data. PMF splits the OA spectrum into different factors that can be related to specific sources. (Paatero, 1999;Paatero and Hopke, 2009). Various factors have been identified by PMF analysis of AMS OA data, with the most common being hydrocarbon-like OA (HOA) and oxygenated OA, that can sometimes be further apportioned to low-volatility oxygenated OA (LV-OOA) and semivolatile oxygenated OA (SV-OOA) (Ulbrich et al., 2009;Lanz et al., 2007;Ng et al., 2010;Jimenez et al., 2009). Other factors include environment specific factors such as biomass burning OA (BBOA) and cooking-related OA (COA). The solution space in this study was investigated by varying the number of factors and starting conditions (seeds, 0 to 50 in increments of 1) and applying rotational parameters (fpeaks, -1 to 1 in increments of 0.1).

2.1.2 Beta plus particle measurement system (BAM)

PM_1 mass was measured and collected onto pre baked (600 °C) quartz 47 mm filters (Pall Tissuquatz p/n 7202) using a Beta plus particle measurement system (BAM, Teledyne API Model 602), every 12 hours. All of the species measured on BAM filters were blank corrected. Particles collected on filters were further analysed for anhydrous sugars, including levoglucosan, by high performance anion exchange chromatography with pulsed amperometric detection and for water soluble ions including potassium (K^+), nitrates (NO_3^-), sulfates (SO_4^{2-}), ammonium (NH_4^+) and chlorides (Cl^-) by ion suppressed chromatography. Levoglucosan and non-sea salt K^+ were used as metrics for BB emissions. BAM PM_1 filters were analysed by a Thermal-Optical Carbon Analyser (DRI Model 2001A) using the IMPROVE-A temperature protocol

Formatted: Subscript

Formatted: Subscript

(Chow et al., 2007) to determine contributions of EC and OC. Water soluble inorganic ions and OC were also used for comparison with AMS-resolved species.

2.1.3 Fourier Transform Infrared Spectrometer (FTIR)

The Spectronus trace gas and isotope Fourier Transform Infrared Spectrometer (FTIR) analyser, built by the Centre of Atmospheric Chemistry at the University of Wollongong, was deployed to monitor gaseous species including carbon monoxide (CO) and carbon dioxide (CO_2) (Griffith et al., 2012;Griffith, 1996). Details about the instrument operation can be found elsewhere (Desservettaz et al., 2016). In order to include dilution effects, OA and ozone data are presented relative to CO. CO is an important BB product that can remain in the atmosphere for a relatively long time period (one to two months depending on the environment) without observed decay or interactions with oxidative agents (Wang and Prinn, 1999;DeCarlo et al., 2010;Edwards et al., 2006). CO has therefore been employed as a long-lived, conservative tracer in many studies (DeCarlo et al., 2010;Kleinman et al., 2008;Brito et al., 2014;Yokelson et al., 2009;Akagi et al., 2012). Gas-phase CO_2 data, as previously mentioned, were applied in the AMS fragmentation table adjustment. CO and CO_2 were also used in modified combustion efficiency (MCE) calculations, with details presented in Desservettaz et al. (2016). MCE refers to the ratio of ΔCO_2 (measured value relative to background value) to the sum of ΔCO_2 and ΔCO (Ward and Radke, 1993). The MCE parameter was used to distinguish smouldering (usually lower than 0.9) from flaming (usually higher than 0.9) fires. The MCE value can also indicate the burning material.

2.1.4 Scanning Mobility Particle Sizer (SMPS)

Aerosol size and number concentration were monitored by a Scanning Mobility Particle Sizer (SMPS, a TSI 3071 long-column electrostatic classifier coupled to a TSI 3772 Condensation Particle Counter). The SMPS measured the particle size distribution from 14 nm up to 670 nm every 5 minutes. Changes in the size distribution due to aging were investigated.

2.1.5 Proton Transfer Reaction-Mass Spectrometer (PTR-MS)

A high sensitivity Proton Transfer Reaction-Mass Spectrometer (PTR-MS, Ionicon Analytik) with a quadrupole mass spectrometer and an H_3O^+ ion source was employed to measure non-methane organic compounds (NMOCs) that include non-methane hydrocarbons and oxygenated volatile organic compounds. These species are important in the formation of SOA and ozone. Isoprene and monoterpenes make up a dominant fraction of global gas-phase NMOCs, contributing significantly to the production of SOA (Guenther et al., 2012). Tropical regions can contribute up to 80 % of global annual isoprene emissions due to warm weather conditions (Guenther, 2006). He et al. (2000) investigated NMOCs emitted from eucalyptus trees, which make up 95 % of all tree species in Australia. Isoprene accounts for 64-100 % of NMOCs emitted from different eucalyptus species. The isoprene/furan fraction (signal at m/z 69) of measured NMOCs is used here in the analysis of isoprene-~~related~~ derived ~~S~~OA. Other studies suggest that the contribution of isoprene to m/z 69 prevails in non-

BB periods while the furan contribution is more significant in BB plumes (Warneke et al., 2011). In order to distinguish furan and isoprene contribution over the sampling period, a gas chromatography-mass spectrometry method was used.

2.1.6 Ozone analyser

Ozone concentration was monitored by an Ultraviolet Photometric Ozone analyser (Model 49i, Thermo Scientific). Ozone enhancement in BB emissions has been used as a proxy for air mass photochemical activity.

2.1.7 Fire data

Information about the location and duration of fires was obtained from the Sentinel Hotspots system. Hotspots data used for this campaign were derived from the MODIS (Moderate Resolution Imaging Spectroradiometer) sensor (Terra and Aqua satellites) and VIIRS (Visible Infrared Imaging Radiometer Suite) sensor (Suomi NPP satellites). Only the hotspots with confidence level higher than 50 % were considered in the analysis. Hotspots are detected by satellite once a day which limited the fire analysis to events that occurred between approximately 11 am and 3 pm. During the SAFIRED campaign thousands of fires were detected in the Northern Territory. Distance-resolved fire frequencies are presented in Mallet et al. (2016). Moreover intense fires characterized by plumes detected without considerable influence from other fire sources, were extracted from the whole dataset (Desservettaz et al., 2016). Five events that were categorised as single, intense fires are analysed here. Air mass backtrajectories were computed using the NOAA/ARL HYSPLIT (Hybrid Single-Particle Lagrangian Integrated Trajectory) model.

Formatted: Font color: Black

3. Results and Discussion

3.1 Aerosol chemical characterization

PM$_1$ ambient aerosols sampled during the SAFIRED campaign were dominated by an organic fraction. Organic carbon made up ~~83~~ 72 % and EC ~~17~~ 15 % of the measured ~~carbonaceous~~ PM$_1$ ~~material~~ on the BAM filters (Fig. 1a). Data from the AMS (Fig. 1b and 1c), indicate that organics made up approximately 90 % of submicron non-refractory mass with an average concentration of 11.1 µg m^{-3} and concentrations of up to 350 µg m^{-3} during intense and nearby BB events. The organic mass (OM) sampled by the BAM was converted from OC using the conversion factor of 1.4, which was determined in PIKA. This value is within the span of OM/OC conversion factors for the biomass burning aerosol suggested by Reid et al. (2005). The BAM OM and mass concentration of organics sampled by the AMS are in good agreement (R value of 0.94), with slightly higher concentrations measured by the BAM (Fig. S2c) probably due to the lower collection efficiency of the AMS above 700 nm. Organic mass has been observed to be the dominant fraction of PM$_1$ ambient aerosols during the early dry season in the Northern Territory (Carr et al., 2005). The organic fraction was also dominant in other studies strongly impacted by BB emissions (Brito et al., 2014;Capes et al., 2008). In this study, the remaining submicron non-refractory mass was made up of

Formatted: Subscript

Formatted: Subscript

Formatted: Subscript

inorganics including sulfates (4.2 %), ammonium (2.8 %), nitrates (1.5 %) and chlorides (1.3 %), with average concentrations of 0.51 ± 0.32 μg m^{-3}, 0.35 ± 0.68 μg m^{-3}, 0.19 ± 0.45 μg m^{-3} and 0.17 ± 1.28 μg m^{-3}, respectively.

The sampling site was constantly impacted by fire emissions with periods of heavy BBs characterized by ~~prominent~~ high aerosol and gas phase ~~signals~~concentrations, for instance CO reaching up to ~10^4 ppb and organics up to 350 μg m^{-3} (Fig. 2). The most intense BB episodes were on the 30th of May, between the 7th and 11th of June, and on the 25th and 26th of June (Fig. 1c) (Mallet et al., 2016). During intense fire periods, organics, CO and particle number concentration showed correlated increases (Fig. 2). Moreover, looking at Sentinel Hot spots during these periods, hot spots were detected within 20 km from the ATARS. Based on this, the dataset was separated into periods of "close BB" (corresponding to high organics, CO and particle number concentration signals and close events (< 20 km)) and "distant BB" (corresponding to less intense organics, CO and particle number concentration signals and distant events (> 20 km)). It is important to emphasize that all periods during the measurement that have not been included in close BB periods have been assigned to distant BB periods, as ATARS was constantly influenced by BBs. The selection does not mean that emissions from distant fires were not present during the close BB periods but that the influence of fires near the measurement station during these periods was dominant. Nine intense BB events were ~~selected~~ identified from close BB periods as single source emissions (Desservettaz et al., 2016).~~ and f~~ Five of ~~them~~ the nine events (Fig. 2) were analysed here (Sect. 3.2.4), due to the instrument not sampling during the remaining events. Most of the ~~fires~~ events occurred in the afternoon/night time (Table ~~S2~~1). ~~During intense fire periods, organics, CO and particle number concentration showed large and correlated increases (Fig. 2). Based on this, the dataset was separated into periods of "close BB" (corresponding to prominent signals and close events) and "distant BB" (corresponding to less prominent signals and distant events). The selection does not mean that emissions from distant fires were not present during the close BB periods but that the influence of fires near the measurement station during these periods was dominant.~~

Coupled with elevated organic concentrations, AMS-measured inorganics also increased during close BB periods (Fig. 1c). A high AMS signals for all monitored species corresponded to close BB periods. During SAFIRED, high correlation was observed between organics and ammonium species (R of 0.92), with better agreement during the close BB (R of 0.92) than in the distant BB periods (R of 0.73) (Table S1), suggesting that these ammonium species originated from fire emissions. Moreover, plume emissions included high chloride concentrations (up to approximately 50 μg m^{-3} during close BB periods). Increased chloride concentration during the close BB periods was also indicated by the BAM data (Fig S3a). This is not surprising since the dominant fine particle inorganic fraction emitted in flaming savannah fires has been shown to be composed of KCl (potassium chloride) and NH_4Cl (ammonium chloride) compounds and/or their mixtures (Liu et al., 2000). There was a better correlation between organics and chlorides for close BB periods (R of 0.67), than for distant BB periods (R of 0.47). This can be explained by the depletion of chloride with transport and aging of BB plumes (Li et al., 2003;Li et al., 2010;Liu et al., 2000). Correlations for nitrate and sulfate with organics show similar patterns in this work regardless of the BB emissions influence (R of 0.72 and 0.77 for nitrate and R of 0.49 and 0.48 for sulfate for close and distant periods, respectively). AMS inorganic species were compared to soluble ions concentrations measured on the filter samples collected using the BAM. There was a strong correlation between all compared species (R values of 0.85, 0.68 and 0.81 for sulfates, ammonium and nitrate, respectively) except in the case of chloride (R of 0.18) (Fig. S2). Mg^{2+}/Na^{+} ratio values for the filters collected during the high oceanic influence (between 3rd and 6th and 19th and 22nd of June) ~~most of the filters~~ were close to the sea salt Mg^{2+}/Na^{+} ratio of 0.12 (Fig. S3b). At the same time low terrestrial fetch (low radon concentration) was observed (Mallet et al., 2016). Moreover, the chlorides collected on filters were prominent during the period of oceanic influence (Fig. S3a). This suggests that a significant portion of chlorides detected on the BAM filters ~~could~~ was ~~be~~ of a sea salt origin, which is refractory and therefore not well measured by the AMS, thereby explaining the poor chloride correlation.

3.2 Biomass burning aerosols and aging

In general, BB-related particulate matter can be easily distinguished from other aerosol sources by chemical composition. Levoglucosan is a common molecular tracer of plume emissions (Simoneit et al., 1999) and has been extensively used as a BB chemical signature (Jordan et al., 2006;Simoneit, 2002). Moreover, the AMS organic signal intensity ~~at m/z 60~~ (fragment $C_2H_4O_2^{+}$) (Org 60) is directly correlated to the concentration of levoglucosan-like species (Alfarra et al., 2007;Simoneit et al., 1999) and can therefore be applied as a valuable BB marker. Fire sources also contribute to high potassium levels (Li et al., 2003). Figure 3 illustrates the time series of Org 60 obtained from the AMS and levoglucosan and soluble non-sea salt potassium sampled by the BAM. Prominent signals of these BB tracers were present during the observed close BB periods, which confirm that the fire source of the detected aerosols is BB.

In order to discriminate BB aerosol from other sources and estimate the degree of BB aerosol aging (processing), a graphical method introduced by Cubison et al. (2011) has been applied here (Fig. 4). The majority of data points (94 % of the dataset) had f60 values above the background limit of 0.003, indicated with a vertical dashed lines in Fig. 4. Thus, the detected OA during SAFIRED can be attributed mostly to BB aerosol.

Chemical aging of BB-related OA typically leads to f60 depletion and increased f44 (Grieshop et al., 2009;Cubison et al., 2011;Ortega et al., 2013;Ng et al., 2010;Zhao et al., 2014;Capes et al., 2008;Jolleys et al., 2015). In general, this trend was observed in this study for distant fires, with the data trending towards the top left corner of the diagram (Fig. 4b). Apart from aerosol processing, changes in f44 and f60 can be attributed to burning conditions and/or materials. The variability observed in f44 vs. f60 for close BB events (Fig. 4a) ~~probably~~ can reflect BB plumes generated during different burning conditions ~~rather than~~ but also different atmospheric processing of BB masses. On average distant BB plumes were characterized by lower fire tracer f60 compared to the close BB emissions. Furthermore, distant fire plumes indicated a higher portion of oxygenated compounds (i.e., higher f44 values), relative to close plumes. The maximum f44 value ranged between 0.20 and 0.23 in this study, which agrees well with previously observed f44 values for oxidized BB emissions in ambient measurements (Cubison et al., 2011). The f44 parameter increased to values characteristic of LV-OOA in the distant BB and yet f60 values were substantially above the background value of 0.003. This confirms that levoglucosan-like species carried by the BB plume did not degrade to background levels even as oxidized species were formed. Thus, f60 is a reasonable marker of distant BB in this study.

All data fall into the f44 vs. f43 triangular plot range for ambient data, introduced by Ng et al. (2010) (Fig. S4). Ng et al. (2010) observed that typical ambient OA data slopes from the bottom right to the top left of the f44 vs. f43 plot, and that this trend can be attributed to photochemical processing of ambient air masses. A similar pattern was observed in this study for distant ~~fires~~ periods (Fig. S4b). A wide range in f44 can be attributed to different processed (aged) BB-related OA, but different burning material and/or conditions cannot be excluded. The observed evolution trend in f44 vs f43 for distant fires can be also influenced by mixing between the plumes. In contrast the f43 values for close BB (Fig. S4a) are located in a narrow f43 range from 0.05 to 0.08 and do not change considerably with increasing f44. This ~~confirms~~ can be a result of ~~that there was no~~ insignificant atmospheric processing in case of close fires. The wide range in f44 can be attributed to difference in burning conditions for close BB. One more factor that can influence f44 vs f60 trend for both close and distant fire is dilution effect.

Formatted: Space After: 0 pt

Formatted: Font: English (U.K.)

3.2.1 Ozone formation

The emissions from BB sources promote ozone production in the troposphere by increasing the concentrations of key ozone-forming precursors (NMOCs, NO_X and CO). Air mass photochemical activity can be estimated through the observation of changes in ozone concentration with aging, particularly the change in the $\Delta O_3/\Delta CO$ ratio, where ΔCO and ΔO_3 refer to enhancements above background concentrations. ΔCO accounts for dilution, as it is a relatively long lived atmospheric species. The minimum CO value of 80 ppb measured during June at the ATARS site was used as the background concentration level. Similarly a minimum ozone concentration of 10 ppb was considered to be the background level in these calculations. On average, the $\Delta O_3/\Delta CO$ ratio increases with f44 and decreases with f60, indicating increased photochemical processing of OA in plumes with atmospheric aging and ozone production (Fig. 4c and Fig. 4d~~5~~).

$\Delta O_3/\Delta CO$ values vary between -0.1 and 0.9 which is within the observed range in other studies (Jaffe and Wigder, 2012). A negative ratio may indicate fresh BB emissions where ozone was removed by atmospheric reaction with nitric oxide (NO) emitted in high amounts from fire sources, as suggested by Yokelson et al. (2003). Close fire emissions were characterized by significantly lower ozone enrichments (average $\Delta O_3/\Delta CO$ of 0.15) compared to plumes detected from the distant BB emissions (average $\Delta O_3/\Delta CO$ of 0.31) which represent higher photochemical activity within more processed air masses. These values agree with observed $\Delta O_3/\Delta CO$ ratio values for plumes aged for less than 1-2 days (average $\Delta O_3/\Delta CO$ of 0.14) and for 2-5 days (average $\Delta O_3/\Delta CO$ of 0.35) in tropical/subtropical regions (Jaffe and Wigder, 2012). The $\Delta O_3/\Delta CO$ enrichments for close BB period indicate that aging of close emissions cannot be excluded. These significant ozone enrichments in BB plumes illustrate high NO_X and NMOC loadings emitted from fire sources and photochemically active air masses.

3.2.2 Secondary organic aerosol (SOA) formation

Since increased photochemical activity was identified in BB air masses, the change in ΔOA/ΔCO ratio was investigated in order to determine whether additional OA was produced in the ~~detected~~ BB plumes (Fig. ~~6~~4e and Fig. 4f). The lowest OA concentration observed during the campaign of 0.09 µg m^{-3} was taken as a background value in these calculations. Figures~~ 6~~ show~~s~~ no particular trend in ΔOA/ΔCO ratio with f44. The ΔOA/ΔCO ratio also remains quite constant despite increases in f44 (Fig. S5). ~~In the case of close fires, different ΔOA/ΔCO ratios can be attributed to different burning conditions (Fig. 6a).~~ In addition, diurnal patterns of the f44, $\Delta O_3/\Delta CO$ and ΔOA/ΔCO ratios were investigated, for close and distant BB periods separately (Fig. 5a and Fig. 5b, respectively). The parameter f44 was used to indicate the level of oxygenation that can be caused by the photochemical changes and $\Delta O_3/\Delta CO$ as a parameter of photochemical activity. It must be noted that simply examining ΔOA/ΔCO vs time of day is a simplified approach which does not fully take into account the total photochemical history of the air mass. ~~The emissions from close fires did not spend enough time in the atmosphere to be significantly processed and subject to SOA formation, and therefore only diurnal trends for distant fires were considered (Fig. 7).~~ There was an increase in ΔOA/ΔCO ratio with an increase in f44 and $\Delta O_3/\Delta CO$ in the late morning and early afternoon for close and for distant BB periods. This is likely due to condensation of organics onto pre-existing particles.~~,~~ ~~and then a d~~The decrease in the ΔOA/ΔCO ratio later in the afternoon~~, which~~ could indicate OA loss due to fragmentation and subsequent evaporation from the particulate phase. As suggested by Kroll et al. (2009), OA loss can reflect dominance of the fragmentation pathways in the formation of more oxidized OA. Therefore it ~~can be concluded~~is suggested that increased photochemical activity of BB-influenced air masses, illustrated by increase in $\Delta O_3/\Delta CO$ and likely due to oxygenation of OA (f44 increase), was accompanied by an increase in ΔOA/ΔCO ratio~~ and probably~~, indicating SOA formation. Moreover, the ~~but also with~~ decrease in ΔOA/ΔCO ratio ~~probably due to~~later in the day can be a result of fragmentation and subsequent evaporation.

Formatted: Subscript

3.2.3 f44-resolved size distribution

Atmospheric aging of plume particles increases particle diameter due to gas to particle transfer of organic and inorganic gaseous species (Martins et al., 1998). In order to estimate whether the aging of BB masses during SAFIRED influenced particle size, average SMPS size distributions and AMS size distributions for organics, both categorised based on different f44 ranges, ~~for distant BB periods~~ were examined (Fig. ~~8~~6). It is important to emphasise that SMPS uses electrical mobility diameter, while AMS uses vacuum aerodynamic diameter. The close and distant BB periods were analysed separately. The f44 values were classified into four groups that represent different aging stages (0.05<f44<0.1, 0.1<f44<0.15, 0.15<f44<0.2, 0.2<f44<0.25). The first f44 bin (0.05<f44<0.1) was not considered in case of the distant BB periods, as only a few data points were in this range (Fig. 4). The same was done for the highest f44 bin (0.2<f44<0.25) for close BB periods. According to SMPS data, the average particle mode varied between 101 – 113 nm and 104 – 106 nm for close and distant BB periods, respectively. The average mode for organics showed larger sizes and varied between 259 – 293 nm and 293 – 305 nm for close and distant BB periods, respectively. Increased f44 was accompanied by a reduction in SMPS particle size for close plumes, going from 113 nm (0.05<f44<0.1) to 101 nm (0.1<f44<0.15). The same trend was observed for the organic aerosols. Considering both AMS and SMPS data for distant fires, ~~There~~ there was ~~a~~ no considerable ~~increase~~ change in ~~particle~~ diameter with aging from less aged BB plumes ~~(83 nm for 0.05<f44<0.1)~~ to more aged BB air masses. The particle modes show only slight differences between different f44 bins. This is not consistent with the observed increase in OA for distant fires. ~~(106 nm for 0.1<f44<0.15). This is consistent with the observed SOA formation. The shift of particle size towards larger particles may be due to condensation of organics onto pre-existing particles.~~ Changes in size distribution will be discussed further in the Sect. 3.2.4 where results related to specific BB events are presented.

3.2.4 Biomass burning events

~~Nine intense BB events were selected as single source emissions (Desservettaz et al., 2016), f~~Five single source BB events ~~of which are~~ were analysed here (Fig. 2). These episodes ~~correspond to~~were within previously defined close BB ~~emissions~~periods. Mass spectra for selected ~~plumes~~ signatures and their time of detection are given in Fig. S6. The spectral signature is similar for these ~~plumes~~events, with prominent BB-related signals at m/z 60, 73, 29 and 39. However, a significant variation in m/z fragments, especially in m/z ~~43 and~~ 44, can be observed. ~~As these plumes were mostly related to sources close to the sampling site (within 2 to 10 km), differences in m/z 44 and 43 can mostly be related to different burning conditions.~~ More detail about these BB events is given in Table ~~S2~~ 1 and discussed in the following paragraphs. Different factors were considered including f44, time of day, $\Delta O_3/\Delta CO$, f60, f60/f73, organic concentration and MCE.

On 30th of May at around 2pm three hot spots (two having confidence level of approximately 50% and one of 70%) were detected within 2km on the NE from the ATARS (Fig S7a-Fig.S7d). These hot spots likely illustrated two fire events. On the same day and time, 11km on the SE from the sampling site, cluster of events was observed, including 4 hot spots with the confidence level between 94% and 100% and one of 78% confidence level. As all of them were spotted at the same tim e and within 1km distance, it is most likely that the one big fire has occured. No other close events were observed over this time period. Cluster of hot spots was detected on the SE approximately 50km from the ATARS and big clusters at 100km and 150km, as well as on the SE. Moreover, 200km on E along the backtrajectories cluster of hot spots was observed.

Two single source events, A and C, were identified and analysed here (Fig.2). The event A illustrated the increased signals in the afternoon hours, when wind was coming from the NE. Therefore, the event A is likely result of the hot spots detected within 2km from the ATARS (Fig S7a and Fig S7b). According to backtrajectories air masses during these time period were passing over the land affected by these fires and they were transported from the fire events to ATARS within approximately 10 min. The average organic concentration was found to be 23 µg m^{-3}, with the concentrations going up to 45 µg m^{-3}. High average MCE value of 0.97 likely suggests flaming fire as emission source and/or grass as a burning material (Desservettaz et al., 2016). The signal named as a C event was detected over the night (Table 1). At that time wind direction was abruptly changed from the NE to SE. Therefore, the signal can be likely associated to cluster of fires 11 km on the SE (Fig S7c and Fig S7d). According to the backtrajectories air masses reached the ATARS within 20 min from the fire cluster. Comparing to the event A, the average organic concentration for the event C was more than threefold with the maximum value of approximately 130 µg m^{-3}. As MCE was found to be similar (0.98) to event A value, most likely higher signals illustrate larger fire. The number of hot spots detected on the same time with high confidence level confirms this. Higher fire intensity can also be a reason for the higher f60 values for the event C (0.027) compared to event A (0.016) (Table 1).

~~Elevated signals on the 30th of May were attributed to emissions from fires within 5 km and labelled as events A and C. High MCE values (MCE of 0.97 and 0.98 for A and C, respectively) suggested flaming fires as emission sources and/or grass as a burning material (Desservettaz et al., 2016). Lower organic mass loadings might therefore be related to flaming burning conditions.~~

On 25th of June three hotspot clusters were observed close to ATARS (2km on E, 5km on NE and 10km on SE) (Fig S7e-Fig S7h). The cluster of hot spots observed 10 km from the sampling site had one of the highest hot spot's power (energy released by the fire) observed close to the ATARS (within 20 km) during the campaign (120 MW/km^2). Besides the close fires two big clusters around 60 km and 120 km on the SE from ATARS were detected on the same day. On the 25th of June, two ~~intense close fires~~single-source events were observed and labelled as events F and G. Event F was related to a close fire (two hot spots of 60 and 100% confidence level, within 2 km on E) whose emissions were clearly visible from ATARS (Fig. S7e and Fig S7f). The detected plumes included a considerable portion of oxygenated OA (average f44 value of 0.13, up to 0.18) that could be caused by ~~reflecting~~ high daytime photochemical activity. The BB event F began at noon and ended at approximately 5 pm, i.e., it occurred during the period of highest photochemical activity. The relatively high ΔO$_3$/ΔCO ratio (0.13) was elevated relative to the other close BB events, which suggests additional photochemical activity in the plume. This value falls into the range for fire emissions aged less than 1-2 days in tropical/subtropical regions (Jaffe and Wigder, 2012). However, the f44 value was highly variable during the event F, ranging from 0.07 to 0.18. Other parameters including f60 and organics varied as well. On that time, the wind direction significantly varied between 140° and 80° and likely influenced changes in detected air mass. One of the explanations can be detection of fresh plume and aged masses coming from the distant fires with the change in wind. The low correlation between f60 and f73 might also be an indicator for detection of different BB air masses (Fig. S8). Relatively low organic mass loading and f60 values may be due to ~~low fire extent~~highly variable wind direction and/or area rather than combustion conditions (MCE of 0.93), as higher organics are expected for this MCE value. In contrast, event G resulted in the highest organic mass loading measured at ATARS (PM$_1$ concentration of ~350 µg m^{-3}). Moreover, the highest chloride concentration observed over the campaign was at the time of G event. The source of emissions was probably within 10 km on SE of the sampling site (Fig S7g and Fig S7h) and the fire magnitude was illustrated by a large burned area observed the following morning (Mallet et al., 2016) and high power of fire observed (30 MW/km^2). Backtrajectories analysis indicated that less than half an hour was needed for the air mass to reach

Formatted: Font:

Formatted: Superscript

Formatted: Subscript

the ATARS. High fire intensity was accompanied with smouldering burning conditions (MCE of 0.90) that resulted in high organic loadings and high levoglucosan concentrations (high f60) (Table 1). A low OOA fraction, f44, $\Delta O_3/\Delta CO$ value (0.01) indicated that the plume was likely not aged, which is to be expected due to the proximity and time of the event (started at 10 pm and finished at 4 am).

Intense signals, including high organic concentrations, were also detected on the 9th of June (Fig S7i and Fig S7j). On that day cluster of hot spots (all with the confidence level higher than 70%) was detected 5 km from ATARS. Number of distant hot spots was detected between 100 km and 200 km, on the SE from the ATARS. Mallet et al. (2016) suggested that possible sources of this event E might be close fires ~~(within 5 km)~~, distant fires ~~(100 and 200 km away)~~ or a combination of both. According to backtrajectories less than 10 min was enough for air masses to cross the distance between 5 km cluster and the research station. Values for f44 (0.08) and $\Delta O_3/\Delta CO$ (0.02) suggested detection of fresh emissions. Moreover, the high f60 value of 0.032 supported this, as distant fires are not likely to be characterized with such a high portion of levoglucosan-like species. However, the possibility of contribution from distant BB plumes cannot be excluded, especially when considering the particle size distribution during event E. The particle size distribution had a mode of 146 nm, while events F and G showed smaller size distributions with modes of 98 and 88 nm, respectively (Table 1). However, different burning material and conditions could also contribute to the larger size distribution mode during event E.

In general, diversity of biomass burning plumes was illustrated through high variability in chemical signature (e.g. large range of f44, from 0.06 to 0.18) for five intense fire events.~~the large range of f44 values (from 0.06 to 0.13) associated with these close events suggested different burning conditions that generated fresh emissions with different fractions of OOA. However, f44 and~~ ~~$\Delta O_3/\Delta CO$~~ ~~values for event F could reflect daytime photochemical activity.~~ Events were characterised with different f60/f73 ratios (varying between 1.2 and 2.5), but there was no trend in the relationship of f60/f73 ratio and burning material/conditions (MCE values) (Fig. S8).

3.3 Positive Matrix Factorization (PMF)

Initially PMF was performed to assist with analysis of the aging observations rather than to apportion sources since the main source (BB) is already known. This approach was intended to estimate whether the ratios of the different factors, e.g., fresh BBOA, aged BBOA or OOA, exhibited relationships with the age of separate BB plumes. The diversity of the plumes (including close fire plumes with spectra presented in Fig. S6), however, made PMF analysis difficult. The thousands of fires that occurred during the SAFIRED campaign contributed to a wide range of OA composition that reflect different burning materials, conditions, mixed fresh and aged emissions and processing in the atmosphere. The ratio of m/z 43 and 44 differed between plumes (Fig. S11~~9~~) and since the AMS mass spectra were dominated by these masses, the PMF analysis returned factors that corresponded to individual plumes, even when distant fires were separately examined. In addition, high residuals during BB events could not be reduced even with an unreasonably large number of factors (Fig. S9~~7~~). The PMF diagnostic plots can be found in Sect. S3.

Instead PMF analysis was applied on “background” data in order to determine the contribution of BB emissions and SOA to regional ambient PM_1 outside of the time periods dominated by BB events. The background time periods were determined by examining the plot of f44 vs. f43 (Fig. S11~~9~~). Cut-offs of 0.15 for m/z 43 and 0.4 for f44 were chosen to remove the influence of periods dominated by BB events which show up as individual lines in f43 vs. f44 space.

PMF performed on the background OA showed significantly smaller residuals (Fig. S12~~0~~) and resulted in three factors, including a biomass burning OA factor (BBOA), oxygenated OA (OOA) and a factor that represented isoprene-derived OA ~~epoxydiols-related SOA (IEPOX-SOA)~~ (Fig. 7~~9~~). A two-factor solution did not extract the biogenic ~~IEPOX-SOA~~isoprene-derived OA factor while a four-factor solution resulted in splitting of profiles (Fig. S13~~1~~). The biomass burning factor, with distinct m/z 60 and 73 signals, contributed to 24 % of the background aerosol. BBOA was also characterized by fragments related to fresh hydrocarbon-like organics, e.g., m/z 27, 29, 41, 43, 55, and 57, and by prominent OOA-related m/z 28 and 44 signals. The large f44 value (an average f44 of 0.09) (Fig. S4) may indicate either the presence of processed BB aerosol and/or fresh emissions that contain oxygenated OA species possibly due to the burning conditions (Heringa et al., 2012;Weimer et al., 2008). A good correlation was observed between the BBOA factor and Org 60 and CO signals (Fig. 7~~9~~d and Fig. 7~~9~~e). An OOA profile with prominent m/z 28 and 44, similar to LV-OOA profiles observed in previous studies, was extracted. Its diurnal trend is marked by a broad daily peak which correlates with the maximum temperature and reflects intense daytime photochemical activity. The OOA dominance (contribution of 47 %) and high degree of oxygenation (an average f44 of 0.23) (Fig. S4) illustrate the significance of OOA for this area. The third PMF factor can be related to background biogenic SOA, and is discussed in more detail in the Sect. 3.3.1.

3.3.1 Isoprene-derived OA ~~epoxydiols-related secondary organic aerosol (IEPOX-SOA)~~

Isoprene epoxydiols (IEPOX) are important gas-phase precursors for IEPOX-SOA and are products of isoprene oxidation, mostly in low-NO_X environments (Paulot et al., 2009). Recent studies have showed that PMF performed on AMS OA data can be used to determine total IEPOX contribution to SOA (Robinson et al., 2011;Lin et al., 2011;Budisulistiorini et al., 2013;Hu et al., 2015;Xu et al., 2016). A similar distinct PMF-resolved factor has been extracted in this study. In order to consider other possible pathways in isoprene-derived OA formation (Schwantes et al., 2015), the PMF factor has been named as isoprene-derived OA (Xu et al., 2016;Pye et al.)~~IEPOX-SOA factor was extracted in this study.~~ The ~~IEPOX-SOA~~isoprene-derived OA mass spectrum can be clearly distinguished from BBOA and OOA by an enhanced m/z 82 signal (Fig. 9a). In the HR analysis of this dataset, $C_5H_6O^+$ is the most dominant peak that contributes to m/z 82 (Fig. S13) and has been confirmed to be a reliable tracer for ~~IEPOX-SOA~~isoprene- derived OA (Hu et al., 2015). There was a strong correlation observed between the ~~IEPOX-SOA~~isoprene- derived OA factor and Org 82 ($C_5H_6O^+$) (R of 0.90) (Fig. 7~~9~~f). The ~~IEPOX-SOA~~isoprene- derived OA factor profile was also characterized with enhanced peaks at m/z 53, 43 and 44. An AMS

Formatted: Subscript

Formatted: Font: (Default) +Headings (Times New Roman), Font color: Text 1

Formatted: Font: (Default) +Headings (Times New Roman), Font color: Text 1 spectrum with the same prominent peaks was reported by Allen et al. (2008) for the Darwin region in the Northern Territory. This was observed during the monsoon-break period during the wet season in February, when fires were not common, and clean air of biogenic origin was suggested as a source. Moreover, our spectrum is similar to ~~IEPOX-SOA~~isoprene-related OA spectra reported previously (Robinson et al., 2011;Lin et al., 2011;Budisulistiorini et al., 2013). The average isoprene concentration measured during the campaign was 0.49 ± 0.78 ppb. However, it should be emphasised that monoterpene-derived OA can also influence the background level of $C_5H_6O^+$ (Hu et al., 2015). The average monoterpenes concentration for this study was found to be 0.22 ± 0.41 ppb.

The main path for isoprene-derived OA formation is proposed to be acid-catalysed IEPOX uptake (Lin et al., 2011;Lambe et al., 2015). According to calculations for the composition depended collection efficiency, 22% of the aerosol were acidic. In order to estimate whether the acidity of the particles had an influence on isoprene- derived OA generation in ATARS, the correlation between sulfate (taken as proxy of aerosol acidity) and the isoprene-derived OA factor was examined. The correlation between the factor and sulfate can be considered as weak (R of 0.3) (Fig S18). However, two periods can be clearly distinguished from the graph: the period before 5th of June and the period after 15th of June. While there is no correlation between sulfate and the isoprene-derived OA factor for the first period, when plotting only data collected from 15th of June, correlation is found to be slightly higher than the correlation for all background data (R of 0.4).

The isoprene/furan concentrations at m/z 69 (PTR-MS) were treated as an isoprene contribution due to the dominance of isoprene signal compared to furan, according to the samples analysed by gas chromatography-mass spectrometry (Fig. S17). The furan contribution was more significant in BB plumes during the close BB period, as suggested previously (Warneke et al., 2011). As expected, the isoprene/furan gas-phase concentration measured by the PTR-MS increased from noon till the late afternoon (Fig. S16). According to diurnal patterns of PMF isoprene- derived OA, there is no considerable change in isoprene- derived OA concentration from noon throughout the day. The ~~IEPOX-SOA~~isoprene- derived OA fraction is expected to increase during daytime hours in accordance with enhancements in isoprene and gas-phase IEPOX (Hu et al., 2015). ~~As expected, the isoprene/furan gas-phase concentration measured by the PTR-MS increased from noon till the late afternoon (Fig. S14). According to diurnal patterns of PMF IEPOX-SOA, there is no considerable change in IEPOX-SOA concentration from noon throughout the day.~~ However, the ~~IEPOX-SOA~~isoprene- derived OA factor was prominent during night and morning hours. Significant ~~IEPOX-SOA~~isoprene- derived OA factor enhancement during the night time might be due to partitioning of lower volatility species onto the particles when the temperature drops and relative humidity increases as suggested by Budisulistiorini et al. (2013), due to transport of distant air masses, or lower boundary layer height. During the night, the boundary level lowers which increases the concentration of gaseous compounds and can induce partitioning of gases onto the particles. Therefore, the lower night-time boundary layer might create conditions for low volatility isoprene-derived OA partitioning and an increase in isoprene-derived OA.

Formatted: Space After: 0 pt

Formatted: Superscript

Formatted: Superscript

Formatted: Superscript

Formatted: Font: English (U.K.)

A plot of f44 (CO_2^+) vs. f82 ($C_5H_6O^+$) (Org CO_2^+/Org and Org $C_5H_6O^+$/Org from HR data analysis, respectively) (Fig. 8~~10~~) introduced by Hu et al. (2015) can be used to distinguish IEPOX-SOA from SOA originating from other sources, including isoprene- derived~~related~~ SOA that are generated from species other than IEPOX. This plot also indicates the degree of aging of the IEPOX-SOA. The general pattern of f44 increase with f82 decrease is observed. With aging, OA becomes more oxidized and the $C_5H_6O^+$ signature decreases. This can be due to oxidation processes or mixing with more aged aerosol masses.

A background value for f82 ($C_5H_6O^+$) in environments strongly influenced by BB was suggested to be 0.0017 and is indicated by the vertical dashed black line (Hu et al., 2015). Looking at our data plotted in f44 vs. f82 a similar observation can be made. All data points are positioned above 0.0016 of f82 with an average value of 0.0061 ± 0.0036. The ~~IEPOX~~isoprene-derived ~~S~~OA factor average values for this campaign and two other ambient studies are marked in the plot. The f82 value for ~~IEPOX-SOA~~isoprene-derived OA factor observed here is similar to the reported f82 value for an urban site (Budisulistiorini et al., 2013), but lower compared to the ~~IEPOX-SOA~~ factor observed for Borneo forest (Robinson et al., 2011). The lower value for SAFIRED compared to Borneo forest, considering that biogenic influence is significant for both environments, can be attributed to the high influence of BB emissions. ~~A low correlation between the IEPOX-SOA time series with both OOA and BBOA was observed (Fig. S15) suggesting that during BB influenced periods either higher NO$_X$ concentrations suppressed IEPOX and consequently IEPOX-SOA generation or the dominant BB aerosol during these periods inhibited measurement of isoprene oxidation products.~~

As the most abundant NMOC, isoprene is a significant contributor to the global SOA budget (Guenther et al., 2012;Hallquist et al., 2009;Paulot et al., 2009). ~~IEPOX-S~~isoprene-derived OA during the SAFIRED campaign accounted for 28 % of the total background OA which is similar to previous observations where the ~~IEPOX-S~~isoprene-derived OA fraction contribution varied from 6-36 %, depending on the environment (Hu et al., 2015). This confirms the importance of isoprene-~~related~~ derived SOA for the Northern Territory environment even in times of high BB influence.

4. Conclusions

A one month long campaign called SAFIRED was conducted in northern Australia during a period of significant burning (early dry season). There was a significant influence of BB plumes on the atmospheric chemical profile at the time of campaign, reflected by high concentrations of gaseous and particle species including CO and PM$_1$ organics, reaching maxima of ~10^4 ppb and 350 µg m^{-3} respectively during heavy BB episodes. Emitted aerosols were predominantly organic species (90 %) with a wide range of levels of oxidation. There was a clear overall increase of the highly oxygenated OA fraction and degradation of BB-related signatures with OA processing. This was shown by an overall trend of f44 increase and f60 decrease for distant fires. Plume emissions formed over the month period were photochemically active resulting in the production of tropospheric ozone. Close fire emissions were characterized by lower ozone enrichments (average

Formatted: Subscript

$\Delta O_3/\Delta CO$ of 0.15) than plumes detected from the distant BB sources (average $\Delta O_3/\Delta CO$ of 0.31) which illustrate higher photochemical activity with more processed air masses. This emphasizes air mass ability for photochemical processing and production of SOA. An increase in the $\Delta OA/\Delta CO$ ratio with increase of f44 also suggests SOA formation. According to results, t~~T~~he OA oxidation level did not significantly influence~~d~~ particle size distribution~~, with a change in the mode from 83 to 106 nm for fresh (0.05<f44<0.1) and aged (0.1 <f44<0.15) BB plumes, respectively~~. Diversity in BB emissions was illustrated through investigation of five selected events. The chemical signature varied for different fire events (e.g. wide range in f44, from 0.06 to 0.18~~3~~).

PMF was employed to estimate BB influence on and SOA portion of background regional aerosol. A significant portion of oxygenated OA, identified through high f44 (majority of data points between 0.1 and 0.25), and a significant portion of aged BBOA (47 and 24 %, respectively) were observed. The latter suggests considerable processing of aerosol in the atmosphere for this area. The remaining OA was attributed to ~~IEPOX-S~~isoprene-derived OA factor (28 %), identified here for the first time in Australia. The OA mass spectrum with ~~IEPOX-S~~isoprene-derived OA characteristics previously reported in the wet season and now observed with prominent BB influence during the dry period, suggests the importance of biogenic isoprene sources for the Northern Territory area at all times of the year.

Observed photochemical activity of air masses and enhancement of OA with aging illustrate the importance of aging and SOA formation in the Northern Territory during the dry early season. SOA is recognized as a significant contributor to climate, environment and adverse human health effects. This study is an important step in addressing suggested further research related to tropical biomass burns and biogenic-related SOA in Australia (Rotstayn et al., 2009). As SOA yields are considerably underestimated and its formation is still not sufficiently understood, this study can facilitate understanding of SOA formation for Northern Territory savannah areas and also for the tropics in general. Additional measurements during late dry season (September-October) are needed as more intense and frequent fires occur during this period (Andersen et al., 2005;Williams et al., 1998). Moreover, the late dry season is suggested to have more aged emissions (Ristovski et al., 2010;Wardoyo et al., 2007). Therefore it is important to characterize SOA formation, and yield during this period.

Data availability. The underlying research data can be accessed upon request to the corresponding author (Branka Miljevic; b.miljevic@qut.edu.au).

Author contributions. Andelija Milic analysed and interpreted the data and prepared the manuscript. Marc Mallet operated the cToF-AMS and contributed to data analysis, interpretation and writing. Branka Miljevic installed the cToF-AMS, contributed to data analysis, interpretation and writing and supervised the work of Andelija Milic. Luke Cravigan set up the SMPS and contributed to data interpretation. Joel Alroe assisted in organizing the QUT instrumentation, data interpretation and writing the manuscript. Zoran Ristovski contributed to campaign organization and data interpretation and supervised the work of Andelija Milic. Leah Williams contributed to setting up the cToF-AMS, preliminary data analysis and data interpretation. Melita Keywood organized and led the campaign. Paul Selleck operated the BAM, analysed the data and contributed to data interpretation. Sarah Lawson operated the PTR-MS and analysed the data. James Ward operated the Ozone analyser and analysed the data. Maximilian Desservettaz operated the FTIR and SMPS and analysed the data. Clare Paton-Walsh contributed to campaign organization and running the campaign. All authors declare that they have no conflict of interest.

Acknowledgements. The authors thank Manjula Canagaratna for valuable discussions about interpreting the PMF analysis. The authors thank Min Cheng for providing the gas chromatography-mass spectrometry data. This work was supported by the Australian Research Council Discovery grant (DP120100126).

References

Aiken, A. C., DeCarlo, P. F., and Jimenez, J. L.: Elemental analysis of organic species with electron ionization high-resolution mass spectrometry, Analytical Chemistry, 79, 8350-8358, 2007.

Aiken, A. C., DeCarlo, P. F., Kroll, J. H., Worsnop, D. R., Huffman, J. A., Docherty, K. S., Ulbrich, I. M., Mohr, C., Kimmel, J. R., Sueper, D., Sun, Y., Zhang, Q., Trimborn, A., Northway, M. J., Ziemann, P. J., Canagaratna, M., Onasch, T., Alfarra, M. R., Prevot, A. S., Dommen, J., Duplissy, J., Metzger, A., Baltensperger, U., and Jimenez, J.: O/C and OM/OC ratios of primary, secondary, and ambient organic aerosols with high-resolution time-of-flight aerosol mass spectrometry, Environmental Science & Technology, 42, 4478-4485, 2008.

Akagi, S., Craven, J., Taylor, J., McMeeking, G., Yokelson, R., Burling, I., Urbanski, S., Wold, C., Seinfeld, J., Coe, H., Alvarado, M., and Weise, D.: Evolution of trace gases and particles emitted by a chaparral fire in California, Atmospheric Chemistry and Physics, 12, 1397-1421, 2012.

Alfarra, M. R., Prevot, A. S., Szidat, S., Sandradewi, J., Weimer, S., Lanz, V. A., Schreiber, D., Mohr, M., and Baltensperger, U.: Identification of the mass spectral signature of organic aerosols from wood burning emissions, Environmental science & technology, 41, 5770-5777, 2007.

Allen, G., Vaughan, G., Bower, K., Williams, P., Crosier, J., Flynn, M., Connolly, P., Hamilton, J., Lee, J., Saxton, J., Watson, N., Gallagher, M., Coe, H., Allan, J., Choularton, T., and Lewis, A.: Aerosol and trace-gas measurements in the Darwin area during the wet season, Journal of Geophysical Research: Atmospheres (1984–2012), 113, 2008.

Andersen, A. N., Cook, G. D., Corbett, L. K., Douglas, M. M., Eager, R. W., Russell-Smith, J., Setterfield, S. A., Williams, R. J., and Woinarski, J. C.: Fire frequency and biodiversity conservation in Australian tropical savannas: implications from the Kapalga fire experiment, Austral Ecology, 30, 155-167, 2005.

Bond, T. C., Streets, D. G., Yarber, K. F., Nelson, S. M., Woo, J. H., and Klimont, Z.: A technology-based global inventory of black and organic carbon emissions from combustion, Journal of Geophysical Research: Atmospheres (1984–2012), 109, 2004.

Bougiatioti, A., Stavroulas, I., Kostenidou, E., Zarmpas, P., Theodosi, C., Kouvarakis, G., Canonaco, F., Prévôt, A., Nenes, A., Pandis, S., and Mihalopoulos, N.: Processing of biomass-burning aerosol in the eastern Mediterranean during summertime, Atmospheric Chemistry and Physics, 14, 4793-4807, 2014.

Bouya, Z., Box, G. P., and Box, M. A.: Seasonal variability of aerosol optical properties in Darwin, Australia, Journal of Atmospheric and Solar-Terrestrial Physics, 72, 726-739, 2010.

Bowman, D. M., Dingle, J. K., Johnston, F. H., Parry, D., and Foley, M.: Seasonal patterns in biomass smoke pollution and the mid 20th-century transition from Aboriginal to European fire management in northern Australia, Global Ecology and Biogeography, 16, 246-256, 2007.

Brito, J., Rizzo, L., Morgan, W., Coe, H., Johnson, B., Haywood, J., Longo, K., Freitas, S., Andreae, M., and Artaxo, P.: Ground-based aerosol characterization during the South American Biomass Burning Analysis (SAMBBA) field experiment, Atmospheric Chemistry and Physics, 14, 12069-12083, 2014.

Budisulistiorini, S. H., Canagaratna, M. R., Croteau, P. L., Marth, W. J., Baumann, K., Edgerton, E. S., Shaw, S. L., Knipping, E. M., Worsnop, D. R., and Jayne, J. T.: Real-time continuous characterization of secondary organic aerosol derived from isoprene epoxydiols in downtown Atlanta, Georgia, using the Aerodyne Aerosol Chemical Speciation Monitor, Environmental science & technology, 47, 5686-5694, 2013.

Capes, G., Johnson, B., McFiggans, G., Williams, P., Haywood, J., and Coe, H.: Aging of biomass burning aerosols over West Africa: Aircraft measurements of chemical composition, microphysical properties, and emission ratios, Journal of Geophysical Research: Atmospheres (1984–2012), 113, 2008.

Carr, S. B., Gras, J., Hackett, M., and Keywood, M.: Aerosol Characteristics in the Northern Territory of Australia During the Dry Season With an Emphasis on Biomass Burning, DTIC Document, 2005.

Chow, J. C., Watson, J. G., Chen, L.-W. A., Chang, M. O., Robinson, N. F., Trimble, D., and Kohl, S.: The IMPROVE_A temperature protocol for thermal/optical carbon analysis: maintaining consistency with a long-term database, Journal of the Air & Waste Management Association, 57, 1014-1023, 2007.

Crutzen, P. J., and Andreae, M. O.: Biomass burning in the tropics: Impact on atmospheric chemistry and biogeochemical cycles, Science, 250, 1669-1678, 1990.

Cubison, M., Ortega, A., Hayes, P., Farmer, D., Day, D., Lechner, M., Brune, W., Apel, E., Diskin, G., and Fisher, J.: Effects of aging on organic aerosol from open biomass burning smoke in aircraft and laboratory studies, Atmospheric Chemistry and Physics, 11, 12049-12064, 2011.

DeCarlo, P., Dunlea, E., Kimmel, J., Aiken, A., Sueper, D., Crounse, J., Wennberg, P., Emmons, L., Shinozuka, Y., and Clarke, A.: Fast airborne aerosol size and chemistry measurements above Mexico City and Central Mexico during the MILAGRO campaign, Atmos. Chem. Phys, 8, 4027-4048, 2008.

DeCarlo, P., Ulbrich, I., Crounse, J., Foy, B. d., Dunlea, E., Aiken, A., Knapp, D., Weinheimer, A., Campos, T., Wennberg, P., and Jimenez, J.: Investigation of the sources and processing of organic aerosol over the Central Mexican Plateau from aircraft measurements during MILAGRO, Atmospheric Chemistry and Physics, 10, 5257-5280, 2010.

Desservettaz, M., Paton-Walsh, C., Griffith, D., Kettlewell, G., Keywood, M., Schoot, M. V., JasonWard, Mallet, M., Ristovski, Z., Miljevic, B., Milic, A., Howard, D., Edwards, G., and Atkinson, B.: Emission factors of trace gases and particles from tropical savanna fires in Australia, submitted to Journal of Geophysical Research 2016.

Edwards, D., Pétron, G., Novelli, P., Emmons, L., Gille, J., and Drummond, J.: Southern Hemisphere carbon monoxide interannual variability observed by Terra/Measurement of Pollution in the Troposphere (MOPITT), Journal of Geophysical Research: Atmospheres, 111, 2006.

Formenti, P., Elbert, W., Maenhaut, W., Haywood, J., Osborne, S., and Andreae, M.: Inorganic and carbonaceous aerosols during the Southern African Regional Science Initiative (SAFARI 2000) experiment: Chemical characteristics, physical properties, and emission data for smoke from African biomass burning, Journal of Geophysical Research: Atmospheres (1984–2012), 108, 2003.

Grieshop, A., Logue, J., Donahue, N., and Robinson, A.: Laboratory investigation of photochemical oxidation of organic aerosol from wood fires 1: measurement and simulation of organic aerosol evolution, Atmospheric Chemistry and Physics, 9, 1263-1277, 2009.

Griffith, D., Deutscher, N., Caldow, C., Kettlewell, G., Riggenbach, M., and Hammer, S.: A Fourier transform infrared trace gas and isotope analyser for atmospheric applications, Atmospheric Measurement Techniques, 5, 2481-2498, 2012.

Griffith, D. W.: Synthetic calibration and quantitative analysis of gas-phase FT-IR spectra, Applied spectroscopy, 50, 59-70, 1996.

Guenther, A., Jiang, X., Heald, C., Sakulyanontvittaya, T., Duhl, T., Emmons, L., and Wang, X.: The Model of Emissions of Gases and Aerosols from Nature version 2.1 (MEGAN2. 1): an extended and updated framework for modeling biogenic emissions, 2012.

Guenther, C.: Estimates of global terrestrial isoprene emissions using MEGAN (Model of Emissions of Gases and Aerosols from Nature), Atmospheric Chemistry and Physics, 6, 2006.

Hallquist, M., Wenger, J., Baltensperger, U., Rudich, Y., Simpson, D., Claeys, M., Dommen, J., Donahue, N., George, C., Goldstein, A., Hamilton, J., Herrmann, H., Hoffmann, D., Iinuma, Y., Jang, M., Jenkin, M., Jimenez, J., Keindler-Scharr, A., Maenhaut, W., McFiggans, G., Mentel, T., Monod, A., Prevot, A., Seinfeld, J., Surratt, J., Szmigielski, R., and Wildt, J.: The formation, properties and impact of secondary organic aerosol: current and emerging issues, Atmos. Chem. Phys, 9, 5155-5236, 2009.

Haywood, J., and Boucher, O.: Estimates of the direct and indirect radiative forcing due to tropospheric aerosols: A review, Reviews of geophysics, 38, 513-543, 2000.

He, C., Murray, F., and Lyons, T.: Monoterpene and isoprene emissions from 15 Eucalyptus species in Australia, Atmospheric Environment, 34, 645-655, 2000.

Heringa, M., DeCarlo, P., Chirico, R., Tritscher, T., Dommen, J., Weingartner, E., Richter, R., Wehrle, G., Prévôt, A., and Baltensperger, U.: Investigations of primary and secondary particulate matter of different wood combustion appliances with a high-resolution time-of-flight aerosol mass spectrometer, Atmos. Chem. Phys, 11, 5945-5957, 2011.

Heringa, M., DeCarlo, P., Chirico, R., Lauber, A., Doberer, A., Good, J., Nussbaumer, T., Keller, A., Burtscher, H., and Richard, A.: Time-resolved characterization of primary emissions from residential wood combustion appliances, Environmental science & technology, 46, 11418-11425, 2012.

Hobbs, P. V., Sinha, P., Yokelson, R. J., Christian, T. J., Blake, D. R., Gao, S., Kirchstetter, T. W., Novakov, T., and Pilewskie, P.: Evolution of gases and particles from a savanna fire in South Africa, Journal of Geophysical Research: Atmospheres (1984–2012), 108, 2003.

Hu, W., Campuzano-Jost, P., Palm, B., Day, D., Ortega, A., Hayes, P., Krechmer, J., Chen, Q., Kuwata, M., Liu, Y., McKinney, K., Martin, S. T., Hu, M., Budisulistiorini, S. H., Riva, M., Surratt, J., Clair, J. M. S., Isaacman, G., Yee, L., Goldstein, A., Carbone, S., Brito, J., Artaxo, P., De Gouw, J., Koss, A., Wisthaler, A., Mikoviny, T., Karl, T., Kaser, L., Jud, W., Hansel, A., Docherty, K., Alexander, M., Robinson, A., Coe, H., Allan, J., Canagaratna, M., Paulot, F., and Jimenez, J.: Characterization of a real-time tracer for isoprene epoxydiols-derived secondary organic aerosol (IEPOX-SOA) from aerosol mass spectrometer measurements, Atmospheric Chemistry and Physics, 15, 11807-11833, 2015.

Hurst, D. F., Griffith, D. W., and Cook, G. D.: Trace gas emissions from biomass burning in tropical Australian savannas, Journal of Geophysical Research: Atmospheres, 99, 16441-16456, 1994.

Jaffe, D. A., and Wigder, N. L.: Ozone production from wildfires: A critical review, Atmospheric Environment, 51, 1-10, 2012.

Jimenez, J., Canagaratna, M., Donahue, N., Prevot, A., Zhang, Q., Kroll, J. H., DeCarlo, P. F., Allan, J. D., Coe, H., Ng, N., Aiken, A., Docherty, K., Ulbrich, I., Grieshop, A. P., Robinson, A., Duplissy, J., Smith, J. D., Wilson, K. R., Lanz, V., Hueglin, C., Sun, J., Tian, J., Laaksonen, A., Raatikainen, T., Rautiainen, J., Vaattovaara, P., Ehn, M., Kulmala, M., Tomlinson, J., Collins, D., Cubison, M. J., Dunlea, E., Huffman, J. A., Onasch, T., Alfarra, M. R., Williams, P., Bower, K. N., Kondo, Y., Schneider, J., Drewnick, F., Borrmann, S., Weimer, S., Demerjian, K. L., Salcedo, D., Cottrell, L., Griffin, R., Takami, A., Miyoshi, T., Hatakeyama, S., Shimono, A., Sun, J., Zhang, J., Dzepina, K., Kimmel, J. R., Sueper, D., Jayne, J. T., Herndon, S., Trimborn, A., Williams, L. R., Wood, E., Middlebrook, A., Kolb, C. E., Baltensperger, U., and Worsnop, D. R.: Evolution of organic aerosols in the atmosphere, Science, 326, 1525-1529, 2009.

Jolleys, M., Coe, H., McFiggans, G., Taylor, J., O'Shea, S., Le Breton, M., Bauguitte, S.-B., Moller, S., Di Carlo, P., and Aruffo, E.: Properties and evolution of biomass burning organic aerosol from Canadian boreal forest fires, Atmospheric Chemistry and Physics, 15, 3077-3095, 2015.

Jordan, T. B., Seen, A. J., and Jacobsen, G. E.: Levoglucosan as an atmospheric tracer for woodsmoke, Atmospheric Environment, 40, 5316-5321, 2006.

Kleinman, L. I., Springston, S. R., Daum, P. H., Lee, Y.-N., Nunnermacker, L., Senum, G., Wang, J., Weinstein-Lloyd, J., Alexander, M., Hubbe, J., Ortega, A., Canagaratna, M., and Jayne, J. T.: The time evolution of aerosol composition over the Mexico City plateau, Atmospheric Chemistry and Physics, 8, 1559-1575, 2008.

Kroll, J. H., Smith, J. D., Che, D. L., Kessler, S. H., Worsnop, D. R., and Wilson, K. R.: Measurement of fragmentation and functionalization pathways in the heterogeneous oxidation of oxidized organic aerosol, Physical Chemistry Chemical Physics, 11, 8005-8014, 2009.

Lacey, C., Walker, J., and Noble, I.: Fire in Australian tropical savannas, in: Ecology of tropical savannas, Springer, 246-272, 1982.

Lambe, A., Chhabra, P., Onasch, T., Brune, W., Hunter, J., Kroll, J., Cummings, M., Brogan, J., Parmar, Y., and Worsnop, D.: Effect of oxidant concentration, exposure time, and seed particles on secondary organic aerosol chemical composition and yield, Atmospheric Chemistry and Physics, 15, 3063-3075, 2015.

Lanz, V., Alfarra, M., Baltensperger, U., Buchmann, B., Hueglin, C., and Prévôt, A.: Source apportionment of submicron organic aerosols at an urban site by factor analytical modelling of aerosol mass spectra, Atmospheric Chemistry and Physics, 7, 1503-1522, 2007.

Li, J., Pósfai, M., Hobbs, P. V., and Buseck, P. R.: Individual aerosol particles from biomass burning in southern Africa: 2, Compositions and aging of inorganic particles, Journal of Geophysical Research: Atmospheres, 108, 2003.

Li, W., Shao, L., and Buseck, P.: Haze types in Beijing and the influence of agricultural biomass burning, Atmospheric Chemistry and Physics, 10, 8119-8130, 2010.

Lin, Y.-H., Zhang, Z., Docherty, K. S., Zhang, H., Budisulistiorini, S. H., Rubitschun, C. L., Shaw, S. L., Knipping, E. M., Edgerton, E. S., Kleindienst, T. E., Gold, A., and Surratt, J.: Isoprene epoxydiols as precursors to secondary organic aerosol formation: acid-catalyzed reactive uptake studies with authentic compounds, Environmental science & technology, 46, 250-258, 2011.

Liu, X., Van Espen, P., Adams, F., Cafmeyer, J., and Maenhaut, W.: Biomass burning in southern Africa: Individual particle characterization of atmospheric aerosols and savanna fire samples, Journal of Atmospheric Chemistry, 36, 135-155, 2000.

Mallet, M. D., Desservettaz, M. J., Miljevic, B., Milic, A., Ristovski, Z. D., Alroe, J., Cravigan, L. T., Jayaratne, E. R., Paton-Walsh, C., Griffith, D. W. T., Wilson, S. R., Kettlewell, G., Vanderschoot, M. V., Selleck, P., Reisen, F., Lawson, S. J., Ward, J., Harnwell, J., Cheng, M., Gillett, R. W., Molloy, S. B., Howard, D., Nelson, P. F., Morrison, A. L., Edwards, G. C., Williams, A. G., Chambers, S. D., Werczynski, S., Williams, L. R., Winton, V. H. L., Atkinson, B., Wang, X., and Keywood, M. D.: Biomass burning emissions in north Australia during the early dry season: an overview of the 2014 SAFIRED campaign, Phys. Discuss., doi:10.5194/acp-2016-866, in review, 2016.

Martins, J. V., Dunlap, M. R., and Liousse, C.: Physical, chemical, and optical properties of regional hazes dominated by smoke in Brazil, Journal of Geophysical Research, 103, 32,059-032,080, 1998.

Middlebrook, A. M., Bahreini, R., Jimenez, J. L., and Canagaratna, M. R.: Evaluation of composition-dependent collection efficiencies for the aerodyne aerosol mass spectrometer using field data, Aerosol Science and Technology, 46, 258-271, 2012.

Mitchell, R., Forgan, B., Campbell, S., and Qin, Y.: The climatology of Australian tropical aerosol: evidence for regional correlation, Geophysical Research Letters, 40, 2384-2389, 2013.

Ng, N., Canagaratna, M., Zhang, Q., Jimenez, J., Tian, J., Ulbrich, I., Kroll, J., Docherty, K., Chhabra, P., Bahreini, R., Murphy, S., Seinfeld, J., Hildebrandt Ruiz, L., Donahue, N. M., DeCarlo, P., Lanz, V., Prevot, A., Dinar, E., Rudich, Y., and Worsnop, D. R.: Organic aerosol components observed in Northern Hemispheric datasets from Aerosol Mass Spectrometry, Atmospheric Chemistry and Physics, 10, 4625-4641, 2010.

O'Brien, D., and Mitchell, R.: Atmospheric heating due to carbonaceous aerosol in northern Australia—confidence limits based on TOMS aerosol index and sun-photometer data, Atmospheric Research, 66, 21-41, 2003.

Ortega, A., Day, D., Cubison, M., Brune, W., Bon, D., de Gouw, J., and Jimenez, J.: Secondary organic aerosol formation and primary organic aerosol oxidation from biomass-burning smoke in a flow reactor during FLAME-3, Atmospheric Chemistry and Physics, 13, 11551-11571, 2013.

Paatero, P., and Tapper, U.: Positive matrix factorization: A non-negative factor model with optimal utilization of error estimates of data values, Environmetrics, 5, 111-126, 1994.

Paatero, P.: The multilinear engine—a table-driven, least squares program for solving multilinear problems, including the n-way parallel factor analysis model, Journal of Computational and Graphical Statistics, 8, 854-888, 1999.

Paatero, P., and Hopke, P. K.: Rotational tools for factor analytic models, Journal of Chemometrics, 23, 91-100, 2009.

Parrington, M., Palmer, P., Lewis, A., Lee, J., Rickard, A., Carlo, P. D., Taylor, J., Hopkins, J., Punjabi, S., Oram, D., Forster, G., Aruffo, E., Moller, S., Bauguitte, S.-B., Allan, J., Coe, H., and Leigh, R.: Ozone photochemistry in boreal biomass burning plumes, Atmospheric Chemistry and Physics, 13, 7321-7341, 2013.

Paulot, F., Crounse, J. D., Kjaergaard, H. G., Kürten, A., Clair, J. M. S., Seinfeld, J. H., and Wennberg, P. O.: Unexpected epoxide formation in the gas-phase photooxidation of isoprene, Science, 325, 730-733, 2009.

Penner, J., Chuang, C., and Grant, K.: Climate forcing by carbonaceous and sulfate aerosols, Clim. Dynamm., 14, 839–851, ISI, 1998.

Pye, H. O., Murphy, B. N., Xu, L., Ng, N. L., Carlton, A. G., Guo, H., Weber, R., Vasilakos, P., Appel, K. W., and Budisulistiorini, S. H.: On the implications of aerosol liquid water and phase separation for organic aerosol mass,

Real, E., Law, K., Weinzierl, B., Fiebig, M., Petzold, A., Wild, O., Methven, J., Arnold, S., Stohl, A., Huntrieser, H., Roiger, A., Schlager, H., Stewart, D., Avery, M., Sachse, G. W., Browell, E., Ferrare, R., and Blake, D. R.: Processes influencing ozone levels in Alaskan forest fire plumes during long-range transport over the North Atlantic, Journal of Geophysical Research: Atmospheres (1984–2012), 112, 2007.

Reid, J., Koppmann, R., Eck, T., and Eleuterio, D.: A review of biomass burning emissions part II: intensive physical properties of biomass burning particles, Atmospheric Chemistry and Physics, 5, 799-825, 2005.

Ristovski, Z. D., Wardoyo, A. Y., Morawska, L., Jamriska, M., Carr, S., and Johnson, G.: Biomass burning influenced particle characteristics in Northern Territory Australia based on airborne measurements, Atmospheric Research, 96, 103-109, 2010.

Roberts, G. C., Artaxo, P., Zhou, J., Swietlicki, E., and Andreae, M. O.: Sensitivity of CCN spectra on chemical and physical properties of aerosol: A case study from the Amazon Basin, Journal of Geophysical Research: Atmospheres (1984–2012), 107, LBA 37-31-LBA 37-18, 2002.

Robinson, N., Hamilton, J., Allan, J., Langford, B., Oram, D., Chen, Q., Docherty, K., Farmer, D., Jimenez, J., and Ward, M.: Evidence for a significant proportion of Secondary Organic Aerosol from isoprene above a maritime tropical forest, Atmospheric Chemistry and Physics, 11, 1039-1050, 2011.

Rotstayn, L. D., Keywood, M. D., Forgan, B. W., Gabric, A. J., Galbally, I. E., Gras, J. L., Luhar, A. K., McTainsh, G. H., Mitchell, R. M., and Young, S. A.: Possible impacts of anthropogenic and natural aerosols on Australian climate: a review, International Journal of Climatology, 29, 461-479, 2009.

Russell-Smith, J., Yates, C. P., Whitehead, P. J., Smith, R., Craig, R., Allan, G. E., Thackway, R., Frakes, I., Cridland, S., Meyer, M. C., and Gill, A.: Bushfires' down under': patterns and implications of contemporary Australian landscape burning, International Journal of Wildland Fire, 16, 361-377, 2007.

Schwantes, R. H., Teng, A. P., Nguyen, T. B., Coggon, M. M., Crounse, J. D., St. Clair, J. M., Zhang, X., Schilling, K. A., Seinfeld, J. H., and Wennberg, P. O.: Isoprene NO3 Oxidation Products from the RO2+ HO2 Pathway, The Journal of Physical Chemistry A, 119, 10158-10171, 2015.

Simoneit, B. R., Schauer, J. J., Nolte, C., Oros, D. R., Elias, V. O., Fraser, M., Rogge, W., and Cass, G. R.: Levoglucosan, a tracer for cellulose in biomass burning and atmospheric particles, Atmospheric Environment, 33, 173-182, 1999.

Simoneit, B. R.: Biomass burning—a review of organic tracers for smoke from incomplete combustion, Applied Geochemistry, 17, 129-162, 2002.

Ulbrich, I., Canagaratna, M., Zhang, Q., Worsnop, D., and Jimenez, J.: Interpretation of organic components from Positive Matrix Factorization of aerosol mass spectrometric data, Atmospheric Chemistry and Physics, 9, 2891-2918, 2009.

Wang, C., and Prinn, R. G.: Impact of emissions, chemistry and climate on atmospheric carbon monoxide: 100-yr predictions from a global chemistry–climate model, Chemosphere-Global Change Science, 1, 73-81, 1999.

Ward, D., and Radke, L.: Emissions measurements from vegetation fires: A comparative evaluation of methods and results, 1993.

Wardoyo, A. Y., Morawska, L., Ristovski, Z. D., Jamriska, M., Carr, S., and Johnson, G.: Size distribution of particles emitted from grass fires in the Northern Territory, Australia, Atmospheric Environment, 41, 8609-8619, 2007.

Warneke, C., Roberts, J., Veres, P., Gilman, J., Kuster, W., Burling, I., Yokelson, R., and de Gouw, J.: VOC identification and inter-comparison from laboratory biomass burning using PTR-MS and PIT-MS, International Journal of Mass Spectrometry, 303, 6-14, 2011.

Weimer, S., Alfarra, M., Schreiber, D., Mohr, M., Prévôt, A., and Baltensperger, U.: Organic aerosol mass spectral signatures from wood-burning emissions: Influence of burning conditions and wood type, Journal of Geophysical Research: Atmospheres (1984–2012), 113, 2008.

Williams, R., Gill, A., and Moore, P.: Seasonal changes in fire behaviour in a tropical savanna in northern Australia, International Journal of Wildland Fire, 8, 227-239, 1998.

Xu, L., Middlebrook, A. M., Liao, J., Gouw, J. A., Guo, H., Weber, R. J., Nenes, A., Lopez-Hilfiker, F. D., Lee, B. H., and Thornton, J. A.: Enhanced formation of isoprene-derived organic aerosol in sulfur-rich power plant plumes during Southeast Nexus, Journal of Geophysical Research: Atmospheres, 121, 2016.

Yokelson, R. J., Bertschi, I. T., Christian, T. J., Hobbs, P. V., Ward, D. E., and Hao, W. M.: Trace gas measurements in nascent, aged, and cloud-processed smoke from African savanna fires by airborne Fourier transform infrared spectroscopy (AFTIR), Journal of Geophysical Research: Atmospheres (1984–2012), 108, 2003.

Yokelson, R. J., Crounse, J., DeCarlo, P., Karl, T., Urbanski, S., Atlas, E., Campos, T., Shinozuka, Y., Kapustin, V., Clarke, A., Weinheimer, A., Knapp, D., Montzga, L., Holloway, J., Weibring, P., Flocke, F., Zheng, W., Toohey, D., Wennberg, P. O., Wiedinmyer, C., Mauldin, R. L., Fried, A., Richter, D., Walega, J., Jimenez, J., Adachi, K., Buseck, P. R., Hall, S., and Shetter, R.: Emissions from biomass burning in the Yucatan, Atmospheric Chemistry and Physics, 9, 5785-5812, 2009.

Zhang, Q., Jimenez, J., Canagaratna, M., Allan, J., Coe, H., Ulbrich, I., Alfarra, M., Takami, A., Middlebrook, A., Sun, Y., Dzepina, K., Dunlea, E., Docherty, K., DeCarlo, P., Salcedo, D., Onasch, T., Jayne, J. T., Miyoshi, T., Shimono, A., Hatakeyama, S., Takegawa, N., Kondo, Y., Schneider, J., Drewnick, F., Borrmann, S., Weimer, S., Demerjian, K. L., Williams, P., Bower, K. N., Bahreini, R., Cottrell, L., Griffin, R., Rautiainen, J., Sun, J., Zhang, Y., and Worsnop, D. R.: Ubiquity and dominance of oxygenated species in organic aerosols in anthropogenically-influenced Northern Hemisphere midlatitudes, Geophysical Research Letters, 34, 2007.

Zhao, R., Mungall, E. L., Lee, A. K., Aljawhary, D., and Abbatt, J. P.: Aqueous-phase photooxidation of levoglucosan–a mechanistic study using Aerosol Time of Flight Chemical Ionization Mass Spectrometry (Aerosol-ToF-CIMS), Atmospheric Chemistry and Physics Discussions, 14, 8819-8850, 2014.

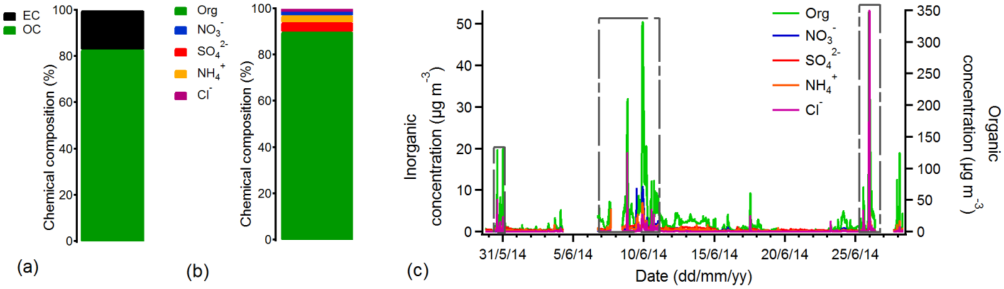

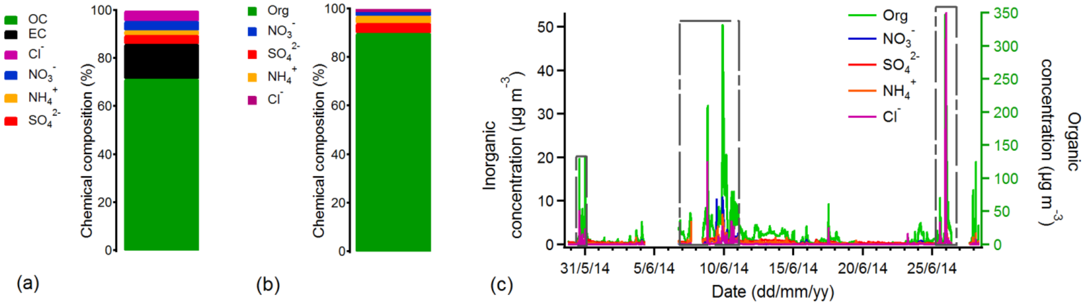

Figure 1: Contributions of (a) EC, ~~and~~ OC and inorganics ~~in carbonaceous material~~ collected on filters and the contribution of (b) AMS organic and inorganics in non-refractory submicron aerosol fraction as well as (c) their time series. Close BB periods ~~is~~ are marked in the AMS time series with grey dashed boxes. The distant BB periods cover all days of the measurement other than days included in close BB periods. Gaps in the AMS time series indicate gaps in the sampling.

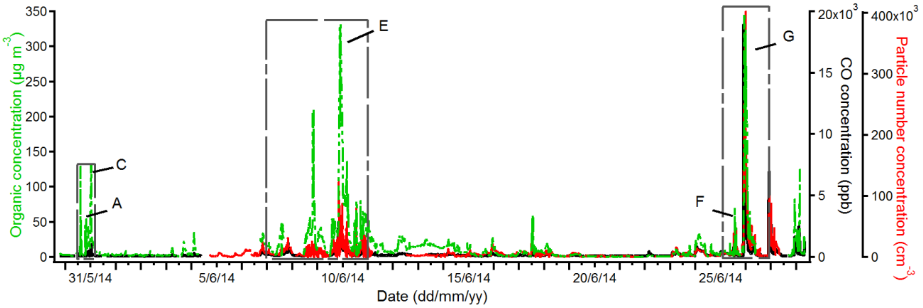

Figure 2: Time series for AMS organics, CO and particle number concentration during the SAFIRED campaign. Close BB periods ~~is~~ are marked with grey dashed boxes and selected BB events are labelled. The distant BB periods cover all days of the measurement other than days included in close BB periods. Gaps in the time series indicate gaps in the sampling (no data for the instrument).

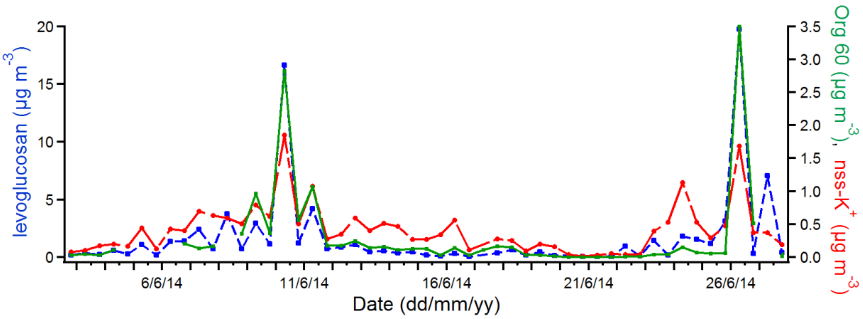

Figure 3: Time series of BB tracers: levoglucosan, soluble non-sea salt potassium (nss-K^+) (both 12h resolution) and AMS Org 60 (averaged to BAM 12h).

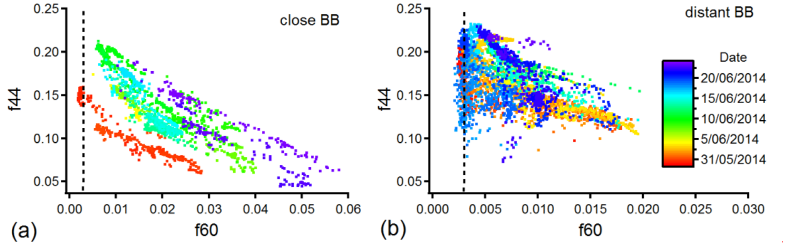

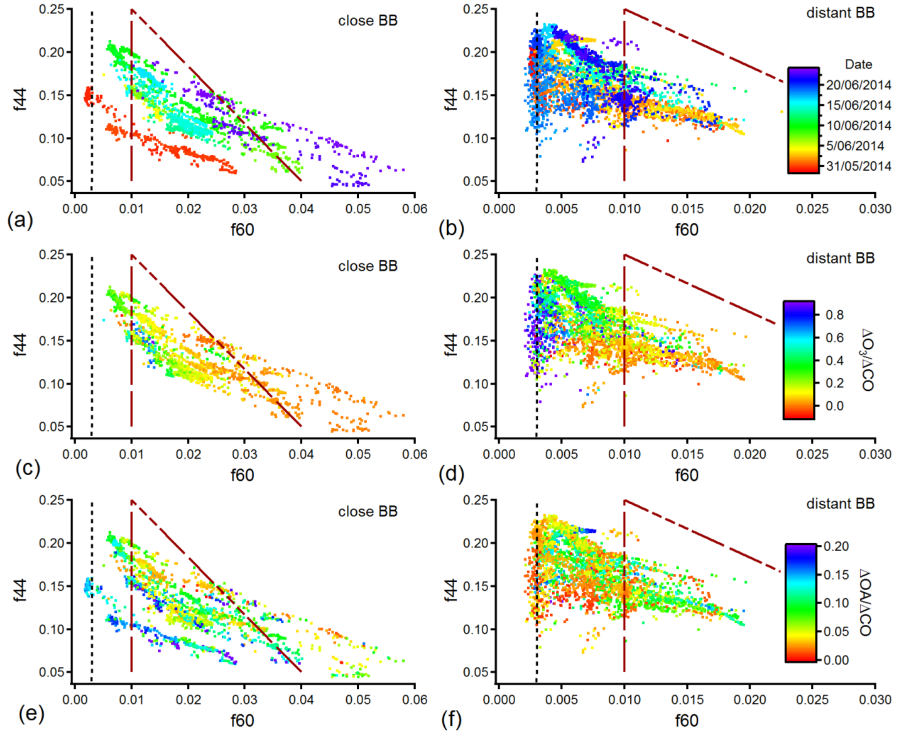

Figure 4: f44 vs. f60 coloured by date for (a) close and (b) distant BB periods, by $\Delta O_3/\Delta CO$ ratio for (c) close and (d) distant BB periods, and by ΔOA/ΔCO ratio for (e) close and (f) distant BB periods (vertical black lines refer to the f60 background level of 0.003). Red dashed lines refer to the ambient BBOA-related data introduced by (Cubison et al., 2011). Note: ozone data from 29th of May until the 1st of June were not available.

Formatted: Subscript

Formatted: Superscript

Formatted: Superscript

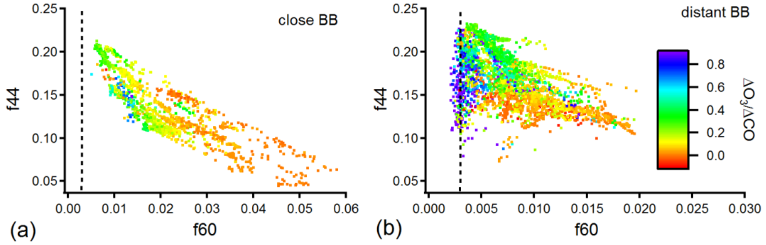

~~**Figure 5: f44 vs. f60 coloured by $\Delta O_3/\Delta CO$ ratio for (a) close and (b) distant BB periods (vertical black lines refer to the f60 background level of 0.003).**~~

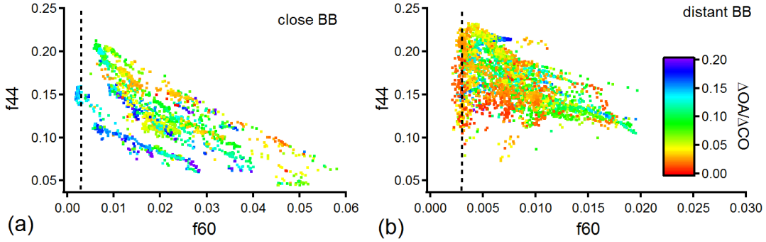

~~**Figure 6: f44 vs. f60 coloured by $\Delta OA/\Delta CO$ ratio for (a) close and (b) distant BB periods (vertical black lines refer to the f60 background level of 0.003).**~~

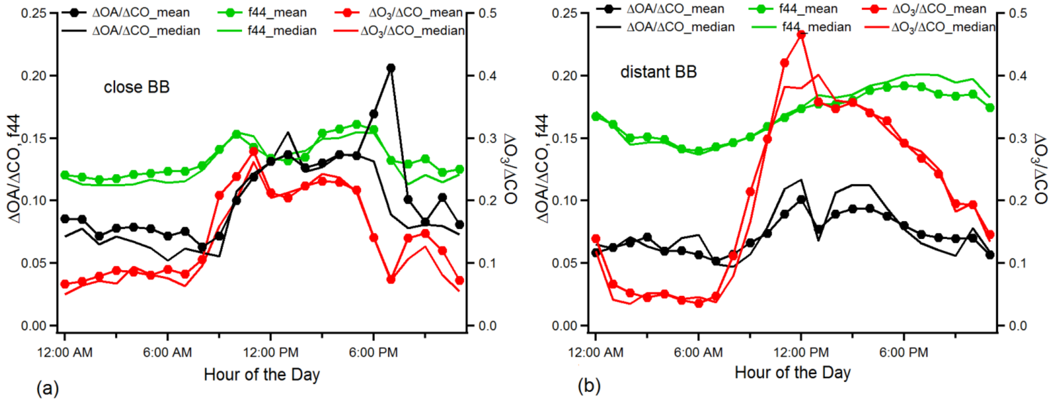

Formatted: Normal

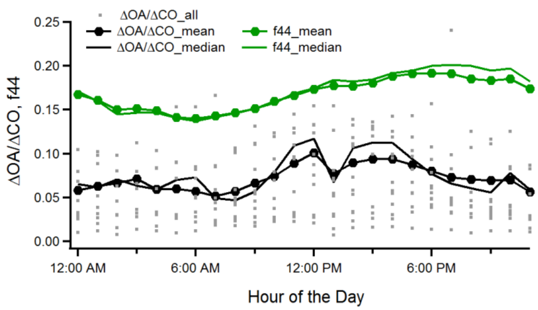

Figure 5~~7~~: Diurnal trend of f44 (mean and median), $\Delta O_3/\Delta CO$ ratio (mean and median) and ΔOA/ΔCO ratio (mean, median)~~ and hourly data points)~~ for close (a) and distant (b) BB ~~emissions~~periods.

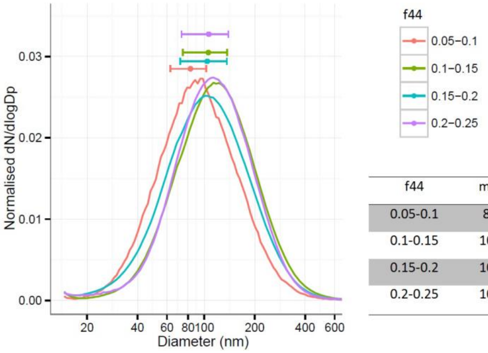

f44	mode	upper	lower
0.05-0.1	82.7	102.7	62.7
0.1-0.15	105.8	137.0	74.5
0.15-0.2	104.1	136.2	72.0
0.2-0.25	106.4	139.4	73.3

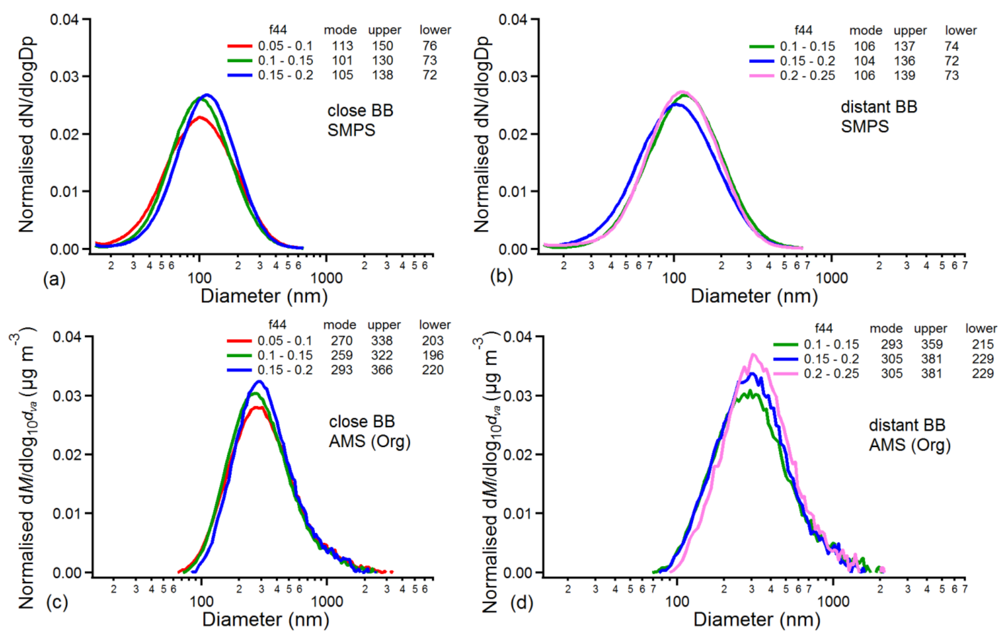

Figure 6~~8~~: SMPS size distributions (dN/dlogDp, normalised to total particle number concentration, versus diameter) binned by the AMS f44 for close (a) and distant (b) BB periods and~~.~~ ~~The average mode and the standard deviation in the mode are given.~~ AMS size distributions (dM/$\mathrm{dlog_{10}d_{va}}$, normalised to total organic concentration, versus diameter) binned by the AMS f44 for close (c) and distant (d) BB periods.

Table 1: Selected BB event values for f44, f60, organic concentration, CO, MCE, mode diameter and $\Delta O_3/\Delta CO$ ratio, along with measurement start and end time. ND refers to no data.

	Date (start/end)	f44±SD (range)	mean f60±SD (range)	mean Org±SD* (range)	mean CO±SD* (range)	MCE	$\Delta O_3/\Delta CO$	Mode diameter (nm)
A	30/05/14 18:34- 30/05/14 19:25	0.087±0.08 (0.079-0.105)	0.016±0.002 (0.010-0.018)	22.6±12.5 (4.6-45.2)	185.9±95.5 (90.2-370.1)	0.97± 0.06	ND	ND
C	30/05/14 23:41- 31/05/14/ 00:59	0.066±0.005 (0.060-0.079)	0.027±0.002 (0.021-0.028)	75.5±40.0 (13.7-131.2)	627.1±345.4 (185.8-1181.6)	0.98± 0.11	ND	ND
E	09/06/14 19:45- 10/06/14 00:32	0.078±0.013 (0.062-0.093)	0.032±0.002 (0.030-0.035)	175.9±105.0 (87.3-331.8)	1558.5±965.5 (671.6-3382.5)	0.91± 0.05	0.024	146
F	25/06/14 12:28- 25/06/14 16:59	0.134±0.031 (0.073-0.178)	0.009±0.002 (0.007-0.014)	13.2±14.5 (2.4-70.8)	479.0±348.8 (139.5-1642.7	0.93± 0.04	0.134	98
G	25/06/14 21:40- 26/06/14 03:59	0.062±0.017 (0.045-0.098)	0.046±0.004 (0.035-0.052)	144.6±104.7 (25.8-347.7)	2744.6±2299.8 (592.8-11275.7)	0.90± 0.06	0.011	88

*unit is µg m^{-3}

Formatted: Justified

Formatted Table

Formatted: Justified

Formatted: Font: 10 pt

Formatted: Normal

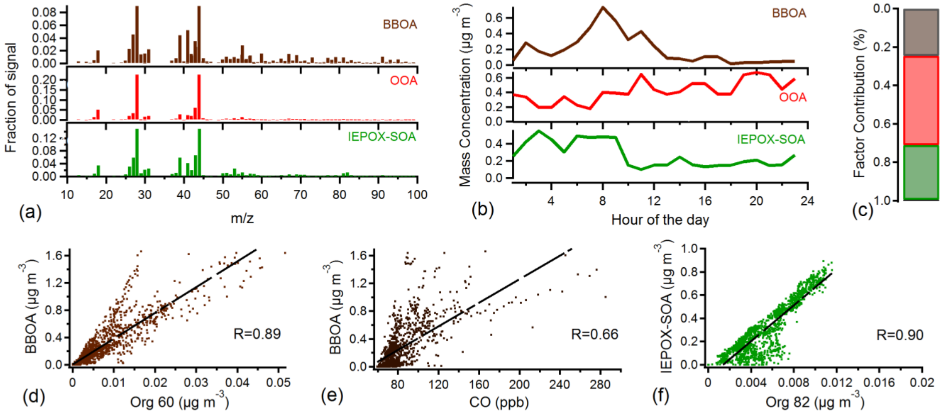

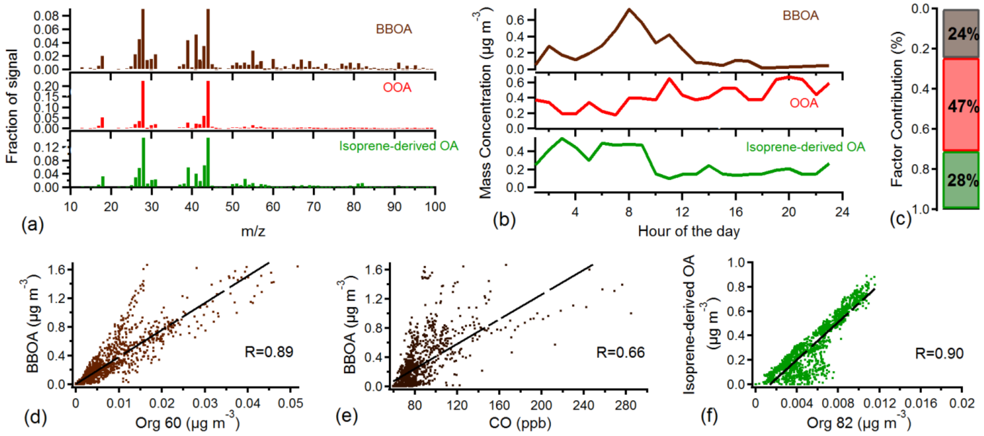

Figure 7~~9~~: (a) Mass spectra, (b) diurnal trends, (c) contribution and (d), (e), (f) correlations for the PMF 3-factor solution for background periods including BBOA, OOA and ~~IEPOX-S~~isoprene-derived OA factors.

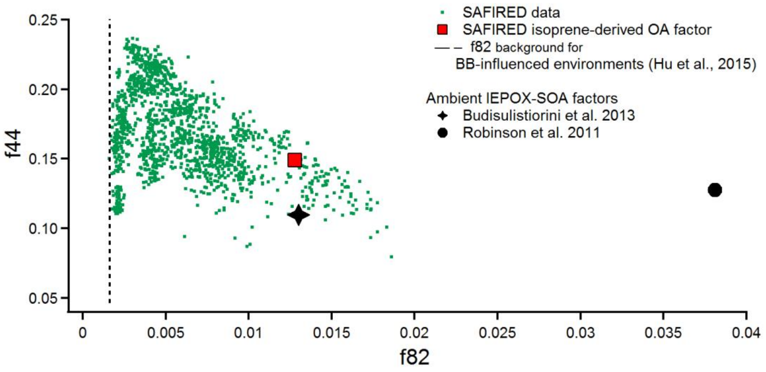

Figure 8~~10~~: f44 (CO_2^+) vs. f82 ($C_5H_6O^+$) for the SAFIRED data; The ~~IEPOX-S~~isoprene-derived OA factor from SAFIRED and two other ambient campaigns (Budisulistiorini et al., 2013;Robinson et al., 2011) are marked. Vertical black dashed line indicates proposed background f82 value in environments strongly influenced by BB (Hu et al., 2015).

S1 Data analysis

High organic loadings during heavy biomass burning (BB) episodes interfered with sulfate detection by the AMS in unit mass resolution (UMR), resulting in negative sulfate readings and scattered data points (Fig. S1a). Adjustments in Squirrel to the fragmentation table addressed the negative data points (Fig. S1b), however significant data dispersion still remained. High resolution (HR) fitting using PIKA improved correlation among different sulfate fragments (Fig. S1c).

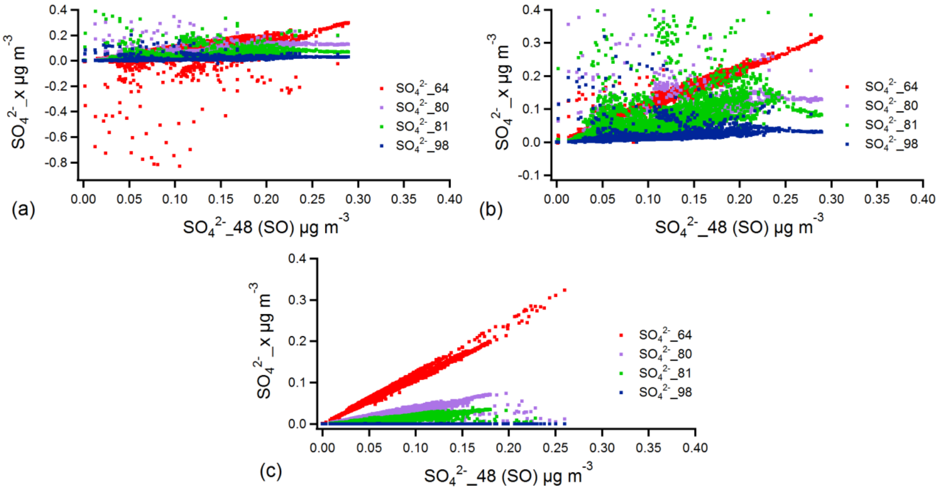

Figure S1: Sulfate fragments plots (a) before and (b) after Squirrel fragmentation table adjustments, and (c) after HR fitting in PIKA; SO_4^{2-}_x indicates sulfate fragments at m/z 64, 80, 81 and 96 plotted against the sulfate fragment at m/z 48.

PM1 soluble ions measured by ion suppressed chromatography and OM (converted from OC that was determined by the Thermal-Optical Carbon Analyser) were compared to the corresponding AMS UMR and HR data. A considerable improvement was observed in the HR analysis results for sulfate (Fig. S2b), with R changing from 0.4 to 0.8. HR fitting did not result in significant change for the other inorganic species or organics. However, improvement in the sulfate signals was significant and HR peak fitting data were used in further ~~data~~ analysis.

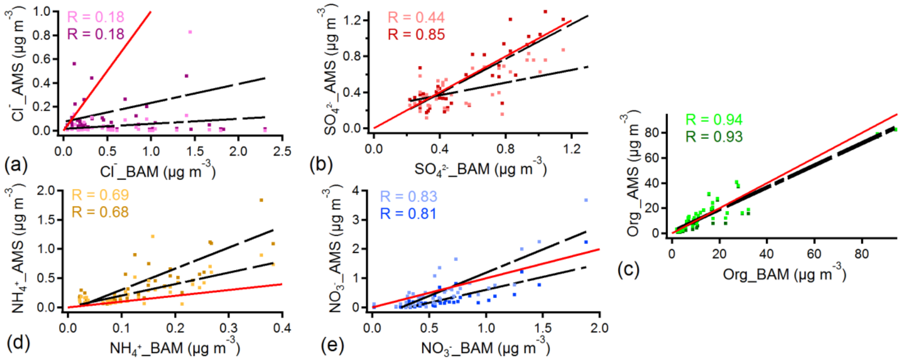

Figure S2: Correlation between BAM PM1 soluble ions and corresponding AMS species including (a) chloride, (b) sulfate, (c) organics, (d) ammonia and (e) nitrate; The lighter points and first number present correlation of BAM data with UMR AMS data, while the darker points and the second number illustrates the correlation for BAM and HR AMS data. Red line represents 1:1 line (absolute concentration between AMS and BAM). BAM organic mass (OM) was converted from OC mass using the conversion coefficient of 1.4. R refers to Pearson correlation coefficient. The AMS data were averaged to BAM 12h data.

Table S1: Correlation values between inorganic species and organics during the campaign, and close and distant periods separately. Inorganic species measured during the whole period (X), close BB periods (X(c)) and distant BB periods (X(d)) were compared to organics measured during the same time period (Org, Org(c), Org(d)).

	Cl^-	Cl^- (c)	Cl^- (d)	NH_4^+	NH_4^+ (c)	NH_4^+ (d)	NO_3^-	NO_3^- (c)	NO_3^- (d)	SO_4^{2-}	SO_4^{2-} (c)	SO_4^{2-} (d)
Org	0.65			0.92			0.75			0.55		
Org(c)		0.67			0.92			0.72			0.49	
Org(d)			0.47			0.73			0.77			0.48

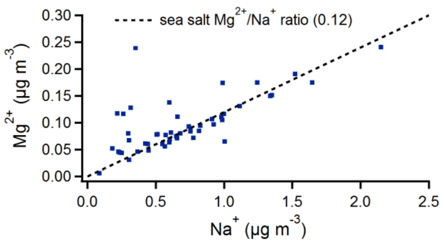

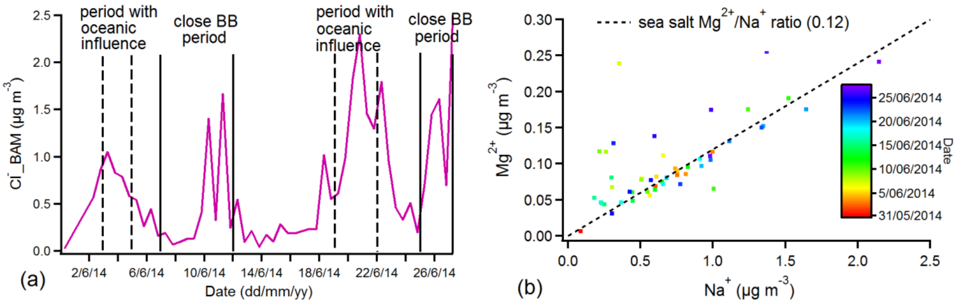

Figure S3: (a) Time series of chlorides collected on the filters (BAM). Dashed lines are defining the periods with oceanic influence, while solid lines illustrate close BB periods. (b) The f~~F~~ilter (BAM) data for magnesium (Mg^{2+}) and sodium (Na^{+}). Black line illustrates Mg^{2+}/Na^{+} ratio for the sea salt (0.12).

S2 Biomass burning aerosols and aging

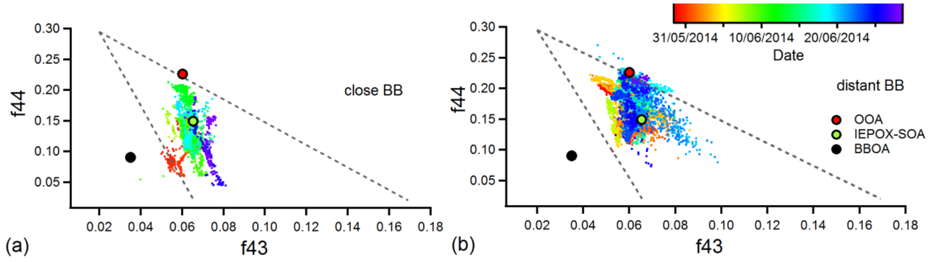

Figure S4: f44 vs. f43 coloured by date for (a) close and (b) distant BB periods. PMF-resolved factors are also indicated. The dashed lines represent boundaries for typical ambient aerosol as presented in Ng et al. (2010).

S2.1 Secondary organic aerosol (SOA) formation

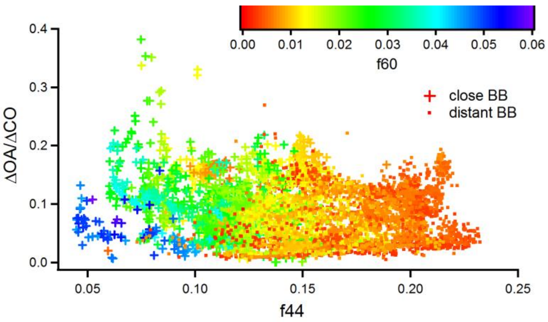

Figure S5: Change in ΔOA/ΔCO ratio with aging (represented by f44 values) for close (crosses) and distant (dots) fires coloured by f60.

S2.2 Biomass burning events

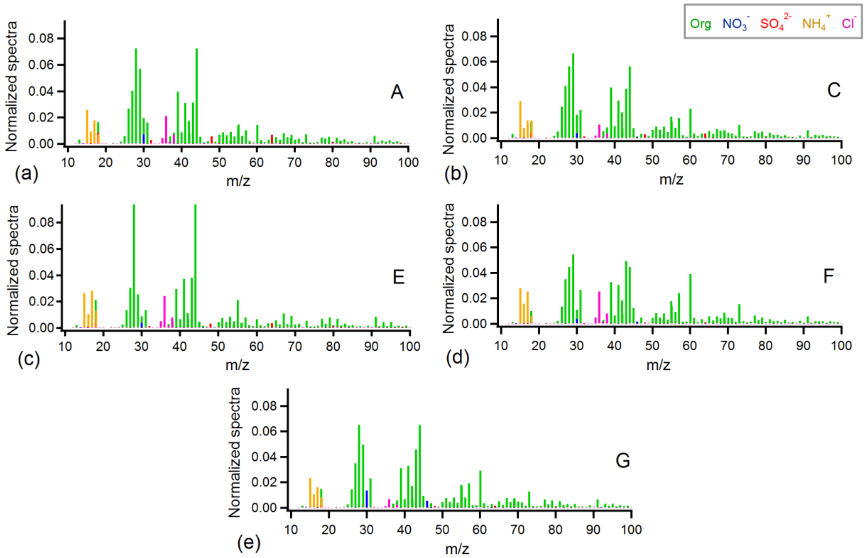
Org
NO_3^-
SO_4^{2-}
NH_4^+
Cl^-
Normalized spectra
0.00
0.02
0.04
0.06
0.08
10
20
30
40
50
60
70
80
90
100
m/z
A
C
E
F
G
(a)
(b)
(c)
(d)
(e)

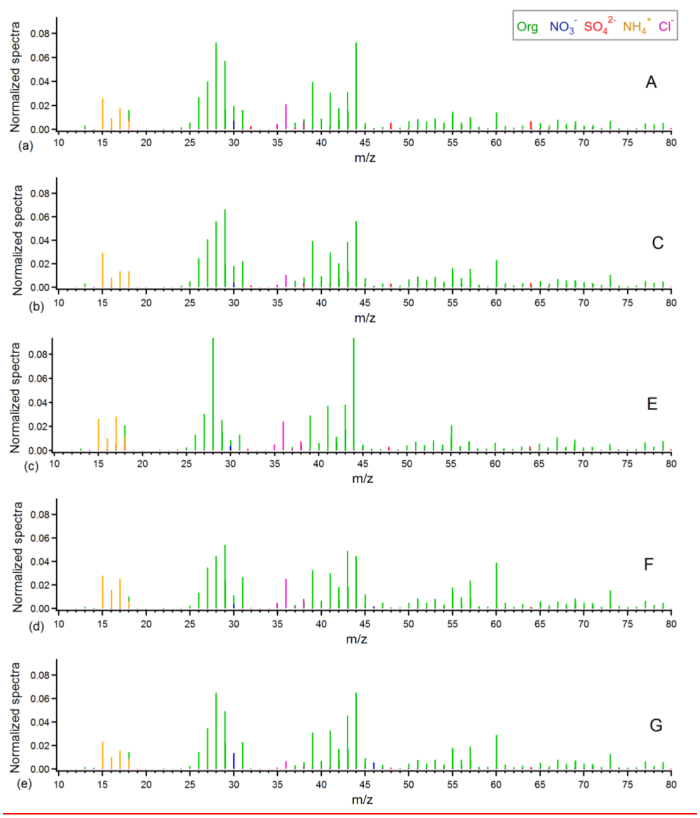

Figure S6: ~~Mass~~ Normalised mass spectra (sum=1) for selected BB events (A (30/05/14, 18:34-19:25), C (30/05/14, 23:41-31/05/14 00:59), E (09/06/14, 19:45-10/06/14 00:32), F (25/06/14, 12:28-16:59) and G (25/06/14, 21:40-26/06/14 03:59) are shown respectively.

~~Table S2: Selected BB event values for f44, f60, organic concentration, CO, MCE and AO~~$_3$~~/ACO ratio, along with measurement start and end time. ND refers to no data.~~

	~~Date (start/end)~~	~~f44±SD (range)~~	~~mean f60±SD (range)~~	~~mean Org±SD* (range)~~	~~mean CO±SD* (range)~~	~~MCE~~	~~AO~~$_3$~~/ACO~~
~~A~~	~~30/05/14 18:34-~~ ~~30/05/14 19:25~~	~~0.087±0.08~~ ~~(0.079-0.105)~~	~~0.016±0.002~~ ~~(0.010-0.018)~~	~~22.6±12.5~~ ~~(4.6-45.2)~~	~~185.9±95.5~~ ~~(90.2-370.1)~~	~~0.97±0.06~~	~~ND~~
~~C~~	~~30/05/14 23:41-~~ ~~31/05/14/ 00:59~~	~~0.066±0.005~~ ~~(0.060-0.079)~~	~~0.027±0.002~~ ~~(0.021-0.028)~~	~~75.5±40.0~~ ~~(13.7-131.2)~~	~~627.1±345.4~~ ~~(185.8-1181.6)~~	~~0.98±0.11~~	~~ND~~
~~E~~	~~09/06/14 19:45-~~ ~~10/06/14 00:32~~	~~0.078±0.013~~ ~~(0.062-0.093)~~	~~0.032±0.002~~ ~~(0.030-0.035)~~	~~175.9±105.0~~ ~~(87.3-331.8)~~	~~1558.5±965.5~~ ~~(671.6-3382.5)~~	~~0.91±0.05~~	~~0.024~~
~~F~~	~~25/06/14 12:28-~~ ~~25/06/14 16:59~~	~~0.134±0.031~~ ~~(0.073-0.178)~~	~~0.009±0.002~~ ~~(0.007-0.014)~~	~~13.2±14.5~~ ~~(2.4-70.8)~~	~~479.0±348.8~~ ~~(139.5-1642.7~~	~~0.93±0.04~~	~~0.134~~
~~G~~	~~25/06/14 21:40-~~ ~~26/06/14 03:59~~	~~0.062±0.017~~ ~~(0.045-0.098)~~	~~0.046±0.004~~ ~~(0.035-0.052)~~	~~144.6±104.7~~ ~~(25.8-347.7)~~	~~2744.6±2299.8~~ ~~(592.8-11275.7)~~	~~0.90±0.06~~	~~0.011~~

~~*unit is µg m^{-3}~~

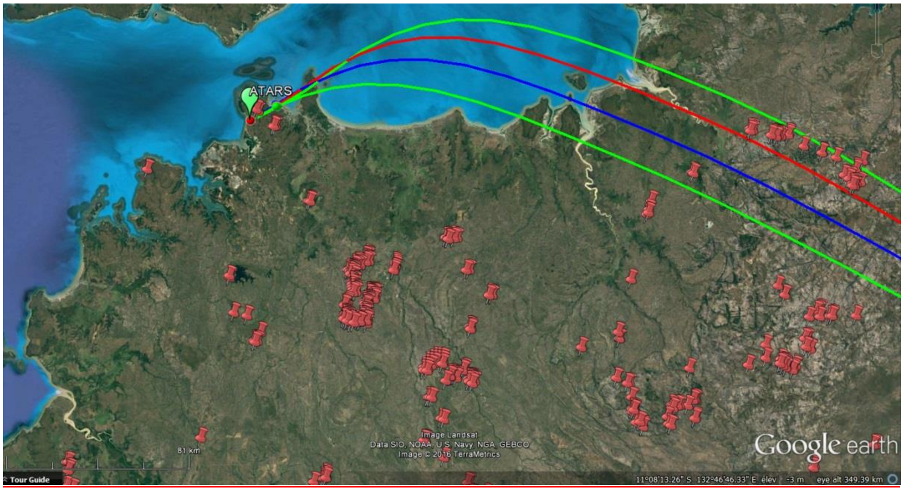

(a)

(b)

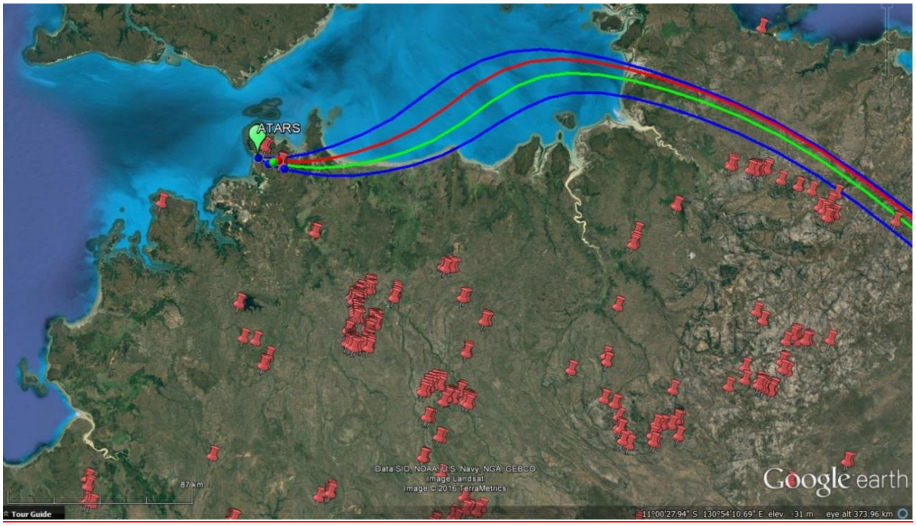
ATARS
87 km
Tour Guide
Data SIO, NOAA, U.S. Navy, NGA, GEBCO
Image Landsat
Image © 2016 TerraMetrics
Google earth
11°00'27.94" S 130°54'10.69" E elev -31 m eye alt 373.96 km

(c)

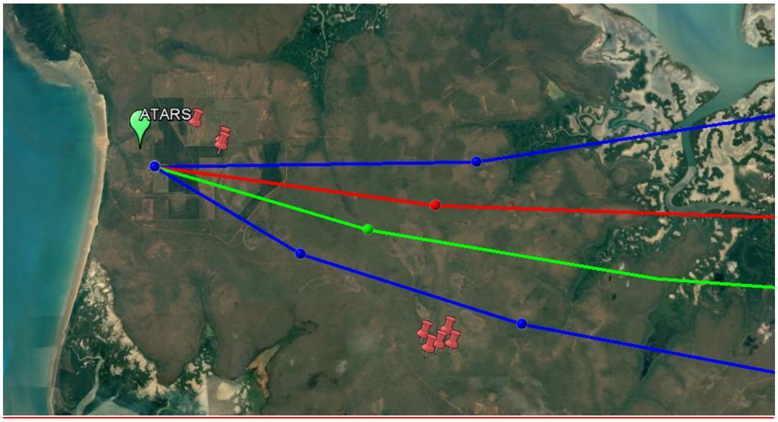
ATARS

(d)

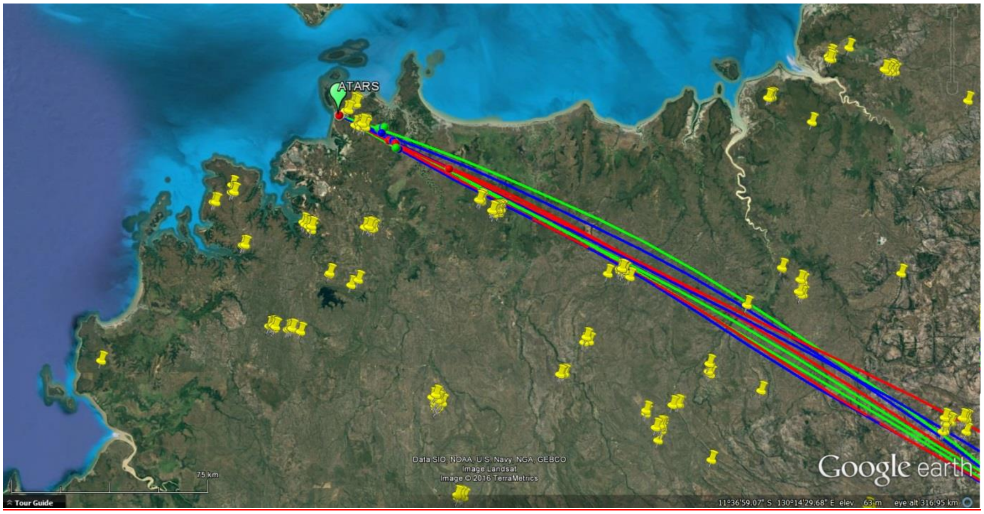
ATARS
75 km
Tour Guide
Data SIO, NOAA, U.S. Navy, NGA, GEBCO
Image Landsat
Image © 2016 TerraMetrics
Google earth
11°36'59.07" S 130°14'29.68" E elev 63 m eye alt 316.95 km

(e)

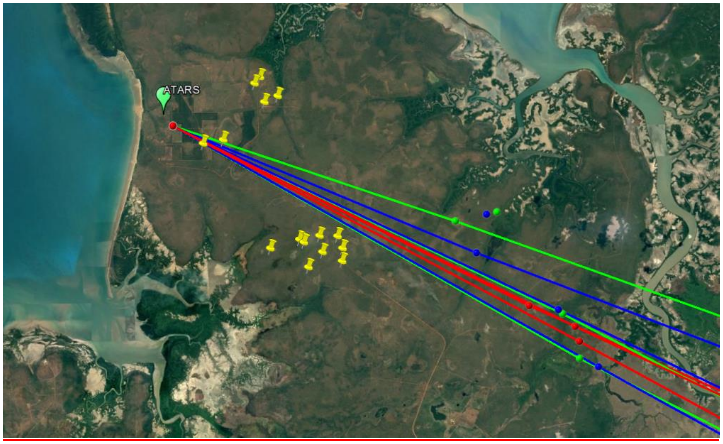
ATARS

(f)

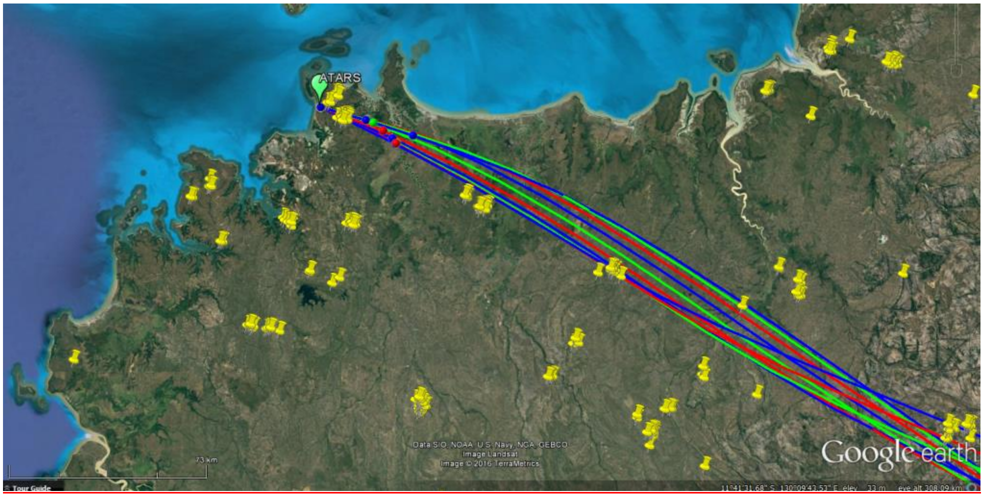
ATARS
Data SIO, NOAA, U.S. Navy, NGA, GEBCO
Image Landsat
Image © 2016 TerraMetrics
73 km
Tour Guide
Google earth
11°41'31.68" S 130°09'43.53" E elev 33 m eye alt 308.09 km

(g)

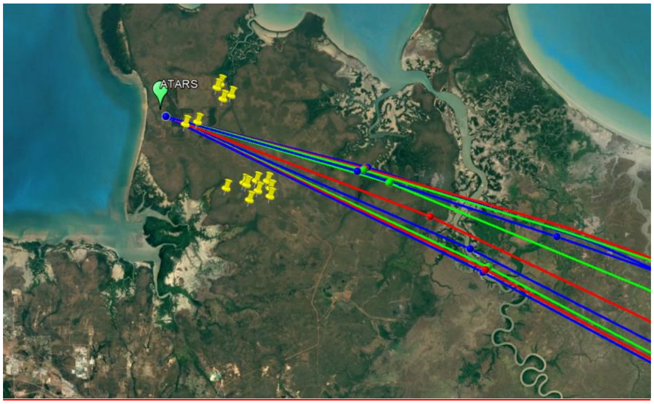
ATARS

(h)

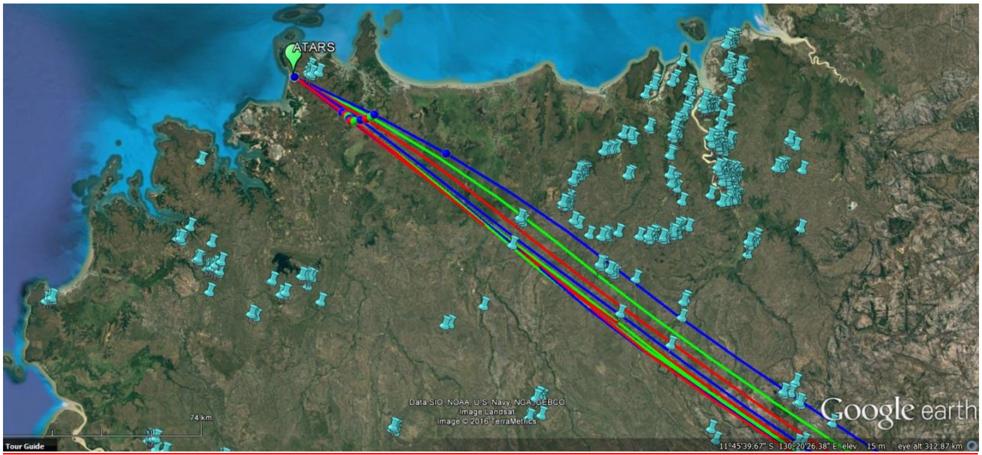

(i)

(j)

Figure S 7: Backtrajectories for event A, with close hot spots (a) and close and distant hot spots (b), for event C, with close hot spots (c) and close and distant hot spots (d), for event F, with close hot spots (e) and close and distant hot spots (f), for event G, with close hot spots (g) and close and distant hot spots (h) and for event E, with close hot spots (i) and close and distant hot spots (j). The backtrajectories were computed using the HYSPLIT (Hybrid Single-Particle Lagrangian Integrated Trajectory) model. All backtrajectories were run for 24h back in time. Different colours illustrate different starting time.

Formatted: Font: 10 pt, English (U.K.)

Formatted: Caption

Formatted: Font:

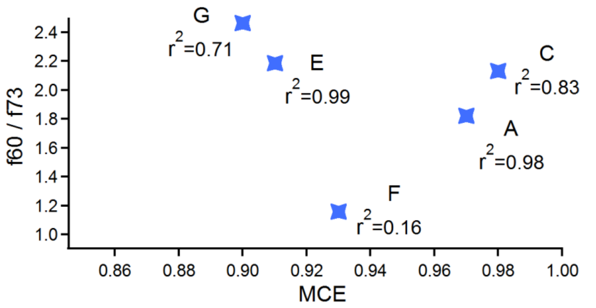

Figure S 8: f60/f73 ratio vs. modified combustion efficiency (MCE) for different events. Each point label indicates name of event and correlation value between f60 and f73.

S3 PMF performed on the whole dataset

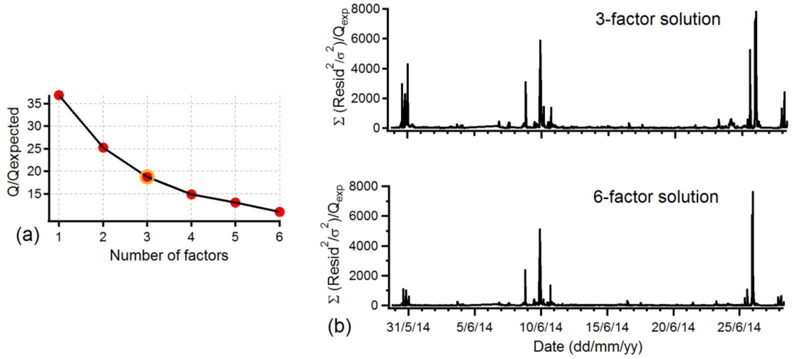

Figure S9~~7~~: (a) Q/Qexpected (Q refers to the sum of squared scaled residuals over the whole dataset) vs. number of factors, illustrating high error and residual values. (b) Time series of Q/Q expected contribution for 3 and 6-factor solutions where it is clear that higher number of factors does not make the residual structure during BB events significantly lower.

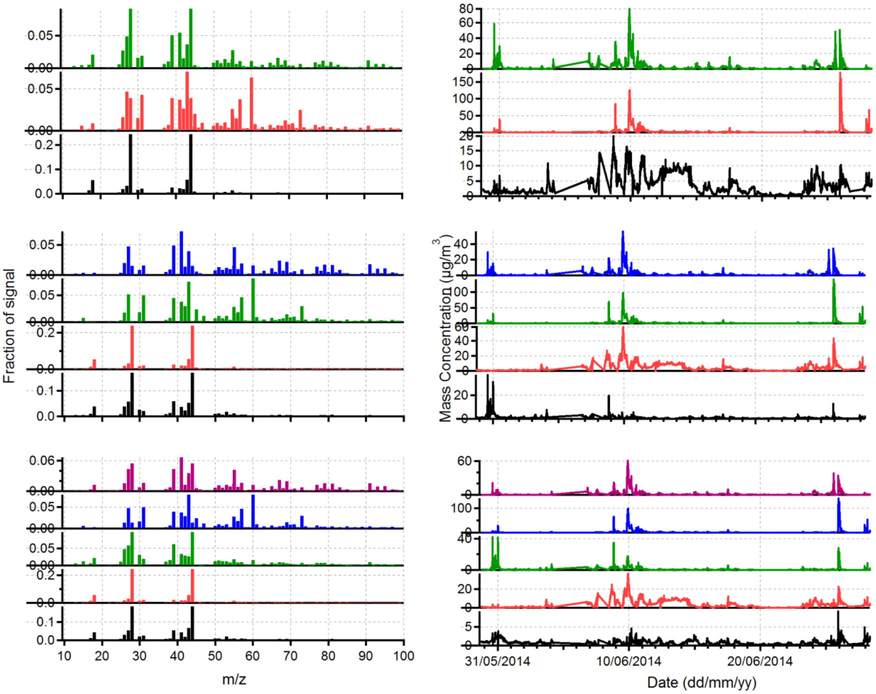

Figure S10~~8~~: Factor profiles and time series for 3, 4 and 5-factor solutions showing BBOA factor splitting, suggesting that plumes are apportioned to different PMF factors.

S4 PMF performed on the background dataset

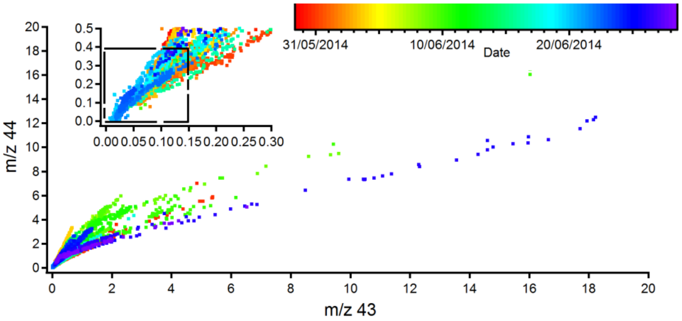

Figure S11~~9~~: m/z 44 vs. m/z 43 coloured by date for the whole dataset and for background periods (inset). Black dashed box in inset graph illustrates cut-offs of 0.15 for m/z 43 and 0.4 for m/z 44 chosen for background data.

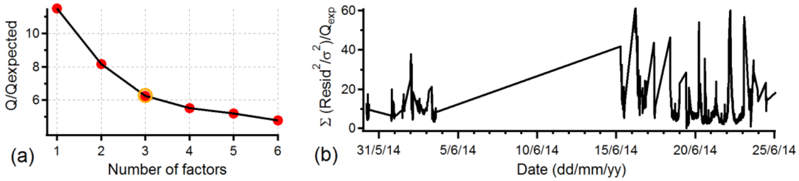

Figure S12~~10~~: (a) Q/Qexpected vs. number of factors and (b) time series of Q/Q expected contribution for the 3-factor solution illustrating significantly smaller residuals in the case of the background dataset, compared to the whole dataset.

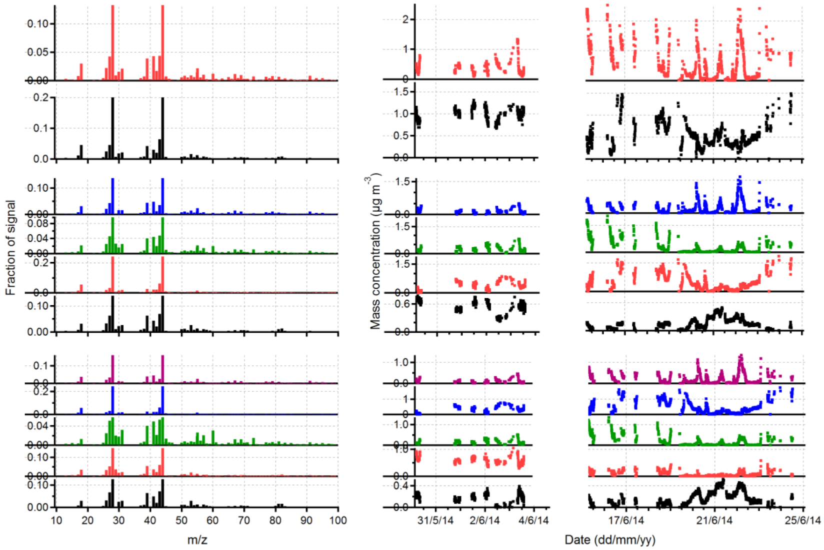

Figure S13~~11~~: Factor profiles and time series for 2, 4 and 5-factor solutions for the background dataset.

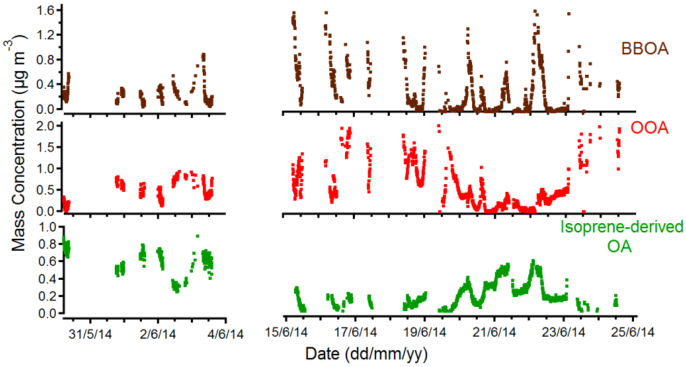

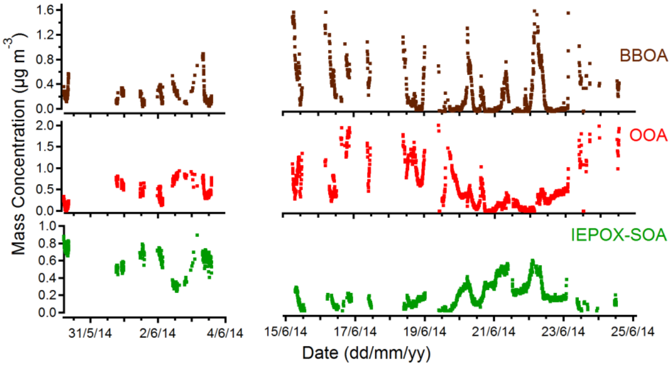

Figure S14~~12~~: Time series for 3-factor solution for the background dataset.

S4.1 Isoprene-derived ~~epoxydiols-related secondary~~ organic aerosol ~~(IEPOX-SOA)~~

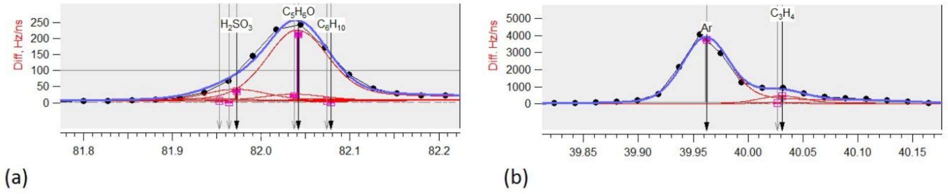

Figure S15~~13~~: HR peak fitting at (a) m/z 82 showing the dominance of the $C_5H_6O^+$ fragment and (b) m/z 40 demonstrating good m/z calibration.

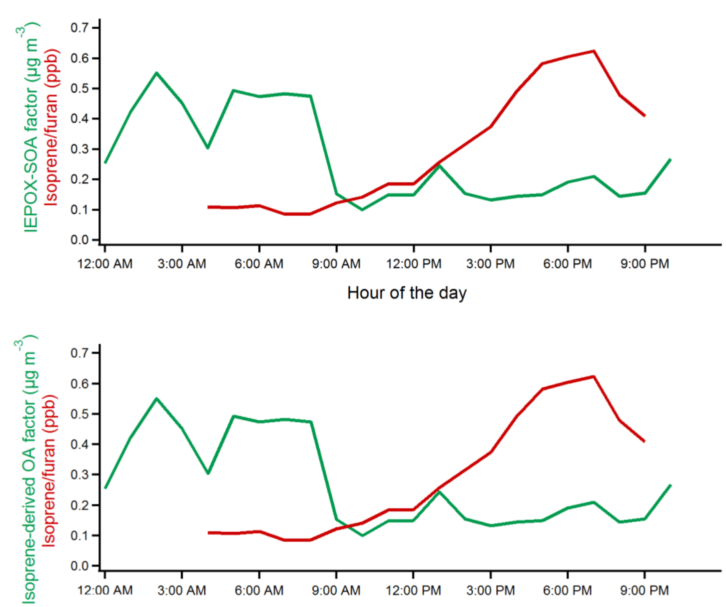

Figure S16~~14~~: Diurnal trend of PMF IEPOX-SOA factor and isoprene/furan concentration measured by PTR-MS.

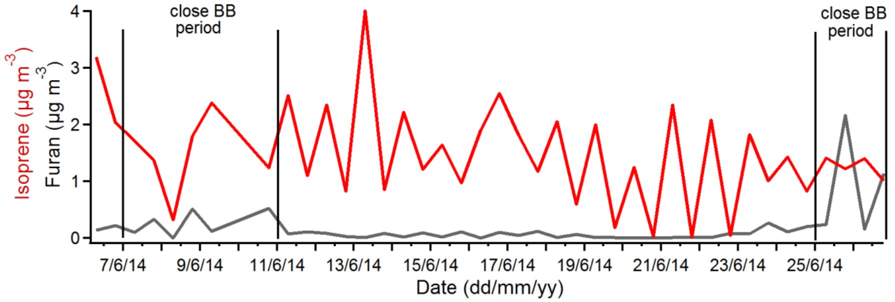

Figure S 17: Time series of isoprene and furan concentrations analysed by the gas chromatography-mass spectrometry. Black lines illustrate close BB periods.

Formatted: Normal

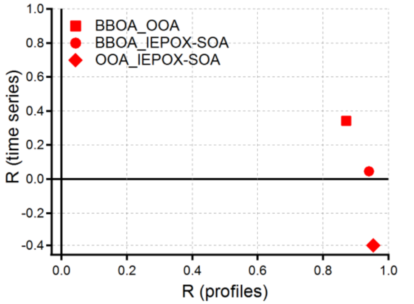

~~Figure S15: Time series and profile correlations between PMF factors.~~

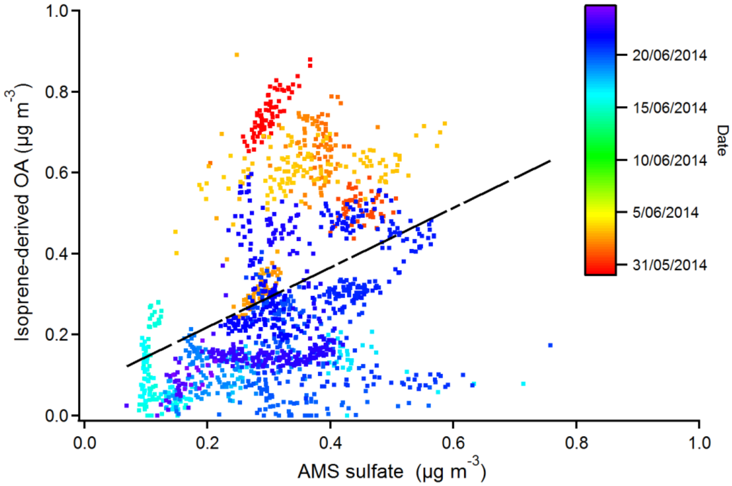

Figure S 18: Correlation between of AMS sulfate with the isoprene-derived OA PMF factor.

Formatted: Normal

~~Aging of~~Fresh and aged aerosols emitted from biomass burning in northern Australia

Andelija Milic[1], Marc D. Mallet[1], Luke T. Cravigan[1], Joel Alroe[1], Zoran D. Ristovski[1], Paul Selleck[2], Sarah J. Lawson[2], Jason Ward[2], Maximilien J. Desservettaz[3], Clare Paton-Walsh[3], Leah R. Williams[4], Melita D. Keywood[2], Branka Miljevic[1]

[1]International Laboratory for Air Quality and Health, Queensland University of Technology, Brisbane, Queensland, 4000, Australia
[2]CSIRO Oceans and Atmosphere, Aspendale, Victoria, 3195, Australia
[3]Centre for Atmospheric Chemistry, University of Wollongong, Wollongong, New South Wales, 2522, Australia
[4]Aerodyne Research, Inc., Billerica, Massachusetts, 01821, USA

Correspondence to: Branka Miljevic (b.miljevic@qut.edu.au)

Abstract. There is a lack of knowledge of how biomass burning aerosols in the tropics age, including those in the fire-prone Northern Territory in Australia. This paper reports chemical characterization ~~and aging~~ of fresh and aged aerosols monitored during the one month long SAFIRED (Savannah Fires in the Early Dry Season) field study, with an emphasis on chemical signature and aging of organic aerosols. The campaign took place in June 2014 during the early dry season when the surface measurement site, the Australian Tropical Atmospheric Research Station (ATARS), located in the Northern Territory, was heavily influenced by thousands of wild and prescribed bushfires. ATARS was equipped with a wide suite of instrumentation for gaseous and aerosol characterization. A compact time-of-flight aerosol mass spectrometer was deployed to monitor aerosol chemical composition. Approximately ~~80 % of submicron carbonaceous mass and~~ 90 % of submicron non-refractory mass was composed of organic material. Ozone enhancement in biomass burning plumes indicated increased air mass photochemistry and increased organic aerosol ~~and particle diameter~~ with the aging parameter (f44) suggested secondary organic aerosol formation. Diversity of biomass burning emissions was illustrated through variability in chemical signature (e.g. wide range in f44, from 0.06 to 0.18~~3~~) for five intense fire events. The background particulate loading was characterized using Positive Matrix Factorization (PMF). A PMF-resolved BBOA (biomass burning organic aerosol) factor comprised 24 % of the submicron non-refractory organic aerosol mass, confirming the significance of fire sources. A dominant PMF factor, OOA (oxygenated organic aerosol), made up 47 % of sampled aerosol fraction, illustrating the importance of aerosol aging in the Northern Territory. Biogenic ~~IEPOX SOA~~isoprene-derived organic aerosol factor ~~(isoprene epoxydiols-related secondary organic aerosol)~~ was the third significant fraction of the background aerosol (28 %).

Keywords. Biomass burning, savannah fires, organic aerosol, aerosol aging

1 Introduction

Tropical regions are some of the most fire-prone areas in the world (Crutzen and Andreae, 1990). As one of them, Northern Australia is observed to be a significant contributor to the global biomass burning (BB) budget (Russell-Smith et al., 2007). Fire emissions are made up of a variety of gaseous and particle-phase species, with the particle-phase consisting primarily of carbonaceous particles, including organic carbon (OC) and elemental ~~(black)~~ carbon (EC) (Bond et al., 2004;Hallquist et al., 2009;Formenti et al., 2003;Crutzen and Andreae, 1990). Open fires are the largest contributors to carbonaceous emissions; approximately 70 % and 40 % of the global annual emissions of OC and EC are formed in open fire events, respectively (Bond et al., 2004). Annually, 60-75 % of Australia's carbon emissions are attributed to BB emissions in tropical savannahs (Hurst et al., 1994). Organic carbon and EC affect the Earth's radiation balance by scattering and absorbing solar radiation, respectively (Penner et al., 1998;Haywood and Boucher, 2000). O'Brien and Mitchell (2003) suggested that atmospheric heating caused by UV absorbing carbonaceous aerosol, related to BB events in the Northern Territory during a dry season, can be significant and will likely have an influence on local (and possibly even global) climate. Carbonaceous species can also serve as condensation nuclei in cloud formation processes (Roberts et al., 2002). It is therefore important to build a comprehensive knowledge of BB emissions as they play a key role in the climate.

The characterization, processing and estimation of impact of BB emissions is a complex and challenging issue due to a wide range of burning material and combustion conditions (flaming/smouldering), as well as complex atmospheric physics and chemistry that BB plumes undergo once emitted (Reid et al., 2005;Weimer et al., 2008). Besides the characterization of fresh BB emissions, it is important to address their evolution in the atmosphere since aging of the BB emissions will alter their properties and thus how they interact with the climate system. Fresh BB emissions are those released directly from BB sources, while processed emissions refer to fresh particle or gaseous species transformed in the atmosphere through photochemical processing (aging). Organic aerosols (OA) can be differentiated as directly emitted primary organic aerosols (POA), aged primary organic aerosols (aged POA) and secondary organic aerosols (SOA) that form via condensation of lower volatility photo-oxidation products. A large fraction of BB-related POA is observed to be semivolatile (Grieshop et al., 2009) and can therefore change upon dilution with background air by evaporation of its content into the gas phase and be exposed to further transformations in the atmosphere.

Processing of BB emissions in the ambient atmosphere and in laboratory experiments is characterized by increases in the oxygenated fraction of OA (OOA) and degradation of species that are indicators of BB origin (Cubison et al., 2011;DeCarlo et al., 2008;Capes et al., 2008). However, there is no agreement on whether the aging of BB emissions leads to additional OA production. Some recent field and laboratory studies investigating the evolution of BB plumes have shown that OA mass increases with aging (DeCarlo et al., 2008;Yokelson et al., 2009;Heringa et al., 2011), while others have found no significant change or a decrease in OA with atmospheric processing (Akagi et al., 2012;Brito et al., 2014;Cubison et al., 2011;Capes et al., 2008). In addition to SOA formation, BB plumes promote the production of another important secondary pollutant, tropospheric ozone (Real et al., 2007). An excess of nitrogen oxides (NO_X), non-methane organic compounds (NMOCs) and carbon monoxide (CO) in the atmosphere from fire emissions promote additional pathways for ozone production (Parrington et al., 2013). Ozone enhancement in BB emissions has been extensively used as a proxy for air mass photochemical activity (Hobbs et al., 2003;Jaffe and Wigder, 2012;Yokelson et al., 2009;Akagi et al., 2012).

An extensive area of the Northern Territory of Australia is burned each year during the dry season (May-October) and the region is strongly affected by BB emissions. Considering that this area is a globally significant source of BB aerosol emissions (Mitchell et al., 2013), and that there have been a limited number of studies on aerosol characterization and aging, there is a need for more research. Information about the composition and degree of aging of OA that makes up the majority of emitted species generated in these fires will facilitate the estimate of the influence of BB in the Northern Territory. This will also contribute to a better understanding of fire emissions in tropical regions. In order to address these issues, the one month long SAFIRED (Savannah Fires in the Early Dry Season) field study was conducted at the Australian Tropical Atmospheric Research Station (ATARS) during a frequent burning period (late May/June 2014). This publication presents insights into fresh and aged aerosol~~s aging~~ emitted during the SAFIRED, while a detailed description of the campaign can be found in Mallet et al. (2016).

2 Measurement site and period

The Australian Tropical Atmospheric Research Station (ATARS) is situated on the Gunn Point peninsula in the Northern Territory (12°14'56.6" S, 131°02'40.8" E). The northern Australian tropical land mass is mostly covered by savannah biomes including scattered eucalypt trees, shrubs and grasses (Lacey et al., 1982). The sampling site can be described as rural background due to its remote location, with the closest populated centre, the city of Darwin, approximately 80 km south west of the ATARS. During the measurement period, the dominant sources of gaseous and aerosol species were wild and prescribed fires. Apart from planned burns, anthropogenic inputs to this region can be considered negligible (Bowman et al., 2007) and observations have highlighted the importance of biogenic sources for this area (Allen et al., 2008). The sampling site can also be impacted by marine aerosols (Bouya et al., 2010); however, fires are the major source of aerosols during the dry season.

The SAFIRED campaign was conducted from the 29th of May until the 30th of June, 2014 at the beginning of the dry season. The early dry period is characterized by natural fires as well as prescribed burns conducted to reduce the extent, intensity and frequency of wildfires in the late dry season (October-November). Thousands of fires in the Northern Territory during the campaign were detected by MODIS and VIIRS satellite sensors (Mallet et al., 2016). Fire emissions sources ranged from approximately two to up to hundreds of kilometres distant from the sampling station.

The early dry season was characterized by dry weather conditions (average relative humidity of 67 ~~%~~ ± 23 %) and warm days with an average daily and nightly temperatures of 27 ± 5 °C (up to 34 °C) and 19 ± 4 °C (with a minimum of 10 °C), respectively. There were no days of rainfall. Wind direction was predominantly southeast, suggesting that the sampled air masses had mainly passed over land affected by fire emissions ~~(Mallet et al., 2016)~~. However, on some days (e.g. between 3rd and 6th of June) in the afternoon hours northeast wind direction was dominant, directing the air masses from land to pass over the ocean before being detected at ATARS. Moreover, an oceanic influence was observed between 19th and 22nd of June (Mallet et al., 2016).

2.1 Instrumentation and method

Ground level characterization was performed using a wide range of instrumentation for gas- and particle-phase measurements. Detailed description of all instruments used in SAFIRED is given in Mallet et al. (2016). The focus of this study was on the aerosol chemical composition and aging using the instrumentation listed in the following paragraphs.

2.1.1 Compact Time-of-Flight Aerosol Mass Spectrometer (cToF-AMS)

A compact time-of-flight aerosol mass spectrometer (cToF-AMS or AMS, Aerodyne Research, Inc.) was deployed to monitor the chemical composition of non-refractory submicron (PM_1) aerosol. Monitored species were submicron particulate organic and inorganic compounds (sulfate, ammonium, nitrates and chlorides). Details about instrument operation during this campaign can be found in Mallet et al. (2016).

Formatted: Subscript

Unit mass resolution (UMR) and high resolution (HR) AMS data analysis was performed in Wavemetrics Igor Pro software (version 6.36) using the standard AMS Analysis Toolkits, Squirrel (Version 1.56D) and PIKA (Version 1.16), respectively. Data collection with a filter at the instrument inlet was used to correct for contributions from air in the fragmentation table (Aiken et al., 2008). Measured time-resolved gas-phase CO_2 concentrations were applied instead of the fragmentation table default value. The AMS collection efficiency was determined using the calculations provided within the ~~Squirrel~~ PIKA Toolkit. The ~~Squirrel~~ composition dependent collection efficiency panel enables an estimate of the collection efficiency based on ammonium nitrate, organic content, aerosol acidity and relative humidity (Middlebrook et al., 2012). The time-resolved collection efficiency (with an average value of 0.61) was applied to the entire dataset. High OA loadings during the campaign caused interferences in the detection of sulfate in the UMR analysis. Significant improvement was made in distinguishing sulfate fragments from organic fragments at the same m/z by performing HR peak fits in PIKA (Sect. S1 in supplementary information). Therefore, HR peak fitting data (PIKA) ~~results~~ were chosen for further ~~data~~ analysis.

AMS fragments analysis

~~Considering that OA~~Organic aerosols measured by the AMS encompassed aerosols that were processed in the atmosphere for different periods of time and included both POA~~, aged POA~~ and SOA. As such, a tool was needed to distinguish BB aerosol from other sources and fresh from processed BB aerosol. An extensively employed fragments analysis using the AMS-extracted parameters f43 (ions $C_3H_7^+$ and $C_2H_3O^+$), f44 (CO_2^+) and f60 ($C_2H_4O_2^+$) was applied here. The ratio of an integrated organic signal, e.g. m/z 43, to total organic signal is referred to as f43. Parameters f43 and f44 were used to estimate the level of OA processing, as they illustrate OA fractions of different aging degree. While f43 is mainly associated with hydrocarbon-like and semivolatile OA fractions (fragments $C_3H_7^+$ and $C_2H_3O^+$, respectively) (Jimenez et al., 2009;Lanz et al., 2007;Zhang et al., 2007;Heringa et al., 2011), f44 is assigned to highly oxygenated OA species (fragment CO_2^+) (Aiken et al., 2007;DeCarlo et al., 2010;Alfarra et al., 2007). The AMS parameter f60 and accompanying f73 ($C_3H_5O_2^+$) are widely used as BB emission signatures as they are directly related to levoglucosan-like species, which are a substantial fraction of organics emitted in pyrolysis of cellulose (Alfarra et al., 2007;Simoneit et al., 1999). The f60 can be applied as a valuable BB marker for time periods of up to one day (Cubison et al., 2011;Bougiatioti et al., 2014). Ambient aerosols characterized by an f60 value higher than 0.003 are considered to be influenced by BB emissions (Cubison et al., 2011). A graphical approach of comparing f44 vs. f60 introduced by Cubison et al. (2011) was used in this study to estimate the degree of aging of BB emissions.

Formatted: Subscript

Formatted: Subscript

Formatted: Subscript

Formatted: Superscript

Positive Matrix Factorization (PMF)

Positive Matrix Factorization (PMF) analysis (Paatero and Tapper, 1994) using the PMF evaluation tool (Ulbrich et al., 2009) was used in source apportionment of the AMS OA data. PMF splits the OA spectrum into different factors that can be related to specific sources. (Paatero, 1999;Paatero and Hopke, 2009). Various factors have been identified by PMF analysis of AMS OA data, with the most common being hydrocarbon-like OA (HOA) and oxygenated OA, that can sometimes be further apportioned to low-volatility oxygenated OA (LV-OOA) and semivolatile oxygenated OA (SV-OOA) (Ulbrich et al., 2009;Lanz et al., 2007;Ng et al., 2010;Jimenez et al., 2009). Other factors include environment specific factors such as biomass burning OA (BBOA) and cooking-related OA (COA). The solution space in this study was investigated by varying the number of factors and starting conditions (seeds, 0 to 50 in increments of 1) and applying rotational parameters (fpeaks, -1 to 1 in increments of 0.1).

2.1.2 Beta plus particle measurement system (BAM)

PM_1 mass was measured and collected onto pre baked (600 °C) quartz 47 mm filters (Pall Tissuquatz p/n 7202) using a Beta plus particle measurement system (BAM, Teledyne API Model 602), every 12 hours. All of the species measured on BAM filters were blank corrected. Particles collected on filters were further analysed for anhydrous sugars, including levoglucosan, by high performance anion exchange chromatography with pulsed amperometric detection and for water soluble ions including potassium (K^+), nitrates (NO_3^-), sulfates (SO_4^{2-}), ammonium (NH_4^+) and chlorides (Cl^-) by ion suppressed chromatography. Levoglucosan and non-sea salt K^+ were used as metrics for BB emissions. BAM PM_1 filters were analysed by a Thermal-Optical Carbon Analyser (DRI Model 2001A) using the IMPROVE-A temperature protocol

Formatted: Subscript

Formatted: Subscript

(Chow et al., 2007) to determine contributions of EC and OC. Water soluble inorganic ions and OC were also used for comparison with AMS-resolved species.

2.1.3 Fourier Transform Infrared Spectrometer (FTIR)

The Spectronus trace gas and isotope Fourier Transform Infrared Spectrometer (FTIR) analyser, built by the Centre of Atmospheric Chemistry at the University of Wollongong, was deployed to monitor gaseous species including carbon monoxide (CO) and carbon dioxide (CO_2) (Griffith et al., 2012;Griffith, 1996). Details about the instrument operation can be found elsewhere (Desservettaz et al., 2016). In order to include dilution effects, OA and ozone data are presented relative to CO. CO is an important BB product that can remain in the atmosphere for a relatively long time period (one to two months depending on the environment) without observed decay or interactions with oxidative agents (Wang and Prinn, 1999;DeCarlo et al., 2010;Edwards et al., 2006). CO has therefore been employed as a long-lived, conservative tracer in many studies (DeCarlo et al., 2010;Kleinman et al., 2008;Brito et al., 2014;Yokelson et al., 2009;Akagi et al., 2012). Gas-phase CO_2 data, as previously mentioned, were applied in the AMS fragmentation table adjustment. CO and CO_2 were also used in modified combustion efficiency (MCE) calculations, with details presented in Desservettaz et al. (2016). MCE refers to the ratio of ΔCO_2 (measured value relative to background value) to the sum of ΔCO_2 and ΔCO (Ward and Radke, 1993). The MCE parameter was used to distinguish smouldering (usually lower than 0.9) from flaming (usually higher than 0.9) fires. The MCE value can also indicate the burning material.

2.1.4 Scanning Mobility Particle Sizer (SMPS)

Aerosol size and number concentration were monitored by a Scanning Mobility Particle Sizer (SMPS, a TSI 3071 long-column electrostatic classifier coupled to a TSI 3772 Condensation Particle Counter). The SMPS measured the particle size distribution from 14 nm up to 670 nm every 5 minutes. Changes in the size distribution due to aging were investigated.

2.1.5 Proton Transfer Reaction-Mass Spectrometer (PTR-MS)

A high sensitivity Proton Transfer Reaction-Mass Spectrometer (PTR-MS, Ionicon Analytik) with a quadrupole mass spectrometer and an H_3O^+ ion source was employed to measure non-methane organic compounds (NMOCs) that include non-methane hydrocarbons and oxygenated volatile organic compounds. These species are important in the formation of SOA and ozone. Isoprene and monoterpenes make up a dominant fraction of global gas-phase NMOCs, contributing significantly to the production of SOA (Guenther et al., 2012). Tropical regions can contribute up to 80 % of global annual isoprene emissions due to warm weather conditions (Guenther, 2006). He et al. (2000) investigated NMOCs emitted from eucalyptus trees, which make up 95 % of all tree species in Australia. Isoprene accounts for 64-100 % of NMOCs emitted from different eucalyptus species. The isoprene/furan fraction (signal at m/z 69) of measured NMOCs is used here in the analysis of isoprene-~~related~~ derived ~~S~~SOA. Other studies suggest that the contribution of isoprene to m/z 69 prevails in non-

BB periods while the furan contribution is more significant in BB plumes (Warneke et al., 2011). In order to distinguish furan and isoprene contribution over the sampling period, a gas chromatography-mass spectrometry method was used.

2.1.6 Ozone analyser

Ozone concentration was monitored by an Ultraviolet Photometric Ozone analyser (Model 49i, Thermo Scientific). Ozone enhancement in BB emissions has been used as a proxy for air mass photochemical activity.

2.1.7 Fire data

Information about the location and duration of fires was obtained from the Sentinel Hotspots system. Hotspots data used for this campaign were derived from the MODIS (Moderate Resolution Imaging Spectroradiometer) sensor (Terra and Aqua satellites) and VIIRS (Visible Infrared Imaging Radiometer Suite) sensor (Suomi NPP satellites). Only the hotspots with confidence level higher than 50 % were considered in the analysis. Hotspots are detected by satellite once a day which limited the fire analysis to events that occurred between approximately 11 am and 3 pm. During the SAFIRED campaign thousands of fires were detected in the Northern Territory. Distance-resolved fire frequencies are presented in Mallet et al. (2016). Moreover intense fires characterized by plumes detected without considerable influence from other fire sources, were extracted from the whole dataset (Desservettaz et al., 2016). Five events that were categorised as single, intense fires are analysed here. Air mass backtrajectories were computed using the NOAA/ARL HYSPLIT (Hybrid Single-Particle Lagrangian Integrated Trajectory) model.

Formatted: Font color: Black

3. Results and Discussion

3.1 Aerosol chemical characterization

PM_1 ambient aerosols sampled during the SAFIRED campaign were dominated by an organic fraction. Organic carbon made up ~~83~~ 72 % and EC ~~17~~ 15 % of the measured ~~carbonaceous~~ PM_1 ~~material~~ on the BAM filters (Fig. 1a). Data from the AMS (Fig. 1b and 1c), indicate that organics made up approximately 90 % of submicron non-refractory mass with an average concentration of 11.1 µg m^{-3} and concentrations of up to 350 µg m^{-3} during intense and nearby BB events. The organic mass (OM) sampled by the BAM was converted from OC using the conversion factor of 1.4, which was determined in PIKA. This value is within the span of OM/OC conversion factors for the biomass burning aerosol suggested by Reid et al. (2005). The BAM OM and mass concentration of organics sampled by the AMS are in good agreement (R value of 0.94), with slightly higher concentrations measured by the BAM (Fig. S2c) probably due to the lower collection efficiency of the AMS above 700 nm. Organic mass has been observed to be the dominant fraction of PM_1 ambient aerosols during the early dry season in the Northern Territory (Carr et al., 2005). The organic fraction was also dominant in other studies strongly impacted by BB emissions (Brito et al., 2014;Capes et al., 2008). In this study, the remaining submicron non-refractory mass was made up of

Formatted: Subscript

Formatted: Subscript

Formatted: Subscript

inorganics including sulfates (4.2 %), ammonium (2.8 %), nitrates (1.5 %) and chlorides (1.3 %), with average concentrations of 0.51 ± 0.32 µg m^{-3}, 0.35 ± 0.68 µg m^{-3}, 0.19 ± 0.45 µg m^{-3} and 0.17 ± 1.28 µg m^{-3}, respectively.

The sampling site was constantly impacted by fire emissions with periods of heavy BBs characterized by ~~prominent~~ high aerosol and gas phase ~~signals~~concentrations, for instance CO reaching up to ~10^4 ppb and organics up to 350 µg m^{-3} (Fig. 2). The most intense BB episodes were on the 30th of May, between the 7th and 11th of June, and on the 25th and 26th of June (Fig. 1c) (Mallet et al., 2016). During intense fire periods, organics, CO and particle number concentration showed correlated increases (Fig. 2). Moreover, looking at Sentinel Hot spots during these periods, hot spots were detected within 20 km from the ATARS. Based on this, the dataset was separated into periods of “close BB” (corresponding to high organics, CO and particle number concentration signals and close events (< 20 km)) and “distant BB” (corresponding to less intense organics, CO and particle number concentration signals and distant events (> 20 km)). It is important to emphasize that all periods during the measurement that have not been included in close BB periods have been assigned to distant BB periods, as ATARS was constantly influenced by BBs. The selection does not mean that emissions from distant fires were not present during the close BB periods but that the influence of fires near the measurement station during these periods was dominant. Nine intense BB events were ~~selected~~ identified from close BB periods as single source emissions (Dessservettaz et al., 2016).~~ and f~~Five of ~~them~~ the nine events (Fig. 2) were analysed here (Sect. 3.2.4), due to the instrument not sampling during the remaining events. Most of the ~~fires~~ events occurred in the afternoon/night time (Table ~~S2~~1). ~~During intense fire periods, organics, CO and particle number concentration showed large and correlated increases (Fig. 2). Based on this, the dataset was separated into periods of “close BB” (corresponding to prominent signals and close events) and “distant BB” (corresponding to less prominent signals and distant events). The selection does not mean that emissions from distant fires were not present during the close BB periods but that the influence of fires near the measurement station during these periods was dominant.~~

Coupled with elevated organic concentrations, AMS-measured inorganics also increased during close BB periods (Fig. 1c). A high AMS signals for all monitored species corresponded to close BB periods. During SAFIRED, high correlation was observed between organics and ammonium species (R of 0.92), with better agreement during the close BB (R of 0.92) than in the distant BB periods (R of 0.73) (Table S1), suggesting that these ammonium species originated from fire emissions. Moreover, plume emissions included high chloride concentrations (up to approximately 50 µg m^{-3} during close BB periods). Increased chloride concentration during the close BB periods was also indicated by the BAM data (Fig S3a). This is not surprising since the dominant fine particle inorganic fraction emitted in flaming savannah fires has been shown to be composed of KCl (potassium chloride) and NH_4Cl (ammonium chloride) compounds and/or their mixtures (Liu et al., 2000). There was a better correlation between organics and chlorides for close BB periods (R of 0.67), than for distant BB periods (R of 0.47). This can be explained by the depletion of chloride with transport and aging of BB plumes (Li et al., 2003;Li et al., 2010;Liu et al., 2000). Correlations for nitrate and sulfate with organics show similar patterns in this work regardless of the BB emissions influence (R of 0.72 and 0.77 for nitrate and R of 0.49 and 0.48 for sulfate for close and distant periods, respectively). AMS inorganic species were compared to soluble ions concentrations measured on the filter samples collected using the BAM. There was a strong correlation between all compared species (R values of 0.85, 0.68 and 0.81 for sulfates, ammonium and nitrate, respectively) except in the case of chloride (R of 0.18) (Fig. S2). Mg^{2+}/Na^+ ratio values for the filters collected during the high oceanic influence (between 3rd and 6th and 19th and 22nd of June) ~~most of the filters~~ were close to the sea salt Mg^{2+}/Na^+ ratio of 0.12 (Fig. S3b). At the same time low terrestrial fetch (low radon concentration) was observed (Mallet et al., 2016). Moreover, the chlorides collected on filters were prominent during the period of oceanic influence (Fig. S3a).This suggests that a significant portion of chlorides detected on the BAM filters ~~could~~ was ~~be~~ of a sea salt origin, which is refractory and therefore not well measured by the AMS, thereby explaining the poor chloride correlation.

3.2 Biomass burning aerosols and aging

In general, BB-related particulate matter can be easily distinguished from other aerosol sources by chemical composition. Levoglucosan is a common molecular tracer of plume emissions (Simoneit et al., 1999) and has been extensively used as a BB chemical signature (Jordan et al., 2006;Simoneit, 2002). Moreover, the AMS organic signal intensity ~~at m/z 60 (~~fragment $C_2H_4O_2^+$) (Org 60) is directly correlated to the concentration of levoglucosan-like species (Alfarra et al., 2007;Simoneit et al., 1999) and can therefore be applied as a valuable BB marker. Fire sources also contribute to high potassium levels (Li et al., 2003). Figure 3 illustrates the time series of Org 60 obtained from the AMS and levoglucosan and soluble non-sea salt potassium sampled by the BAM. Prominent signals of these BB tracers were present during the observed close BB periods, which confirm that the fire source of the detected aerosols is BB.

In order to discriminate BB aerosol from other sources and estimate the degree of BB aerosol aging (processing), a graphical method introduced by Cubison et al. (2011) has been applied here (Fig. 4). The majority of data points (94 % of the dataset) had f60 values above the background limit of 0.003, indicated with a vertical dashed lines in Fig. 4. Thus, the detected OA during SAFIRED can be attributed mostly to BB aerosol.

Chemical aging of BB-related OA typically leads to f60 depletion and increased f44 (Grieshop et al., 2009;Cubison et al., 2011;Ortega et al., 2013;Ng et al., 2010;Zhao et al., 2014;Capes et al., 2008;Jolleys et al., 2015). In general, this trend was observed in this study for distant fires, with the data trending towards the top left corner of the diagram (Fig. 4b). Apart from aerosol processing, changes in f44 and f60 can be attributed to burning conditions and/or materials. The variability observed in f44 vs. f60 for close BB events (Fig. 4a) ~~probably~~ can reflect BB plumes generated during different burning conditions ~~rather than~~ but also different atmospheric processing of BB masses. On average distant BB plumes were characterized by lower fire tracer f60 compared to the close BB emissions. Furthermore, distant fire plumes indicated a higher portion of oxygenated compounds (i.e., higher f44 values), relative to close plumes. The maximum f44 value ranged between 0.20 and 0.23 in this study, which agrees well with previously observed f44 values for oxidized BB emissions in ambient measurements (Cubison et al., 2011). The f44 parameter increased to values characteristic of LV-OOA in the distant BB and yet f60 values were substantially above the background value of 0.003. This confirms that levoglucosan-like species carried by the BB plume did not degrade to background levels even as oxidized species were formed. Thus, f60 is a reasonable marker of distant BB in this study.

All data fall into the f44 vs. f43 triangular plot range for ambient data, introduced by Ng et al. (2010) (Fig. S4). Ng et al. (2010) observed that typical ambient OA data slopes from the bottom right to the top left of the f44 vs. f43 plot, and that this trend can be attributed to photochemical processing of ambient air masses. A similar pattern was observed in this study for distant ~~fires~~ periods (Fig. S4b). A wide range in f44 can be attributed to different processed (aged) BB-related OA, but different burning material and/or conditions cannot be excluded. The observed evolution trend in f44 vs f43 for distant fires can be also influenced by mixing between the plumes. In contrast the f43 values for close BB (Fig. S4a) are located in a narrow f43 range from 0.05 to 0.08 and do not change considerably with increasing f44. This ~~confirms~~ can be a result of ~~that there was no~~ insignificant atmospheric processing in case of close fires. The wide range in f44 can be attributed to difference in burning conditions for close BB. One more factor that can influence f44 vs f60 trend for both close and distant fire is dilution effect.

Formatted: Space After: 0 pt

Formatted: Font: English (U.K.)

3.2.1 Ozone formation

The emissions from BB sources promote ozone production in the troposphere by increasing the concentrations of key ozone-forming precursors (NMOCs, NO_X and CO). Air mass photochemical activity can be estimated through the observation of changes in ozone concentration with aging, particularly the change in the $\Delta O_3/\Delta CO$ ratio, where ΔCO and ΔO_3 refer to enhancements above background concentrations. ΔCO accounts for dilution, as it is a relatively long lived atmospheric species. The minimum CO value of 80 ppb measured during June at the ATARS site was used as the background concentration level. Similarly a minimum ozone concentration of 10 ppb was considered to be the background level in these calculations. On average, the $\Delta O_3/\Delta CO$ ratio increases with f44 and decreases with f60, indicating increased photochemical processing of OA in plumes with atmospheric aging and ozone production (Fig. 4c and Fig. 4d~~5~~).

$\Delta O_3/\Delta CO$ values vary between -0.1 and 0.9 which is within the observed range in other studies (Jaffe and Wigder, 2012). A negative ratio may indicate fresh BB emissions where ozone was removed by atmospheric reaction with nitric oxide (NO) emitted in high amounts from fire sources, as suggested by Yokelson et al. (2003). Close fire emissions were characterized by significantly lower ozone enrichments (average $\Delta O_3/\Delta CO$ of 0.15) compared to plumes detected from the distant BB emissions (average $\Delta O_3/\Delta CO$ of 0.31) which represent higher photochemical activity within more processed air masses. These values agree with observed $\Delta O_3/\Delta CO$ ratio values for plumes aged for less than 1-2 days (average $\Delta O_3/\Delta CO$ of 0.14) and for 2-5 days (average $\Delta O_3/\Delta CO$ of 0.35) in tropical/subtropical regions (Jaffe and Wigder, 2012). The $\Delta O_3/\Delta CO$ enrichments for close BB period indicate that aging of close emissions cannot be excluded. These significant ozone enrichments in BB plumes illustrate high NO_X and NMOC loadings emitted from fire sources and photochemically active air masses.

3.2.2 Secondary organic aerosol (SOA) formation

Since increased photochemical activity was identified in BB air masses, the change in ΔOA/ΔCO ratio was investigated in order to determine whether additional OA was produced in the ~~detected~~ BB plumes (Fig. ~~6~~4e and Fig. 4f). The lowest OA concentration observed during the campaign of 0.09 µg m^{-3} was taken as a background value in these calculations. Figures~~ 6~~ show~~s~~ no particular trend in ΔOA/ΔCO ratio with f44. The ΔOA/ΔCO ratio also remains quite constant despite increases in f44 (Fig. S5). ~~In the case of close fires, different ΔOA/ΔCO ratios can be attributed to different burning conditions (Fig. 6a).~~ In addition, diurnal patterns of the f44, $\Delta O_3/\Delta CO$ and ΔOA/ΔCO ratios were investigated, for close and distant BB periods separately (Fig. 5a and Fig. 5b, respectively). The parameter f44 was used to indicate the level of oxygenation that can be caused by the photochemical changes and $\Delta O_3/\Delta CO$ as a parameter of photochemical activity. It must be noted that simply examining ΔOA/ΔCO vs time of day is a simplified approach which does not fully take into account the total photochemical history of the air mass. ~~The emissions from close fires did not spend enough time in the atmosphere to be significantly processed and subject to SOA formation, and therefore only diurnal trends for distant fires were considered (Fig. 7).~~ There was an increase in ΔOA/ΔCO ratio with an increase in f44 and $\Delta O_3/\Delta CO$ in the late morning and early afternoon for close and for distant BB periods. This is likely due to condensation of organics onto pre-existing particles.~~,~~ ~~and then a d~~The decrease in the ΔOA/ΔCO ratio later in the afternoon~~, which~~ could indicate OA loss due to fragmentation and subsequent evaporation from the particulate phase. As suggested by Kroll et al. (2009), OA loss can reflect dominance of the fragmentation pathways in the formation of more oxidized OA. Therefore it ~~can be concluded~~is suggested that increased photochemical activity of BB-influenced air masses, illustrated by increase in $\Delta O_3/\Delta CO$ and likely due to oxygenation of OA (f44 increase), was accompanied by an increase in ΔOA/ΔCO ratio ~~and probably~~, indicating SOA formation Moreover, the ~~but also with~~ decrease in ΔOA/ΔCO ratio ~~probably due to~~later in the day can be a result of fragmentation and subsequent evaporation.

Formatted: Subscript

3.2.3 f44-resolved size distribution

Atmospheric aging of plume particles increases particle diameter due to gas to particle transfer of organic and inorganic gaseous species (Martins et al., 1998). In order to estimate whether the aging of BB masses during SAFIRED influenced particle size, average SMPS size distributions and AMS size distributions for organics, both categorised based on different f44 ranges, ~~for distant BB periods~~ were examined (Fig. ~~8~~6). It is important to emphasise that SMPS uses electrical mobility diameter, while AMS uses vacuum aerodynamic diameter. The close and distant BB periods were analysed separately. The f44 values were classified into four groups that represent different aging stages (0.05<f44<0.1, 0.1<f44<0.15, 0.15<f44<0.2, 0.2<f44<0.25). The first f44 bin (0.05<f44<0.1) was not considered in case of the distant BB periods, as only a few data points were in this range (Fig. 4). The same was done for the highest f44 bin (0.2<f44<0.25) for close BB periods. According to SMPS data, the average particle mode varied between 101 – 113 nm and 104 – 106 nm for close and distant BB periods, respectively. The average mode for organics showed larger sizes and varied between 259 – 293 nm and 293 - 305 nm for close and distant BB periods, respectively. Increased f44 was accompanied by a reduction in SMPS particle size for close plumes, going from 113 nm (0.05<f44<0.1) to 101 nm (0.1<f44<0.15). The same trend was observed for the organic aerosols. Considering both AMS and SMPS data for distant fires, ~~There~~ there was ~~a~~ no considerable ~~increase~~ change in ~~particle~~ diameter with aging from less aged BB plumes ~~(83 nm for 0.05<f44<0.1)~~ to more aged BB air masses. The particle modes show only slight differences between different f44 bins. This is not consistent with the observed increase in OA for distant fires. ~~(106 nm for 0.1<f44<0.15). This is consistent with the observed SOA formation. The shift of particle size towards larger particles may be due to condensation of organics onto pre-existing particles.~~ Changes in size distribution will be discussed further in the Sect. 3.2.4 where results related to specific BB events are presented.

3.2.4 Biomass burning events

~~Nine intense BB events were selected as single source emissions (Desservettaz et al., 2016), f~~Five single source BB events ~~of which are~~ were analysed here (Fig. 2). These episodes ~~correspond to~~were within previously defined close BB ~~emissions~~periods. Mass spectra for selected ~~plumes~~ signatures and their time of detection are given in Fig. S6. The spectral signature is similar for these ~~plumes~~events, with prominent BB-related signals at m/z 60, 73, 29 and 39. However, a significant variation in m/z fragments, especially in m/z ~~43 and~~ 44, can be observed. ~~As these plumes were mostly related to sources close to the sampling site (within 2 to 10 km), differences in m/z 44 and 43 can mostly be related to different burning conditions.~~ More detail about these BB events is given in Table ~~S2~~ 1 and discussed in the following paragraphs. Different factors were considered including f44, time of day, $\Delta O_3/\Delta CO$, f60, f60/f73, organic concentration and MCE.

On 30th of May at around 2pm three hot spots (two having confidence level of approximately 50% and one of 70%) were detected within 2km on the NE from the ATARS (Fig S7a-Fig.S7d). These hot spots likely illustrate two fire events. On the same day and time, 11km on the SE from the sampling site, cluster of events was observed, including 4 hot spots with the confidence level between 94% and 100% and one of 78% confidence level. As all of them were spotted at the same time and within 1km distance, it is most likely that the one big fire has occured. No other close events were observed over this time period. Cluster of hot spots was detected on the SE approximately 50km from the ATARS and big clusters at 100km and 150km, as well as on the SE. Moreover, 200km on E along the backtrajectories cluster of hot spots was observed.

Two single source events, A and C, were identified and analysed here (Fig.2). The event A illustrated the increased signals in the afternoon hours, when wind was coming from the NE. Therefore, the event A is likely result of the hot spots detected within 2km from the ATARS (Fig S7a and Fig S7b). According to backtrajectories air masses during these time period were passing over the land affected by these fires and they were transported from the fire events to ATARS within approximately 10 min. The average organic concentration was found to be 23 µg m^{-3}, with the concentrations going up to 45 µg m^{-3}. High average MCE value of 0.97 likely suggests flaming fire as emission source and/or grass as a burning material (Desservettaz et al., 2016). The signal named as a C event was detected over the night (Table 1). At that time wind direction was abruptly changed from the NE to SE. Therefore, the signal can be likely associated to cluster of fires 11 km on the SE (Fig S7c and Fig S7d). According to the backtrajectories air masses reached the ATARS within 20 min from the fire cluster. Comparing to the event A, the average organic concentration for the event C was more than threefold with the maximum value of approximately 130 µg m^{-3}. As MCE was found to be similar (0.98) to event A value, most likely higher signals illustrate larger fire. The number of hot spots detected on the same time with high confidence level confirms this. Higher fire intensity can also be a reason for the higher f60 values for the event C (0.027) compared to event A (0.016) (Table 1).

~~Elevated signals on the 30th of May were attributed to emissions from fires within 5 km and labelled as events A and C. High MCE values (MCE of 0.97 and 0.98 for A and C, respectively) suggested flaming fires as emission sources and/or grass as a burning material (Desservettaz et al., 2016). Lower organic mass loadings might therefore be related to flaming burning conditions.~~

On 25th of June three hotspot clusters were observed close to ATARS (2km on E, 5km on NE and 10km on SE) (Fig S7e-Fig S7h). The cluster of hot spots observed 10 km from the sampling site had one of the highest hot spot's power (energy released by the fire) observed close to the ATARS (within 20 km) during the campaign (120 MW/km^2). Besides the close fires two big clusters around 60 km and 120 km on the SE from ATARS were detected on the same day. On the 25th of June, two ~~intense close fires~~single-source events were observed and labelled as events F and G. Event F was related to a close fire (two hot spots of 60 and 100% confidence level, within 2 km on E) whose emissions were clearly visible from ATARS (Fig. S7e and Fig S7f). The detected plumes included a considerable portion of oxygenated OA (average f44 value of 0.13, up to 0.18) that could be caused by ~~reflecting~~ high daytime photochemical activity. The BB event F began at noon and ended at approximately 5 pm, i.e., it occurred during the period of highest photochemical activity. The relatively high $\Delta O_3/\Delta CO$ ratio (0.13) was elevated relative to the other close BB events, which suggests additional photochemical activity in the plume. This value falls into the range for fire emissions aged less than 1-2 days in tropical/subtropical regions (Jaffe and Wigder, 2012). However, the f44 value was highly variable during the event F, ranging from 0.07 to 0.18. Other parameters including f60 and organics varied as well. On that time, the wind direction significantly varied between 140° and 80° and likely influenced changes in detected air mass. One of the explanations can be detection of fresh plume and aged masses coming from the distant fires with the change in wind. The low correlation between f60 and f73 might also be an indicator for detection of different BB air masses (Fig. S8). Relatively low organic mass loading and f60 values may be due to ~~low fire extent~~highly variable wind direction and/or area rather than combustion conditions (MCE of 0.93), as higher organics are expected for this MCE value. In contrast, event G resulted in the highest organic mass loading measured at ATARS (PM_1 concentration of ~350 µg m^{-3}). Moreover, the highest chloride concentration observed over the campaign was at the time of G event. The source of emissions was probably within 10 km on SE of the sampling site (Fig S7g and Fig S7h) and the fire magnitude was illustrated by a large burned area observed the following morning (Mallet et al., 2016) and high power of fire observed (30 MW/km^2). Backtrajectories analysis indicated that less than half an hour was needed for the air mass to reach the ATARS. High fire intensity was accompanied with smouldering burning conditions (MCE of 0.90) that resulted in high

Formatted: Font:

Formatted: Superscript

Formatted: Subscript

organic loadings and high levoglucosan concentrations (high f60) (Table 1). A low OOA fraction, f44, $\Delta O_3/\Delta CO$ value (0.01) indicated that the plume was likely not aged, which is to be expected due to the proximity and time of the event (started at 10 pm and finished at 4 am).

Intense signals, including high organic concentrations, were also detected on the 9th of June (Fig S7i and Fig S7j). On that day cluster of hot spots (all with the confidence level higher than 70%) was detected 5 km from ATARS. Number of distant hot spots was detected between 100 km and 200 km, on the SE from the ATARS. Mallet et al. (2016) suggested that possible sources of this event E might be close fires ~~(within 5 km)~~, distant fires ~~(100 and 200 km away)~~ or a combination of both. According to backtrajectories less than 10 min was enough for air masses to cross the distance between 5 km cluster and the research station. Values for f44 (0.08) and $\Delta O_3/\Delta CO$ (0.02) suggested detection of fresh emissions. Moreover, the high f60 value of 0.032 supported this, as distant fires are not likely to be characterized with such a high portion of levoglucosan-like species. However, the possibility of contribution from distant BB plumes cannot be excluded, especially when considering the particle size distribution during event E. The particle size distribution had a mode of 146 nm, while events F and G showed smaller size distributions with modes of 98 and 88 nm, respectively (Table 1). However, different burning material and conditions could also contribute to the larger size distribution mode during event E.

In general, diversity of biomass burning plumes was illustrated through high variability in chemical signature (e.g. large range of f44, from 0.06 to 0.18) for five intense fire events.~~the large range of f44 values (from 0.06 to 0.13) associated with these close events suggested different burning conditions that generated fresh emissions with different fractions of OOA. However, f44 and $\Delta O_3/\Delta CO$ values for event F could reflect daytime photochemical activity.~~ Events were characterised with different f60/f73 ratios (varying between 1.2 and 2.5), but there was no trend in the relationship of f60/f73 ratio and burning material/conditions (MCE values) (Fig. S8).

3.3 Positive Matrix Factorization (PMF)

Initially PMF was performed to assist with analysis of the aging observations rather than to apportion sources since the main source (BB) is already known. This approach was intended to estimate whether the ratios of the different factors, e.g., fresh BBOA, aged BBOA or OOA, exhibited relationships with the age of separate BB plumes. The diversity of the plumes (including close fire plumes with spectra presented in Fig. S6), however, made PMF analysis difficult. The thousands of fires that occurred during the SAFIRED campaign contributed to a wide range of OA composition that reflect different burning materials, conditions, mixed fresh and aged emissions and processing in the atmosphere. The ratio of m/z 43 and 44 differed between plumes (Fig. S11~~9~~) and since the AMS mass spectra were dominated by these masses, the PMF analysis returned factors that corresponded to individual plumes, even when distant fires were separately examined. In addition, high residuals during BB events could not be reduced even with an unreasonably large number of factors (Fig. S9~~7~~). The PMF diagnostic plots can be found in Sect. S3.

Instead PMF analysis was applied on “background” data in order to determine the contribution of BB emissions and SOA to regional ambient PM_1 outside of the time periods dominated by BB events. The background time periods were determined by examining the plot of f44 vs. f43 (Fig. S11~~9~~). Cut-offs of 0.15 for m/z 43 and 0.4 for f44 were chosen to remove the influence of periods dominated by BB events which show up as individual lines in f43 vs. f44 space.

PMF performed on the background OA showed significantly smaller residuals (Fig. S12~~0~~) and resulted in three factors, including a biomass burning OA factor (BBOA), oxygenated OA (OOA) and a factor that represented isoprene-derived OA ~~epoxydiols-related SOA (IEPOX-SOA)~~ (Fig. 7~~9~~). A two-factor solution did not extract the biogenic ~~IEPOX-SOA~~isoprene-derived OA factor while a four-factor solution resulted in splitting of profiles (Fig. S13~~1~~). The biomass burning factor, with distinct m/z 60 and 73 signals, contributed to 24 % of the background aerosol. BBOA was also characterized by fragments related to fresh hydrocarbon-like organics, e.g., m/z 27, 29, 41, 43, 55, and 57, and by prominent OOA-related m/z 28 and 44 signals. The large f44 value (an average f44 of 0.09) (Fig. S4) may indicate either the presence of processed BB aerosol and/or fresh emissions that contain oxygenated OA species possibly due to the burning conditions (Heringa et al., 2012;Weimer et al., 2008). A good correlation was observed between the BBOA factor and Org 60 and CO signals (Fig. 7~~9~~d and Fig. 7~~9~~e). An OOA profile with prominent m/z 28 and 44, similar to LV-OOA profiles observed in previous studies, was extracted. Its diurnal trend is marked by a broad daily peak which correlates with the maximum temperature and reflects intense daytime photochemical activity. The OOA dominance (contribution of 47 %) and high degree of oxygenation (an average f44 of 0.23) (Fig. S4) illustrate the significance of OOA for this area. The third PMF factor can be related to background biogenic SOA, and is discussed in more detail in the Sect. 3.3.1.

3.3.1 Isoprene-derived OA ~~epoxydiols-related secondary organic aerosol (IEPOX-SOA)~~

Isoprene epoxydiols (IEPOX) are important gas-phase precursors for IEPOX-SOA and are products of isoprene oxidation, mostly in low-NO_X environments (Paulot et al., 2009). Recent studies have showed that PMF performed on AMS OA data can be used to determine total IEPOX contribution to SOA (Robinson et al., 2011;Lin et al., 2011;Budisulistiorini et al., 2013;Hu et al., 2015;Xu et al., 2016). A similar distinct PMF-resolved factor has been extracted in this study. In order to consider other possible pathways in isoprene-derived OA formation (Schwantes et al., 2015), the PMF factor has been named as isoprene-derived OA (Xu et al., 2016;Pye et al.)~~IEPOX-SOA factor was extracted in this study.~~ The ~~IEPOX-SOA~~isoprene-derived OA mass spectrum can be clearly distinguished from BBOA and OOA by an enhanced m/z 82 signal (Fig. 9a). In the HR analysis of this dataset, $C_5H_6O^+$ is the most dominant peak that contributes to m/z 82 (Fig. S13) and has been confirmed to be a reliable tracer for ~~IEPOX-SOA~~isoprene- derived OA (Hu et al., 2015). There was a strong correlation observed between the ~~IEPOX-SOA~~isoprene- derived OA factor and Org 82 ($C_5H_6O^+$) (R of 0.90) (Fig. 7~~9~~f). The ~~IEPOX-SOA~~isoprene- derived OA factor profile was also characterized with enhanced peaks at m/z 53, 43 and 44. An AMS spectrum with the same prominent peaks was reported by Allen et al. (2008) for the Darwin region in the Northern Territory. This was observed during the monsoon-break period during the wet season in February, when fires were not common, and

Formatted: Subscript

Formatted: Font: (Default) +Headings (Times New Roman), Font color: Text 1

Formatted: Font: (Default) +Headings (Times New Roman), Font color: Text 1 clean air of biogenic origin was suggested as a source. Moreover, our spectrum is similar to ~~IEPOX-SOA~~isoprene-related OA spectra reported previously (Robinson et al., 2011;Lin et al., 2011;Budisulistiorini et al., 2013). The average isoprene concentration measured during the campaign was 0.49 ± 0.78 ppb. However, it should be emphasised that monoterpene-derived OA can also influence the background level of $C_5H_6O^+$ (Hu et al., 2015). The average monoterpenes concentration for this study was found to be 0.22 ± 0.41 ppb.

The main path for isoprene-derived OA formation is proposed to be acid-catalysed IEPOX uptake (Lin et al., 2011;Lambe et al., 2015). According to calculations for the composition depended collection efficiency, 22% of the aerosol were acidic. In order to estimate whether the acidity of the particles had an influence on isoprene- derived OA generation in ATARS, the correlation between sulfate (taken as proxy of aerosol acidity) and the isoprene-derived OA factor was examined. The correlation between the factor and sulfate can be considered as weak (R of 0.3) (Fig S18). However, two periods can be clearly distinguished from the graph: the period before 5th of June and the period after 15th of June. While there is no correlation between sulfate and the isoprene-derived OA factor for the first period, when plotting only data collected from 15th of June, correlation is found to be slighly higher than the correlation for all background data (R of 0.4).

The isoprene/furan concentrations at m/z 69 (PTR-MS) were treated as an isoprene contribution due to the dominance of isoprene signal compared to furan, according to the samples analysed by gas chromatography-mass spectrometry (Fig. S17). The furan contribution was more significant in BB plumes during the close BB period, as suggested previously (Warneke et al., 2011). As expected, the isoprene/furan gas-phase concentration measured by the PTR-MS increased from noon till the late afternoon (Fig. S16). According to diurnal patterns of PMF isoprene- derived OA, there is no considerable change in isoprene- derived OA concentration from noon throughout the day. The ~~IEPOX-SOA~~isoprene- derived OA fraction is expected to increase during daytime hours in accordance with enhancements in isoprene and gas-phase IEPOX (Hu et al., 2015). ~~As expected, the isoprene/furan gas-phase concentration measured by the PTR-MS increased from noon till the late afternoon (Fig. S14). According to diurnal patterns of PMF IEPOX-SOA, there is no considerable change in IEPOX-SOA concentration from noon throughout the day.~~ However, the ~~IEPOX-SOA~~isoprene- derived OA factor was prominent during night and morning hours. Significant ~~IEPOX-SOA~~isoprene- derived OA factor enhancement during the night time might be due to partitioning of lower volatility species onto the particles when the temperature drops and relative humidity increases as suggested by Budisulistiorini et al. (2013), due to transport of distant air masses, or lower boundary layer height. During the night, the boundary level lowers which increases the concentration of gaseous compounds and can induce partitioning of gases onto the particles. Therefore, the lower night-time boundary layer might create conditions for low volatility isoprene-derived OA partitioning and an increase in isoprene-derived OA.

A plot of f44 (CO_2^+) vs. f82 ($C_5H_6O^+$) (Org CO_2^+/Org and Org $C_5H_6O^+$/Org from HR data analysis, respectively) (Fig. 8~~10~~) introduced by Hu et al. (2015) can be used to distinguish IEPOX-SOA from SOA originating from other sources, including isoprene- derived~~related~~ SOA that are generated from species other than IEPOX. This plot also indicates the degree of aging

Formatted: Space After: 0 pt

Formatted: Superscript

Formatted: Superscript

Formatted: Superscript

Formatted: Font: English (U.K.)

of the IEPOX-SOA. The general pattern of f44 increase with f82 decrease is observed. With aging, OA becomes more oxidized and the $C_5H_6O^+$ signature decreases. This can be due to oxidation processes or mixing with more aged aerosol masses.

A background value for f82 ($C_5H_6O^+$) in environments strongly influenced by BB was suggested to be 0.0017 and is indicated by the vertical dashed black line (Hu et al., 2015). Looking at our data plotted in f44 vs. f82 a similar observation can be made. All data points are positioned above 0.0016 of f82 with an average value of 0.0061 ± 0.0036. The ~~IEPOX~~isoprene-derived ~~S~~OA factor average values for this campaign and two other ambient studies are marked in the plot. The f82 value for ~~IEPOX-SOA~~isoprene-derived OA factor observed here is similar to the reported f82 value for an urban site (Budisulistiorini et al., 2013), but lower compared to the ~~IEPOX-SOA~~ factor observed for Borneo forest (Robinson et al., 2011). The lower value for SAFIRED compared to Borneo forest, considering that biogenic influence is significant for both environments, can be attributed to the high influence of BB emissions. ~~A low correlation between the IEPOX-SOA time series with both OOA and BBOA was observed (Fig. S15) suggesting that during BB influenced periods either higher NO$_X$ concentrations suppressed IEPOX and consequently IEPOX-SOA generation or the dominant BB aerosol during these periods inhibited measurement of isoprene oxidation products.~~

As the most abundant NMOC, isoprene is a significant contributor to the global SOA budget (Guenther et al., 2012;Hallquist et al., 2009;Paulot et al., 2009). ~~IEPOX-S~~isoprene-derived OA during the SAFIRED campaign accounted for 28 % of the total background OA which is similar to previous observations where the ~~IEPOX-S~~isoprene-derived OA fraction contribution varied from 6-36 %, depending on the environment (Hu et al., 2015). This confirms the importance of isoprene-~~related~~ derived SOA for the Northern Territory environment even in times of high BB influence.

4. Conclusions

A one month long campaign called SAFIRED was conducted in northern Australia during a period of significant burning (early dry season). There was a significant influence of BB plumes on the atmospheric chemical profile at the time of campaign, reflected by high concentrations of gaseous and particle species including CO and PM$_1$ organics, reaching maxima of ~10^4 ppb and 350 µg m^{-3} respectively during heavy BB episodes. Emitted aerosols were predominantly organic species (90 %) with a wide range of levels of oxidation. There was a clear overall increase of the highly oxygenated OA fraction and degradation of BB-related signatures with OA processing. This was shown by an overall trend of f44 increase and f60 decrease for distant fires. Plume emissions formed over the month period were photochemically active resulting in the production of tropospheric ozone. Close fire emissions were characterized by lower ozone enrichments (average $\Delta O_3/\Delta CO$ of 0.15) than plumes detected from the distant BB sources (average $\Delta O_3/\Delta CO$ of 0.31) which illustrate higher photochemical activity with more processed air masses. This emphasizes air mass ability for photochemical processing and production of SOA. An increase in the $\Delta OA/\Delta CO$ ratio with increase of f44 also suggests SOA formation. According to

Formatted: Subscript

results, t~~T~~he OA oxidation level did not significantly influence~~d~~ particle size distribution~~, with a change in the mode from 83 to 106 nm for fresh (0.05<f44<0.1) and aged (0.1 <f44<0.15) BB plumes, respectively~~. Diversity in BB emissions was illustrated through investigation of five selected events. The chemical signature varied for different fire events (e.g. wide range in f44, from 0.06 to 0.18~~3~~).

PMF was employed to estimate BB influence on and SOA portion of background regional aerosol. A significant portion of oxygenated OA, identified through high f44 (majority of data points between 0.1 and 0.25), and a significant portion of aged BBOA (47 and 24 %, respectively) were observed. The latter suggests considerable processing of aerosol in the atmosphere for this area. The remaining OA was attributed to ~~IEPOX-S~~isoprene-derived OA factor (28 %), identified here for the first time in Australia. The OA mass spectrum with ~~IEPOX-S~~isoprene-derived OA characteristics previously reported in the wet season and now observed with prominent BB influence during the dry period, suggests the importance of biogenic isoprene sources for the Northern Territory area at all times of the year.

Observed photochemical activity of air masses and enhancement of OA with aging illustrate the importance of aging and SOA formation in the Northern Territory during the dry early season. SOA is recognized as a significant contributor to climate, environment and adverse human health effects. This study is an important step in addressing suggested further research related to tropical biomass burns and biogenic-related SOA in Australia (Rotstayn et al., 2009). As SOA yields are considerably underestimated and its formation is still not sufficiently understood, this study can facilitate understanding of SOA formation for Northern Territory savannah areas and also for the tropics in general. Additional measurements during late dry season (September-October) are needed as more intense and frequent fires occur during this period (Andersen et al., 2005;Williams et al., 1998). Moreover, the late dry season is suggested to have more aged emissions (Ristovski et al., 2010;Wardoyo et al., 2007). Therefore it is important to characterize SOA formation, and yield during this period.

Data availability. The underlying research data can be accessed upon request to the corresponding author (Branka Miljevic; b.miljevic@qut.edu.au).

Author contributions. Andelija Milic analysed and interpreted the data and prepared the manuscript. Marc Mallet operated the cToF-AMS and contributed to data analysis, interpretation and writing. Branka Miljevic installed the cToF-AMS, contributed to data analysis, interpretation and writing and supervised the work of Andelija Milic. Luke Cravigan set up the SMPS and contributed to data interpretation. Joel Alroe assisted in organizing the QUT instrumentation, data interpretation and writing the manuscript. Zoran Ristovski contributed to campaign organization and data interpretation and supervised the work of Andelija Milic. Leah Williams contributed to setting up the cToF-AMS, preliminary data analysis and data interpretation. Melita Keywood organized and led the campaign. Paul Selleck operated the BAM, analysed the data and contributed to data interpretation. Sarah Lawson operated the PTR-MS and analysed the data. James Ward operated the Ozone analyser and analysed the data. Maximilian Desservettaz operated the FTIR and SMPS and analysed the data. Clare

Paton-Walsh contributed to campaign organization and running the campaign. All authors declare that they have no conflict of interest.

Acknowledgements. The authors thank Manjula Canagaratna for valuable discussions about interpreting the PMF analysis. The authors thank Min Cheng for providing the gas chromatography-mass spectrometry data. This work was supported by the Australian Research Council Discovery grant (DP120100126).

References

Aiken, A. C., DeCarlo, P. F., and Jimenez, J. L.: Elemental analysis of organic species with electron ionization high-resolution mass spectrometry, Analytical Chemistry, 79, 8350-8358, 2007.
Aiken, A. C., DeCarlo, P. F., Kroll, J. H., Worsnop, D. R., Huffman, J. A., Docherty, K. S., Ulbrich, I. M., Mohr, C., Kimmel, J. R., Sueper, D., Sun, Y., Zhang, Q., Trimborn, A., Northway, M. J., Ziemann, P. J., Canagaratna, M., Onasch, T., Alfarra, M. R., Prevot, A. S., Dommen, J., Duplissy, J., Metzger, A., Baltensperger, U., and Jimenez, J.: O/C and OM/OC ratios of primary, secondary, and ambient organic aerosols with high-resolution time-of-flight aerosol mass spectrometry, Environmental Science & Technology, 42, 4478-4485, 2008.
Akagi, S., Craven, J., Taylor, J., McMeeking, G., Yokelson, R., Burling, I., Urbanski, S., Wold, C., Seinfeld, J., Coe, H., Alvarado, M., and Weise, D.: Evolution of trace gases and particles emitted by a chaparral fire in California, Atmospheric Chemistry and Physics, 12, 1397-1421, 2012.
Alfarra, M. R., Prevot, A. S., Szidat, S., Sandradewi, J., Weimer, S., Lanz, V. A., Schreiber, D., Mohr, M., and Baltensperger, U.: Identification of the mass spectral signature of organic aerosols from wood burning emissions, Environmental science & technology, 41, 5770-5777, 2007.
Allen, G., Vaughan, G., Bower, K., Williams, P., Crosier, J., Flynn, M., Connolly, P., Hamilton, J., Lee, J., Saxton, J., Watson, N., Gallagher, M., Coe, H., Allan, J., Choularton, T., and Lewis, A.: Aerosol and trace-gas measurements in the Darwin area during the wet season, Journal of Geophysical Research: Atmospheres (1984–2012), 113, 2008.
Andersen, A. N., Cook, G. D., Corbett, L. K., Douglas, M. M., Eager, R. W., Russell-Smith, J., Setterfield, S. A., Williams, R. J., and Woinarski, J. C.: Fire frequency and biodiversity conservation in Australian tropical savannas: implications from the Kapalga fire experiment, Austral Ecology, 30, 155-167, 2005.
Bond, T. C., Streets, D. G., Yarber, K. F., Nelson, S. M., Woo, J. H., and Klimont, Z.: A technology-based global inventory of black and organic carbon emissions from combustion, Journal of Geophysical Research: Atmospheres (1984–2012), 109, 2004.
Bougiatioti, A., Stavroulas, I., Kostenidou, E., Zarmpas, P., Theodosi, C., Kouvarakis, G., Canonaco, F., Prévôt, A., Nenes, A., Pandis, S., and Mihalopoulos, N.: Processing of biomass-burning aerosol in the eastern Mediterranean during summertime, Atmospheric Chemistry and Physics, 14, 4793-4807, 2014.
Bouya, Z., Box, G. P., and Box, M. A.: Seasonal variability of aerosol optical properties in Darwin, Australia, Journal of Atmospheric and Solar-Terrestrial Physics, 72, 726-739, 2010.
Bowman, D. M., Dingle, J. K., Johnston, F. H., Parry, D., and Foley, M.: Seasonal patterns in biomass smoke pollution and the mid 20th-century transition from Aboriginal to European fire management in northern Australia, Global Ecology and Biogeography, 16, 246-256, 2007.
Brito, J., Rizzo, L., Morgan, W., Coe, H., Johnson, B., Haywood, J., Longo, K., Freitas, S., Andreae, M., and Artaxo, P.: Ground-based aerosol characterization during the South American Biomass Burning Analysis (SAMBBA) field experiment, Atmospheric Chemistry and Physics, 14, 12069-12083, 2014.
Budisulistiorini, S. H., Canagaratna, M. R., Croteau, P. L., Marth, W. J., Baumann, K., Edgerton, E. S., Shaw, S. L., Knipping, E. M., Worsnop, D. R., and Jayne, J. T.: Real-time continuous characterization of secondary organic aerosol derived from isoprene epoxydiols in downtown Atlanta, Georgia, using the Aerodyne Aerosol Chemical Speciation Monitor, Environmental science & technology, 47, 5686-5694, 2013.

Capes, G., Johnson, B., McFiggans, G., Williams, P., Haywood, J., and Coe, H.: Aging of biomass burning aerosols over West Africa: Aircraft measurements of chemical composition, microphysical properties, and emission ratios, Journal of Geophysical Research: Atmospheres (1984–2012), 113, 2008.

Carr, S. B., Gras, J., Hackett, M., and Keywood, M.: Aerosol Characteristics in the Northern Territory of Australia During the Dry Season With an Emphasis on Biomass Burning, DTIC Document, 2005.

Chow, J. C., Watson, J. G., Chen, L.-W. A., Chang, M. O., Robinson, N. F., Trimble, D., and Kohl, S.: The IMPROVE_A temperature protocol for thermal/optical carbon analysis: maintaining consistency with a long-term database, Journal of the Air & Waste Management Association, 57, 1014-1023, 2007.

Crutzen, P. J., and Andreae, M. O.: Biomass burning in the tropics: Impact on atmospheric chemistry and biogeochemical cycles, Science, 250, 1669-1678, 1990.

Cubison, M., Ortega, A., Hayes, P., Farmer, D., Day, D., Lechner, M., Brune, W., Apel, E., Diskin, G., and Fisher, J.: Effects of aging on organic aerosol from open biomass burning smoke in aircraft and laboratory studies, Atmospheric Chemistry and Physics, 11, 12049-12064, 2011.

DeCarlo, P., Dunlea, E., Kimmel, J., Aiken, A., Sueper, D., Crounse, J., Wennberg, P., Emmons, L., Shinozuka, Y., and Clarke, A.: Fast airborne aerosol size and chemistry measurements above Mexico City and Central Mexico during the MILAGRO campaign, Atmos. Chem. Phys, 8, 4027-4048, 2008.

DeCarlo, P., Ulbrich, I., Crounse, J., Foy, B. d., Dunlea, E., Aiken, A., Knapp, D., Weinheimer, A., Campos, T., Wennberg, P., and Jimenez, J.: Investigation of the sources and processing of organic aerosol over the Central Mexican Plateau from aircraft measurements during MILAGRO, Atmospheric Chemistry and Physics, 10, 5257-5280, 2010.

Desservettaz, M., Paton-Walsh, C., Griffith, D., Kettlewell, G., Keywood, M., Schoot, M. V., JasonWard, Mallet, M., Ristovski, Z., Miljevic, B., Milic, A., Howard, D., Edwards, G., and Atkinson, B.: Emission factors of trace gases and particles from tropical savanna fires in Australia, submitted to Journal of Geophysical Research 2016.

Edwards, D., Pétron, G., Novelli, P., Emmons, L., Gille, J., and Drummond, J.: Southern Hemisphere carbon monoxide interannual variability observed by Terra/Measurement of Pollution in the Troposphere (MOPITT), Journal of Geophysical Research: Atmospheres, 111, 2006.

Formenti, P., Elbert, W., Maenhaut, W., Haywood, J., Osborne, S., and Andreae, M.: Inorganic and carbonaceous aerosols during the Southern African Regional Science Initiative (SAFARI 2000) experiment: Chemical characteristics, physical properties, and emission data for smoke from African biomass burning, Journal of Geophysical Research: Atmospheres (1984–2012), 108, 2003.

Grieshop, A., Logue, J., Donahue, N., and Robinson, A.: Laboratory investigation of photochemical oxidation of organic aerosol from wood fires 1: measurement and simulation of organic aerosol evolution, Atmospheric Chemistry and Physics, 9, 1263-1277, 2009.

Griffith, D., Deutscher, N., Caldow, C., Kettlewell, G., Riggenbach, M., and Hammer, S.: A Fourier transform infrared trace gas and isotope analyser for atmospheric applications, Atmospheric Measurement Techniques, 5, 2481-2498, 2012.

Griffith, D. W.: Synthetic calibration and quantitative analysis of gas-phase FT-IR spectra, Applied spectroscopy, 50, 59-70, 1996.

Guenther, A., Jiang, X., Heald, C., Sakulyanontvittaya, T., Duhl, T., Emmons, L., and Wang, X.: The Model of Emissions of Gases and Aerosols from Nature version 2.1 (MEGAN2. 1): an extended and updated framework for modeling biogenic emissions, 2012.

Guenther, C.: Estimates of global terrestrial isoprene emissions using MEGAN (Model of Emissions of Gases and Aerosols from Nature), Atmospheric Chemistry and Physics, 6, 2006.

Hallquist, M., Wenger, J., Baltensperger, U., Rudich, Y., Simpson, D., Claeys, M., Dommen, J., Donahue, N., George, C., Goldstein, A., Hamilton, J., Herrmann, H., Hoffmann, D., Iinuma, Y., Jang, M., Jenkin, M., Jimenez, J., Keindler-Scharr, A., Maenhaut, W., McFiggans, G., Mentel, T., Monod, A., Prevot, A., Seinfeld, J., Surratt, J., Szmigielski, R., and Wildt, J.: The formation, properties and impact of secondary organic aerosol: current and emerging issues, Atmos. Chem. Phys, 9, 5155-5236, 2009.

Haywood, J., and Boucher, O.: Estimates of the direct and indirect radiative forcing due to tropospheric aerosols: A review, Reviews of geophysics, 38, 513-543, 2000.

He, C., Murray, F., and Lyons, T.: Monoterpene and isoprene emissions from 15 Eucalyptus species in Australia, Atmospheric Environment, 34, 645-655, 2000.

Heringa, M., DeCarlo, P., Chirico, R., Tritscher, T., Dommen, J., Weingartner, E., Richter, R., Wehrle, G., Prévôt, A., and Baltensperger, U.: Investigations of primary and secondary particulate matter of different wood combustion appliances with a high-resolution time-of-flight aerosol mass spectrometer, Atmos. Chem. Phys, 11, 5945-5957, 2011.

Heringa, M., DeCarlo, P., Chirico, R., Lauber, A., Doberer, A., Good, J., Nussbaumer, T., Keller, A., Burtscher, H., and Richard, A.: Time-resolved characterization of primary emissions from residential wood combustion appliances, Environmental science & technology, 46, 11418-11425, 2012.

Hobbs, P. V., Sinha, P., Yokelson, R. J., Christian, T. J., Blake, D. R., Gao, S., Kirchstetter, T. W., Novakov, T., and Pilewskie, P.: Evolution of gases and particles from a savanna fire in South Africa, Journal of Geophysical Research: Atmospheres (1984–2012), 108, 2003.

Hu, W., Campuzano-Jost, P., Palm, B., Day, D., Ortega, A., Hayes, P., Krechmer, J., Chen, Q., Kuwata, M., Liu, Y., McKinney, K., Martin, S. T., Hu, M., Budisulistiorini, S. H., Riva, M., Surratt, J., Clair, J. M. S., Isaacman, G., Yee, L., Goldstein, A., Carbone, S., Brito, J., Artaxo, P., De Gouw, J., Koss, A., Wisthaler, A., Mikoviny, T., Karl, T., Kaser, L., Jud, W., Hansel, A., Docherty, K., Alexander, M., Robinson, A., Coe, H., Allan, J., Canagaratna, M., Paulot, F., and Jimenez, J.: Characterization of a real-time tracer for isoprene epoxydiols-derived secondary organic aerosol (IEPOX-SOA) from aerosol mass spectrometer measurements, Atmospheric Chemistry and Physics, 15, 11807-11833, 2015.

Hurst, D. F., Griffith, D. W., and Cook, G. D.: Trace gas emissions from biomass burning in tropical Australian savannas, Journal of Geophysical Research: Atmospheres, 99, 16441-16456, 1994.

Jaffe, D. A., and Wigder, N. L.: Ozone production from wildfires: A critical review, Atmospheric Environment, 51, 1-10, 2012.

Jimenez, J., Canagaratna, M., Donahue, N., Prevot, A., Zhang, Q., Kroll, J. H., DeCarlo, P. F., Allan, J. D., Coe, H., Ng, N., Aiken, A., Docherty, K., Ulbrich, I., Grieshop, A. P., Robinson, A., Duplissy, J., Smith, J. D., Wilson, K. R., Lanz, V., Hueglin, C., Sun, J., Tian, J., Laaksonen, A., Raatikainen, T., Rautiainen, J., Vaattovaara, P., Ehn, M., Kulmala, M., Tomlinson, J., Collins, D., Cubison, M. J., Dunlea, E., Huffman, J. A., Onasch, T., Alfarra, M. R., Williams, P., Bower, K. N., Kondo, Y., Schneider, J., Drewnick, F., Borrmann, S., Weimer, S., Demerjian, K. L., Salcedo, D., Cottrell, L., Griffin, R., Takami, A., Miyoshi, T., Hatakeyama, S., Shimono, A., Sun, J., Zhang, J., Dzepina, K., Kimmel, J. R., Sueper, D., Jayne, J. T., Herndon, S., Trimborn, A., Williams, L. R., Wood, E., Middlebrook, A., Kolb, C. E., Baltensperger, U., and Worsnop, D. R.: Evolution of organic aerosols in the atmosphere, Science, 326, 1525-1529, 2009.

Jolleys, M., Coe, H., McFiggans, G., Taylor, J., O'Shea, S., Le Breton, M., Bauguitte, S.-B., Moller, S., Di Carlo, P., and Aruffo, E.: Properties and evolution of biomass burning organic aerosol from Canadian boreal forest fires, Atmospheric Chemistry and Physics, 15, 3077-3095, 2015.

Jordan, T. B., Seen, A. J., and Jacobsen, G. E.: Levoglucosan as an atmospheric tracer for woodsmoke, Atmospheric Environment, 40, 5316-5321, 2006.

Kleinman, L. I., Springston, S. R., Daum, P. H., Lee, Y.-N., Nunnermacker, L., Senum, G., Wang, J., Weinstein-Lloyd, J., Alexander, M., Hubbe, J., Ortega, A., Canagaratna, M., and Jayne, J. T.: The time evolution of aerosol composition over the Mexico City plateau, Atmospheric Chemistry and Physics, 8, 1559-1575, 2008.

Kroll, J. H., Smith, J. D., Che, D. L., Kessler, S. H., Worsnop, D. R., and Wilson, K. R.: Measurement of fragmentation and functionalization pathways in the heterogeneous oxidation of oxidized organic aerosol, Physical Chemistry Chemical Physics, 11, 8005-8014, 2009.

Lacey, C., Walker, J., and Noble, I.: Fire in Australian tropical savannas, in: Ecology of tropical savannas, Springer, 246-272, 1982.

Lambe, A., Chhabra, P., Onasch, T., Brune, W., Hunter, J., Kroll, J., Cummings, M., Brogan, J., Parmar, Y., and Worsnop, D.: Effect of oxidant concentration, exposure time, and seed particles on secondary organic aerosol chemical composition and yield, Atmospheric Chemistry and Physics, 15, 3063-3075, 2015.

Lanz, V., Alfarra, M., Baltensperger, U., Buchmann, B., Hueglin, C., and Prévôt, A.: Source apportionment of submicron organic aerosols at an urban site by factor analytical modelling of aerosol mass spectra, Atmospheric Chemistry and Physics, 7, 1503-1522, 2007.

Li, J., Pósfai, M., Hobbs, P. V., and Buseck, P. R.: Individual aerosol particles from biomass burning in southern Africa: 2, Compositions and aging of inorganic particles, Journal of Geophysical Research: Atmospheres, 108, 2003.

Li, W., Shao, L., and Buseck, P.: Haze types in Beijing and the influence of agricultural biomass burning, Atmospheric Chemistry and Physics, 10, 8119-8130, 2010.

Lin, Y.-H., Zhang, Z., Docherty, K. S., Zhang, H., Budisulistiorini, S. H., Rubitschun, C. L., Shaw, S. L., Knipping, E. M., Edgerton, E. S., Kleindienst, T. E., Gold, A., and Surratt, J.: Isoprene epoxydiols as precursors to secondary organic aerosol formation: acid-catalyzed reactive uptake studies with authentic compounds, Environmental science & technology, 46, 250-258, 2011.

Liu, X., Van Espen, P., Adams, F., Cafmeyer, J., and Maenhaut, W.: Biomass burning in southern Africa: Individual particle characterization of atmospheric aerosols and savanna fire samples, Journal of Atmospheric Chemistry, 36, 135-155, 2000.

Mallet, M. D., Desservettaz, M. J., Miljevic, B., Milic, A., Ristovski, Z. D., Alroe, J., Cravigan, L. T., Jayaratne, E. R., Paton-Walsh, C., Griffith, D. W. T., Wilson, S. R., Kettlewell, G., Vanderschoot, M. V., Selleck, P., Reisen, F., Lawson, S. J., Ward, J., Harnwell, J., Cheng, M., Gillett, R. W., Molloy, S. B., Howard, D., Nelson, P. F., Morrison, A. L., Edwards, G. C., Williams, A. G., Chambers, S. D., Werczynski, S., Williams, L. R., Winton, V. H. L., Atkinson, B., Wang, X., and Keywood, M. D.: Biomass burning emissions in north Australia during the early dry season: an overview of the 2014 SAFIRED campaign, Phys. Discuss., doi:10.5194/acp-2016-866, in review, 2016, 2016.

Martins, J. V., Dunlap, M. R., and Liousse, C.: Physical, chemical, and optical properties of regional hazes dominated by smoke in Brazil, Journal of Geophysical Research, 103, 32,059-032,080, 1998.

Middlebrook, A. M., Bahreini, R., Jimenez, J. L., and Canagaratna, M. R.: Evaluation of composition-dependent collection efficiencies for the aerodyne aerosol mass spectrometer using field data, Aerosol Science and Technology, 46, 258-271, 2012.

Mitchell, R., Forgan, B., Campbell, S., and Qin, Y.: The climatology of Australian tropical aerosol: evidence for regional correlation, Geophysical Research Letters, 40, 2384-2389, 2013.

Ng, N., Canagaratna, M., Zhang, Q., Jimenez, J., Tian, J., Ulbrich, I., Kroll, J., Docherty, K., Chhabra, P., Bahreini, R., Murphy, S., Seinfeld, J., Hildebrandt Ruiz, L., Donahue, N. M., DeCarlo, P., Lanz, V., Prevot, A., Dinar, E., Rudich, Y., and Worsnop, D. R.: Organic aerosol components observed in Northern Hemispheric datasets from Aerosol Mass Spectrometry, Atmospheric Chemistry and Physics, 10, 4625-4641, 2010.

O'Brien, D., and Mitchell, R.: Atmospheric heating due to carbonaceous aerosol in northern Australia—confidence limits based on TOMS aerosol index and sun-photometer data, Atmospheric Research, 66, 21-41, 2003.

Ortega, A., Day, D., Cubison, M., Brune, W., Bon, D., de Gouw, J., and Jimenez, J.: Secondary organic aerosol formation and primary organic aerosol oxidation from biomass-burning smoke in a flow reactor during FLAME-3, Atmospheric Chemistry and Physics, 13, 11551-11571, 2013.

Paatero, P., and Tapper, U.: Positive matrix factorization: A non-negative factor model with optimal utilization of error estimates of data values, Environmetrics, 5, 111-126, 1994.

Paatero, P.: The multilinear engine—a table-driven, least squares program for solving multilinear problems, including the n-way parallel factor analysis model, Journal of Computational and Graphical Statistics, 8, 854-888, 1999.

Paatero, P., and Hopke, P. K.: Rotational tools for factor analytic models, Journal of Chemometrics, 23, 91-100, 2009.

Parrington, M., Palmer, P., Lewis, A., Lee, J., Rickard, A., Carlo, P. D., Taylor, J., Hopkins, J., Punjabi, S., Oram, D., Forster, G., Aruffo, E., Moller, S., Bauguitte, S.-B., Allan, J., Coe, H., and Leigh, R.: Ozone photochemistry in boreal biomass burning plumes, Atmospheric Chemistry and Physics, 13, 7321-7341, 2013.

Paulot, F., Crounse, J. D., Kjaergaard, H. G., Kürten, A., Clair, J. M. S., Seinfeld, J. H., and Wennberg, P. O.: Unexpected epoxide formation in the gas-phase photooxidation of isoprene, Science, 325, 730-733, 2009.

Penner, J., Chuang, C., and Grant, K.: Climate forcing by carbonaceous and sulfate aerosols, Clim. Dynamm., 14, 839–851, ISI, 1998.

Pye, H. O., Murphy, B. N., Xu, L., Ng, N. L., Carlton, A. G., Guo, H., Weber, R., Vasilakos, P., Appel, K. W., and Budisulistiorini, S. H.: On the implications of aerosol liquid water and phase separation for organic aerosol mass,

Real, E., Law, K., Weinzierl, B., Fiebig, M., Petzold, A., Wild, O., Methven, J., Arnold, S., Stohl, A., Huntrieser, H., Roiger, A., Schlager, H., Stewart, D., Avery, M., Sachse, G. W., Browell, E., Ferrare, R., and Blake, D. R.: Processes influencing ozone levels in Alaskan forest fire plumes during long-range transport over the North Atlantic, Journal of Geophysical Research: Atmospheres (1984–2012), 112, 2007.

Reid, J., Koppmann, R., Eck, T., and Eleuterio, D.: A review of biomass burning emissions part II: intensive physical properties of biomass burning particles, Atmospheric Chemistry and Physics, 5, 799-825, 2005.

Ristovski, Z. D., Wardoyo, A. Y., Morawska, L., Jamriska, M., Carr, S., and Johnson, G.: Biomass burning influenced particle characteristics in Northern Territory Australia based on airborne measurements, Atmospheric Research, 96, 103-109, 2010.

Roberts, G. C., Artaxo, P., Zhou, J., Swietlicki, E., and Andreae, M. O.: Sensitivity of CCN spectra on chemical and physical properties of aerosol: A case study from the Amazon Basin, Journal of Geophysical Research: Atmospheres (1984–2012), 107, LBA 37-31-LBA 37-18, 2002.

Robinson, N., Hamilton, J., Allan, J., Langford, B., Oram, D., Chen, Q., Docherty, K., Farmer, D., Jimenez, J., and Ward, M.: Evidence for a significant proportion of Secondary Organic Aerosol from isoprene above a maritime tropical forest, Atmospheric Chemistry and Physics, 11, 1039-1050, 2011.

Rotstayn, L. D., Keywood, M. D., Forgan, B. W., Gabric, A. J., Galbally, I. E., Gras, J. L., Luhar, A. K., McTainsh, G. H., Mitchell, R. M., and Young, S. A.: Possible impacts of anthropogenic and natural aerosols on Australian climate: a review, International Journal of Climatology, 29, 461-479, 2009.

Russell-Smith, J., Yates, C. P., Whitehead, P. J., Smith, R., Craig, R., Allan, G. E., Thackway, R., Frakes, I., Cridland, S., Meyer, M. C., and Gill, A.: Bushfires' down under': patterns and implications of contemporary Australian landscape burning, International Journal of Wildland Fire, 16, 361-377, 2007.

Schwantes, R. H., Teng, A. P., Nguyen, T. B., Coggon, M. M., Crounse, J. D., St. Clair, J. M., Zhang, X., Schilling, K. A., Seinfeld, J. H., and Wennberg, P. O.: Isoprene NO3 Oxidation Products from the RO2+ HO2 Pathway, The Journal of Physical Chemistry A, 119, 10158-10171, 2015.

Simoneit, B. R., Schauer, J. J., Nolte, C., Oros, D. R., Elias, V. O., Fraser, M., Rogge, W., and Cass, G. R.: Levoglucosan, a tracer for cellulose in biomass burning and atmospheric particles, Atmospheric Environment, 33, 173-182, 1999.

Simoneit, B. R.: Biomass burning—a review of organic tracers for smoke from incomplete combustion, Applied Geochemistry, 17, 129-162, 2002.

Ulbrich, I., Canagaratna, M., Zhang, Q., Worsnop, D., and Jimenez, J.: Interpretation of organic components from Positive Matrix Factorization of aerosol mass spectrometric data, Atmospheric Chemistry and Physics, 9, 2891-2918, 2009.

Wang, C., and Prinn, R. G.: Impact of emissions, chemistry and climate on atmospheric carbon monoxide: 100-yr predictions from a global chemistry–climate model, Chemosphere-Global Change Science, 1, 73-81, 1999.

Ward, D., and Radke, L.: Emissions measurements from vegetation fires: A comparative evaluation of methods and results, 1993.

Wardoyo, A. Y., Morawska, L., Ristovski, Z. D., Jamriska, M., Carr, S., and Johnson, G.: Size distribution of particles emitted from grass fires in the Northern Territory, Australia, Atmospheric Environment, 41, 8609-8619, 2007.

Warneke, C., Roberts, J., Veres, P., Gilman, J., Kuster, W., Burling, I., Yokelson, R., and de Gouw, J.: VOC identification and inter-comparison from laboratory biomass burning using PTR-MS and PIT-MS, International Journal of Mass Spectrometry, 303, 6-14, 2011.

Weimer, S., Alfarra, M., Schreiber, D., Mohr, M., Prévôt, A., and Baltensperger, U.: Organic aerosol mass spectral signatures from wood-burning emissions: Influence of burning conditions and wood type, Journal of Geophysical Research: Atmospheres (1984–2012), 113, 2008.

Williams, R., Gill, A., and Moore, P.: Seasonal changes in fire behaviour in a tropical savanna in northern Australia, International Journal of Wildland Fire, 8, 227-239, 1998.

Xu, L., Middlebrook, A. M., Liao, J., Gouw, J. A., Guo, H., Weber, R. J., Nenes, A., Lopez-Hilfiker, F. D., Lee, B. H., and Thornton, J. A.: Enhanced formation of isoprene-derived organic aerosol in sulfur-rich power plant plumes during Southeast Nexus, Journal of Geophysical Research: Atmospheres, 121, 2016.

Yokelson, R. J., Bertschi, I. T., Christian, T. J., Hobbs, P. V., Ward, D. E., and Hao, W. M.: Trace gas measurements in nascent, aged, and cloud-processed smoke from African savanna fires by airborne Fourier transform infrared spectroscopy (AFTIR), Journal of Geophysical Research: Atmospheres (1984–2012), 108, 2003.

Yokelson, R. J., Crounse, J., DeCarlo, P., Karl, T., Urbanski, S., Atlas, E., Campos, T., Shinozuka, Y., Kapustin, V., Clarke, A., Weinheimer, A., Knapp, D., Montzga, L., Holloway, J., Weibring, P., Flocke, F., Zheng, W., Toohey, D., Wennberg, P. O., Wiedinmyer, C., Mauldin, R. L., Fried, A., Richter, D., Walega, J., Jimenez, J., Adachi, K., Buseck, P. R., Hall, S., and Shetter, R.: Emissions from biomass burning in the Yucatan, Atmospheric Chemistry and Physics, 9, 5785-5812, 2009.

Zhang, Q., Jimenez, J., Canagaratna, M., Allan, J., Coe, H., Ulbrich, I., Alfarra, M., Takami, A., Middlebrook, A., Sun, Y., Dzepina, K., Dunlea, E., Docherty, K., DeCarlo, P., Salcedo, D., Onasch, T., Jayne, J. T., Miyoshi, T., Shimono, A., Hatakeyama, S., Takegawa, N., Kondo, Y., Schneider, J., Drewnick, F., Borrmann, S., Weimer, S., Demerjian, K. L., Williams, P., Bower, K. N., Bahreini, R., Cottrell, L., Griffin, R., Rautiainen, J., Sun, J., Zhang, Y., and Worsnop, D. R.: Ubiquity and dominance of oxygenated species in organic aerosols in anthropogenically-influenced Northern Hemisphere midlatitudes, Geophysical Research Letters, 34, 2007.

Zhao, R., Mungall, E. L., Lee, A. K., Aljawhary, D., and Abbatt, J. P.: Aqueous-phase photooxidation of levoglucosan–a mechanistic study using Aerosol Time of Flight Chemical Ionization Mass Spectrometry (Aerosol-ToF-CIMS), Atmospheric Chemistry and Physics Discussions, 14, 8819-8850, 2014.

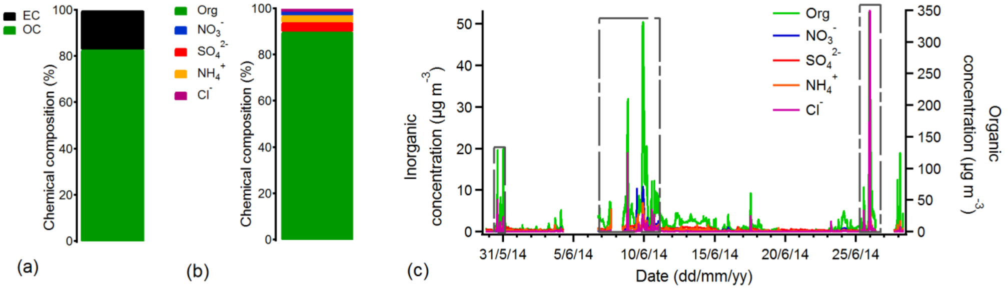

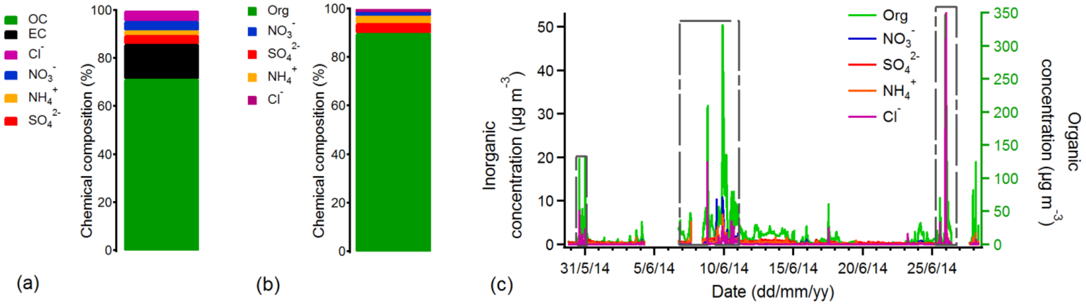

Figure 1: Contributions of (a) EC, ~~and~~ OC and inorganics ~~in carbonaceous material~~ collected on filters and the contribution of (b) AMS organic and inorganics in non-refractory submicron aerosol fraction as well as (c) their time series. Close BB periods ~~is~~ are marked in the AMS time series with grey dashed boxes. The distant BB periods cover all days of the measurement other than days included in close BB periods. Gaps in the AMS time series indicate gaps in the sampling.

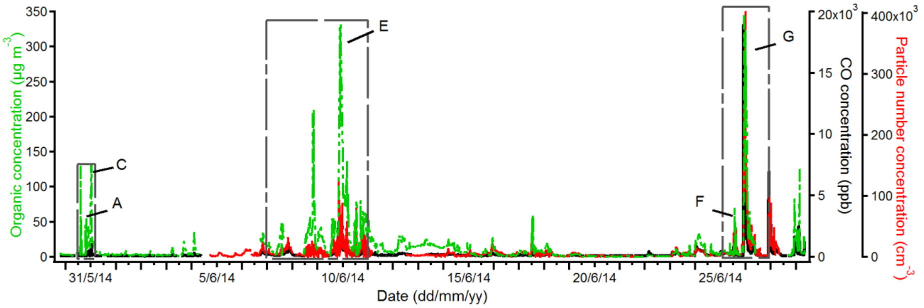

Figure 2: Time series for AMS organics, CO and particle number concentration during the SAFIRED campaign. Close BB periods ~~is~~ are marked with grey dashed boxes and selected BB events are labelled. The distant BB periods cover all days of the measurement other than days included in close BB periods. Gaps in the time series indicate gaps in the sampling (no data for the instrument).

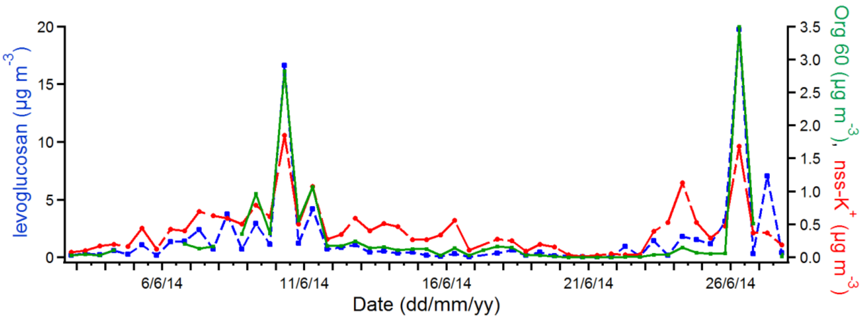

Figure 3: Time series of BB tracers: levoglucosan, soluble non-sea salt potassium (nss-K$^+$) (both 12h resolution) and AMS Org 60 (averaged to BAM 12h).

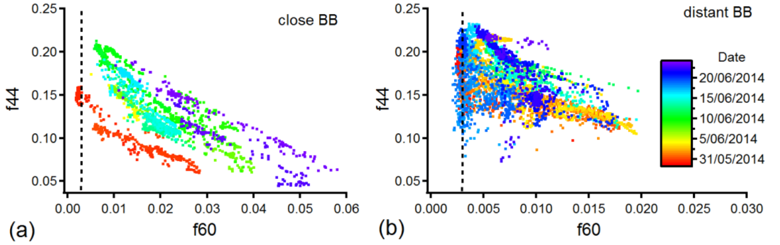

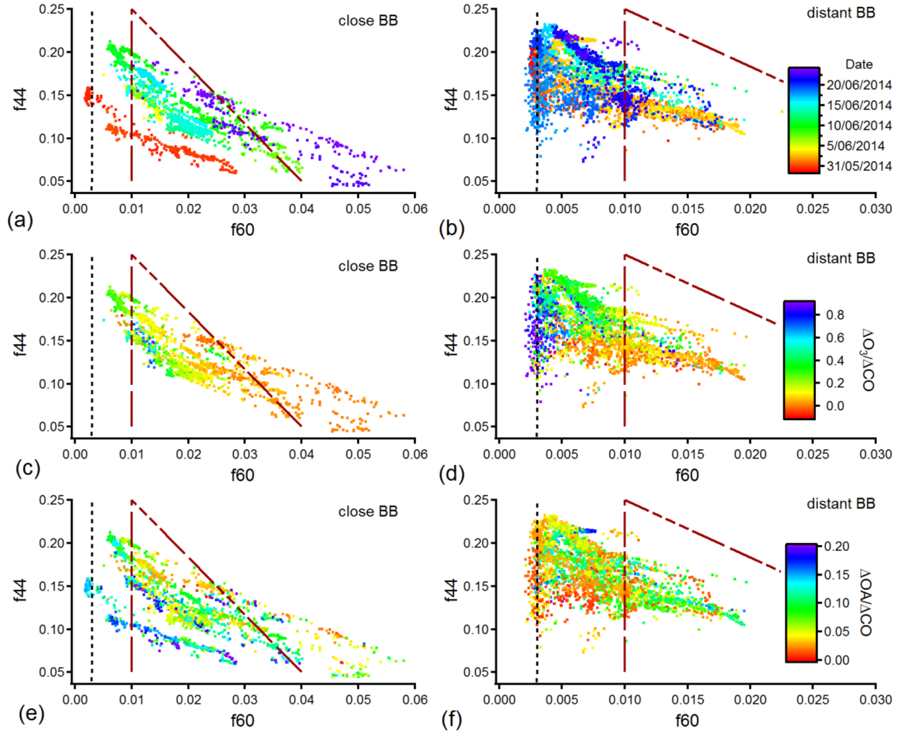

Figure 4: f44 vs. f60 coloured by date for (a) close and (b) distant BB periods, by ΔO_3/ΔCO ratio for (c) close and (d) distant BB periods, and by ΔOA/ΔCO ratio for (e) close and (f) distant BB periods (vertical black lines refer to the f60 background level of 0.003). Red dashed lines refer to the ambient BBOA-related data introduced by (Cubison et al., 2011). Note: ozone data from 29th of May until the 1st of June were not available.

Formatted: Subscript

Formatted: Superscript

Formatted: Superscript

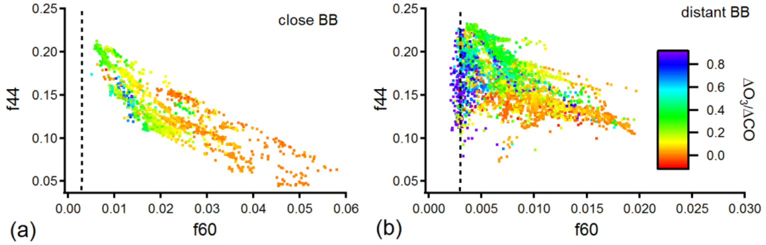

~~Figure 5: f44 vs. f60 coloured by $\Delta O_3/\Delta CO$ ratio for (a) close and (b) distant BB periods (vertical black lines refer to the f60 background level of 0.003).~~

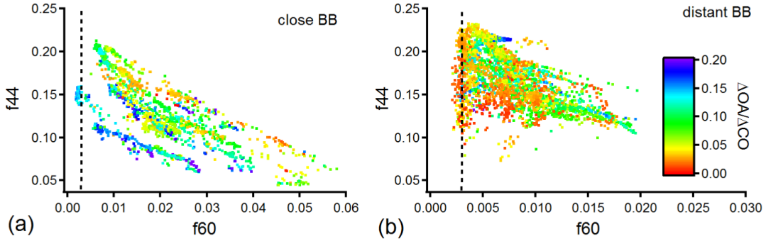

~~Figure 6: f44 vs. f60 coloured by ΔOA/ΔCO ratio for (a) close and (b) distant BB periods (vertical black lines refer to the f60 background level of 0.003).~~

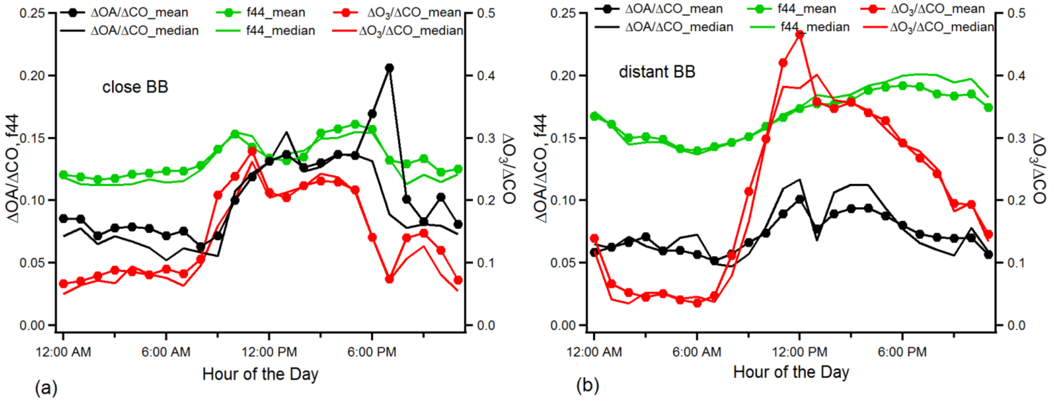

Formatted: Normal

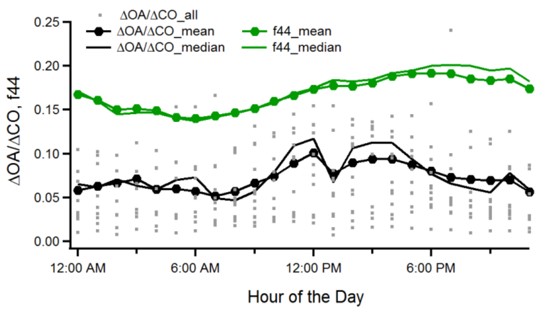

Figure 5~~7~~: Diurnal trend of f44 (mean and median), ΔO$_3$/ΔCO ratio (mean and median) and ΔOA/ΔCO ratio (mean, median)~~ and hourly data points)~~ for close (a) and distant (b) BB ~~emissions~~periods.

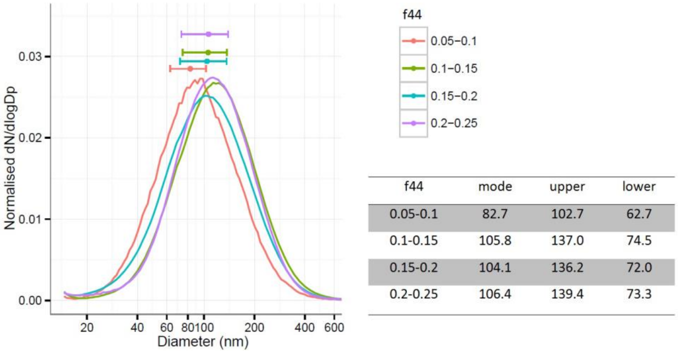

f44	mode	upper	lower
0.05-0.1	82.7	102.7	62.7
0.1-0.15	105.8	137.0	74.5
0.15-0.2	104.1	136.2	72.0
0.2-0.25	106.4	139.4	73.3

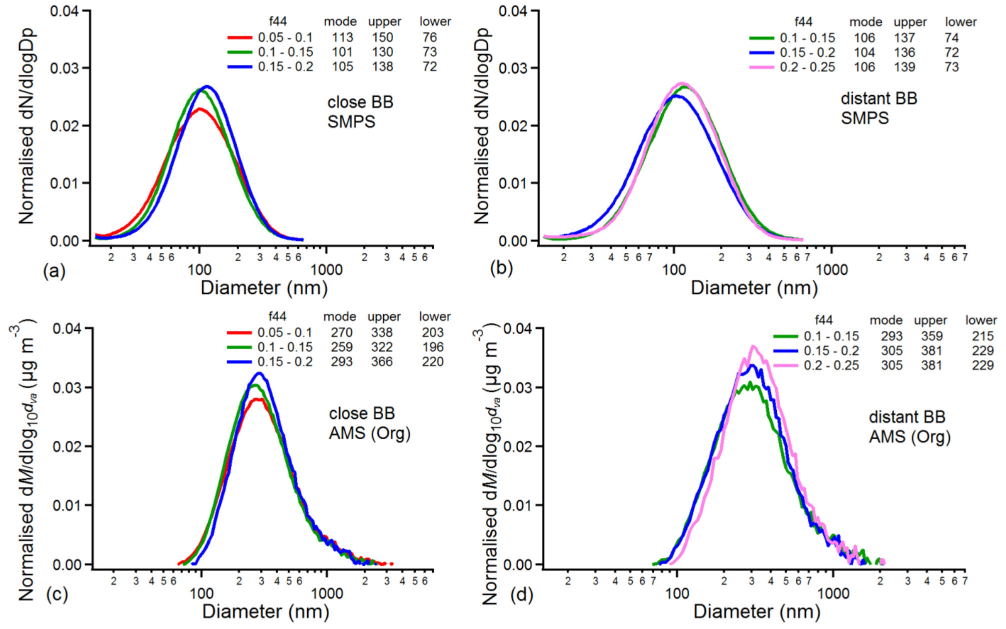

(a)

f44	mode	upper	lower
0.05 - 0.1	113	150	76
0.1 - 0.15	101	130	73
0.15 - 0.2	105	138	72

(b)

f44	mode	upper	lower
0.1 - 0.15	106	137	74
0.15 - 0.2	104	136	72
0.2 - 0.25	106	139	73

(c)

f44	mode	upper	lower
0.05 - 0.1	270	338	203
0.1 - 0.15	259	322	196
0.15 - 0.2	293	366	220

(d)

f44	mode	upper	lower
0.1 - 0.15	293	359	215
0.15 - 0.2	305	381	229
0.2 - 0.25	305	381	229

Figure 68: SMPS size distributions (dN/dlogDp, normalised to total particle number concentration, versus diameter) binned by the AMS f44 for close (a) and distant (b) BB periods and~~.~~ ~~The average mode and the standard deviation in the mode are given.~~ AMS size distributions (dM/dlog$_{10}$d$_{va}$, normalised to total organic concentration, versus diameter) binned by the AMS f44 for close (c) and distant (d) BB periods.

Table 1: Selected BB event values for f44, f60, organic concentration, CO, MCE, mode diameter and $\Delta O_3/\Delta CO$ ratio, along with measurement start and end time. ND refers to no data.

	Date (start/end)	f44±SD (range)	mean f60±SD (range)	mean Org±SD*	mean CO±SD* (range)	MCE	$\Delta O_3/\Delta CO$	Mode diameter

Formatted Table

Formatted: Justified

Formatted: Justified

				(range)				(nm)
A	30/05/14 18:34- 30/05/14 19:25	0.087±0.08 (0.079-0.105)	0.016±0.002 (0.010-0.018)	22.6±12.5 (4.6-45.2)	185.9±95.5 (90.2-370.1)	0.97± 0.06	ND	ND
C	30/05/14 23:41- 31/05/14/ 00:59	0.066±0.005 (0.060-0.079)	0.027±0.002 (0.021-0.028)	75.5±40.0 (13.7-131.2)	627.1±345.4 (185.8-1181.6)	0.98± 0.11	ND	ND
E	09/06/14 19:45- 10/06/14 00:32	0.078±0.013 (0.062-0.093)	0.032±0.002 (0.030-0.035)	175.9±105.0 (87.3-331.8)	1558.5±965.5 (671.6-3382.5)	0.91± 0.05	0.024	146
F	25/06/14 12:28- 25/06/14 16:59	0.134±0.031 (0.073-0.178)	0.009±0.002 (0.007-0.014)	13.2±14.5 (2.4-70.8)	479.0±348.8 (139.5-1642.7	0.93± 0.04	0.134	98
G	25/06/14 21:40- 26/06/14 03:59	0.062±0.017 (0.045-0.098)	0.046±0.004 (0.035-0.052)	144.6±104.7 (25.8-347.7)	2744.6±2299.8 (592.8-11275.7)	0.90± 0.06	0.011	88

*unit is $\mu g\ m^{-3}$

Formatted: Font: 10 pt

Formatted: Normal

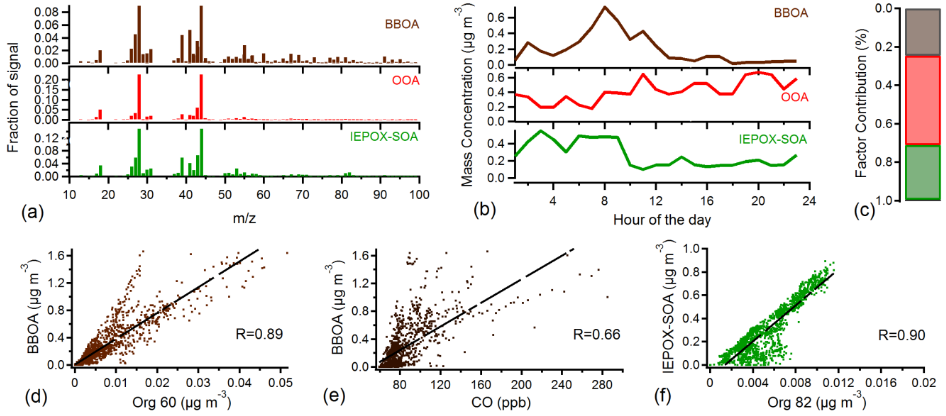

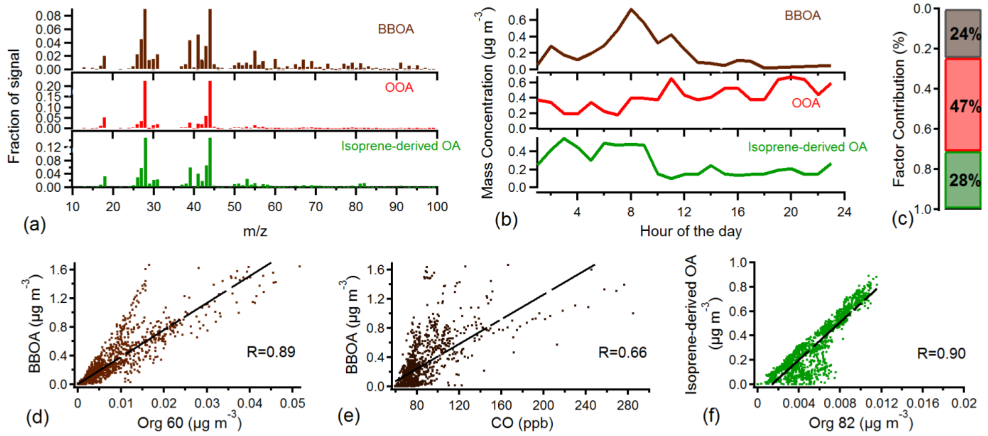

Figure 7~~9~~: (a) Mass spectra, (b) diurnal trends, (c) contribution and (d), (e), (f) correlations for the PMF 3-factor solution for background periods including BBOA, OOA and ~~IEPOX-S~~isoprene-derived OA factors.

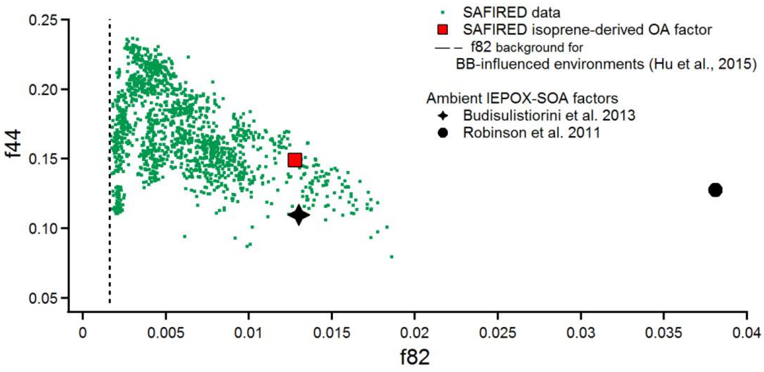

Figure 8~~10~~: f44 (CO_2^+) vs. f82 ($C_5H_6O^+$) for the SAFIRED data; The ~~IEPOX-S~~isoprene-derived OA factor from SAFIRED and two other ambient campaigns (Budisulistiorini et al., 2013;Robinson et al., 2011) are marked. Vertical black dashed line indicates proposed background f82 value in environments strongly influenced by BB (Hu et al., 2015).

Supplementary material

S1 Data analysis

High organic loadings during heavy biomass burning (BB) episodes interfered with sulfate detection by the AMS in unit mass resolution (UMR), resulting in negative sulfate readings and scattered data points (Fig. S1a). Adjustments in Squirrel to the fragmentation table addressed the negative data points (Fig. S1b), however significant data dispersion still remained. High resolution (HR) fitting using PIKA improved correlation among different sulfate fragments (Fig. S1c).

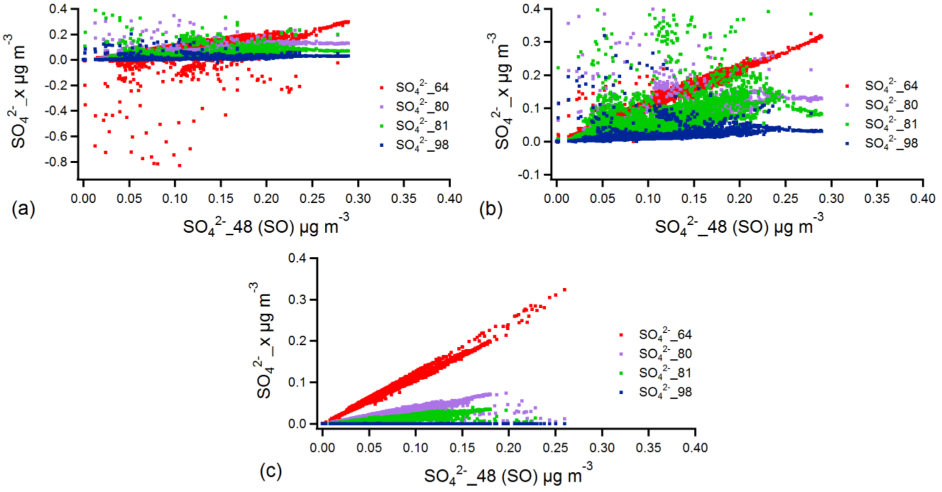

Figure S1: Sulfate fragments plots (a) before and (b) after Squirrel fragmentation table adjustments, and (c) after HR fitting in PIKA; SO$_4^{2-}$_x indicates sulfate fragments at m/z 64, 80, 81 and 96 plotted against the sulfate fragment at m/z 48.

PM1 soluble ions measured by ion suppressed chromatography and OM (converted from OC that was determined by the Thermal-Optical Carbon Analyser) were compared to the corresponding AMS UMR and HR data. A considerable improvement was observed in the HR analysis results for sulfate (Fig. S2b), with R changing from 0.4 to 0.8. HR fitting did not result in significant change for the other inorganic species or organics. However, improvement in the sulfate signals was significant and HR peak fitting data were used in further ~~data~~ analysis.

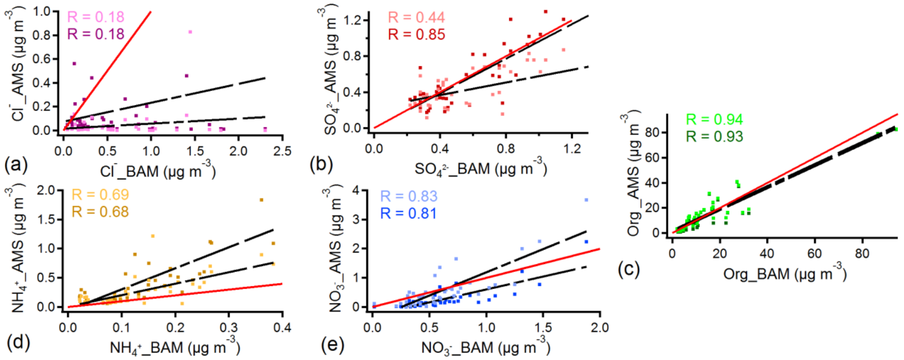

Figure S2: Correlation between BAM PM1 soluble ions and corresponding AMS species including (a) chloride, (b) sulfate, (c) organics, (d) ammonia and (e) nitrate; The lighter points and first number present correlation of BAM data with UMR AMS data, while the darker points and the second number illustrates the correlation for BAM and HR AMS data. Red line represents 1:1 line (absolute concentration between AMS and BAM). BAM organic mass (OM) was converted from OC mass using the conversion coefficient of 1.4. R refers to Pearson correlation coefficient. The AMS data were averaged to BAM 12h data.

Table S1: Correlation values between inorganic species and organics during the campaign, and close and distant periods separately. Inorganic species measured during the whole period (X), close BB periods (X(c)) and distant BB periods (X(d)) were compared to organics measured during the same time period (Org, Org(c), Org(d)).

	Cl^-	Cl^- (c)	Cl^- (d)	NH_4^+	NH_4^+ (c)	NH_4^+ (d)	NO_3^-	NO_3^- (c)	NO_3^- (d)	SO_4^{2-}	SO_4^{2-} (c)	SO_4^{2-} (d)
Org	0.65			0.92			0.75			0.55		
Org(c)		0.67			0.92			0.72			0.49	
Org(d)			0.47			0.73			0.77			0.48

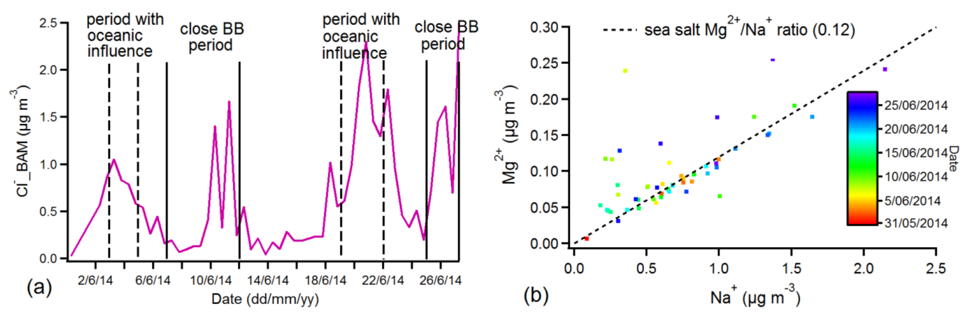

Figure S3: (a) Time series of chlorides collected on the filters (BAM). Dashed lines are defining the periods with oceanic influence, while solid lines illustrate close BB periods. (b) The filter (BAM) data for magnesium (Mg^{2+}) and sodium (Na^+). Black line illustrates Mg^{2+}/Na^+ ratio for the sea salt (0.12).

S2 Biomass burning aerosols and aging

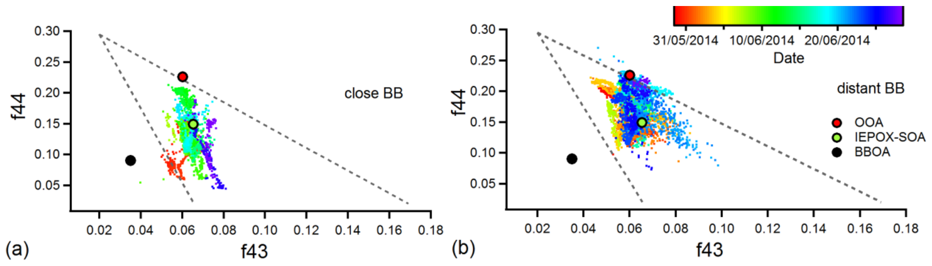

Figure S4: f44 vs. f43 coloured by date for (a) close and (b) distant BB periods. PMF-resolved factors are also indicated. The dashed lines represent boundaries for typical ambient aerosol as presented in Ng et al. (2010).

S2.1 Secondary organic aerosol (SOA) formation

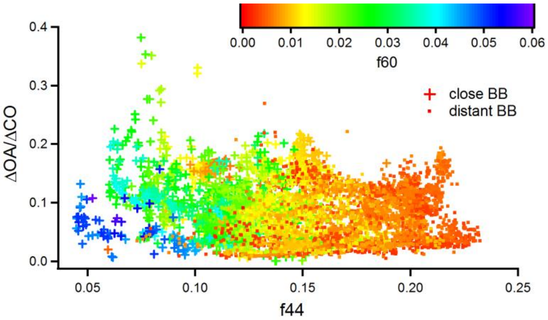

Figure S5: Change in ΔOA/ΔCO ratio with aging (represented by f44 values) for close (crosses) and distant (dots) fires coloured by f60.

S2.2 Biomass burning events

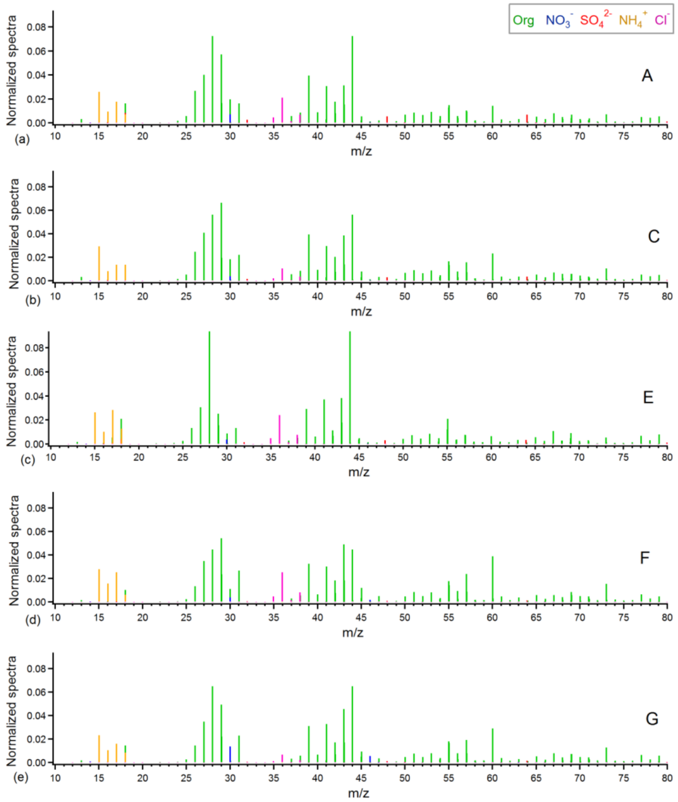

Figure S6: Normalised mass spectra (sum=1) for selected BB events (A (30/05/14, 18:34-19:25), C (30/05/14, 23:41-31/05/14 00:59), E (09/06/14, 19:45-10/06/14 00:32), F (25/06/14, 12:28-16:59) and G (25/06/14, 21:40-26/06/14 03:59) are shown respectively.

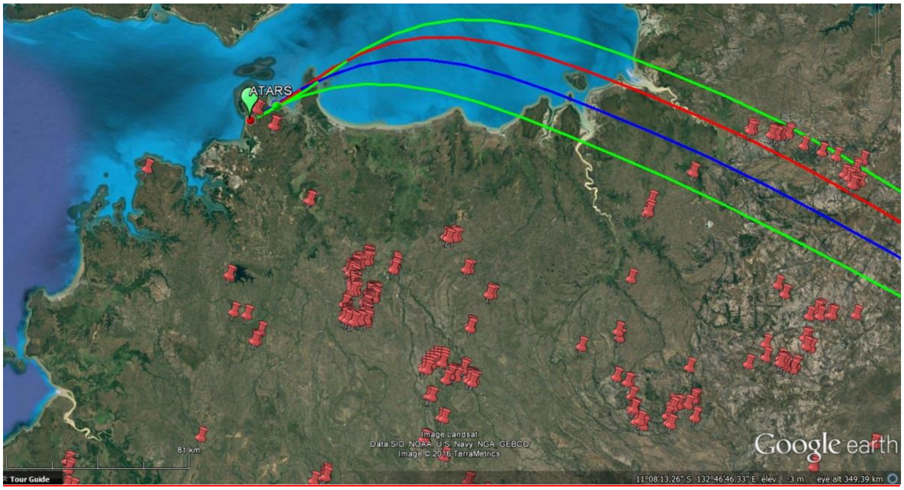
ATARS
Image Landsat
Data SIO, NOAA, U.S. Navy, NGA, GEBCO
Image © 2016 TerraMetrics
Google earth
81 km
Tour Guide
11°08'13.26" S 132°46'46.33" E elev -3 m eye alt 349.39 km

(a)


ATARS

(b)

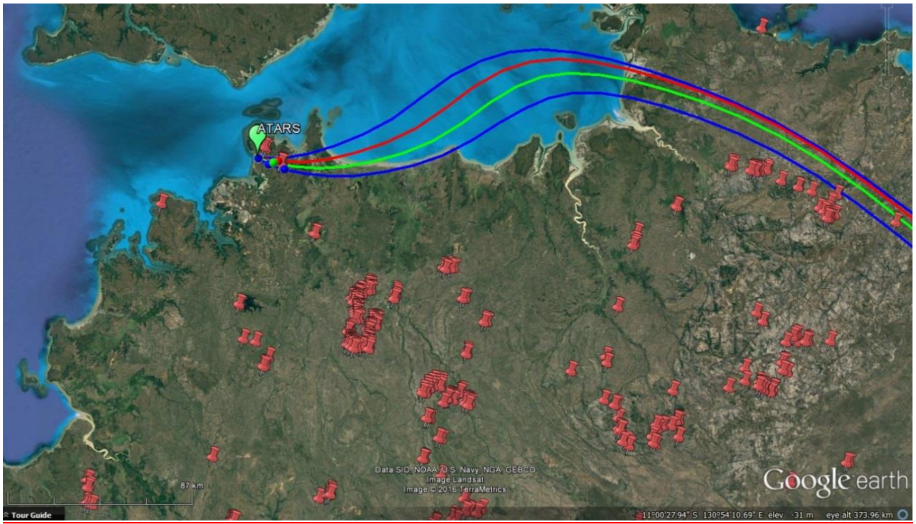
ATARS
87 km
Tour Guide
Data SIO, NOAA, U.S. Navy, NGA, GEBCO
Image Landsat
Image © 2016 TerraMetrics
Google earth
11°00'27.94" S 130°54'10.69" E elev -31 m eye alt 373.96 km

(c)

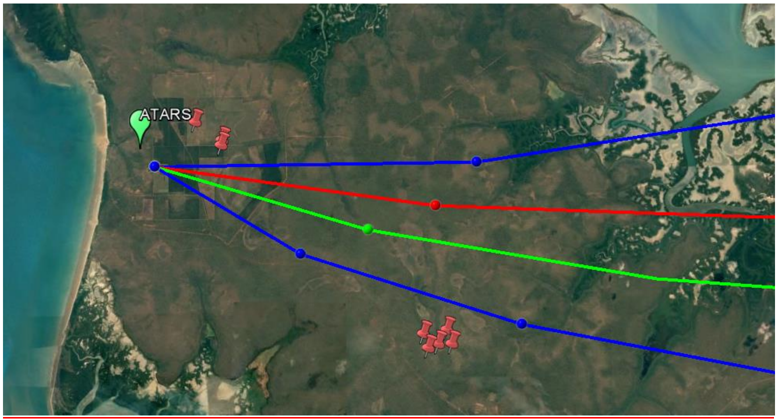
ATARS

(d)

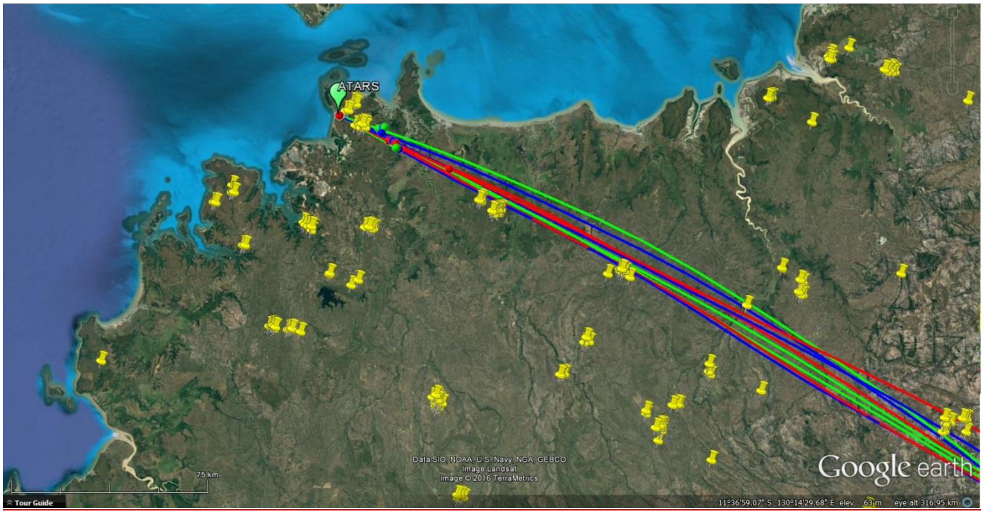
ATARS
Data SIO, NOAA, U.S. Navy, NGA, GEBCO
Image Landsat
Image © 2016 TerraMetrics
Google earth
75 km
Tour Guide
11°36'59.07" S 130°14'29.68" E elev 63 m eye alt 316.95 km

(e)

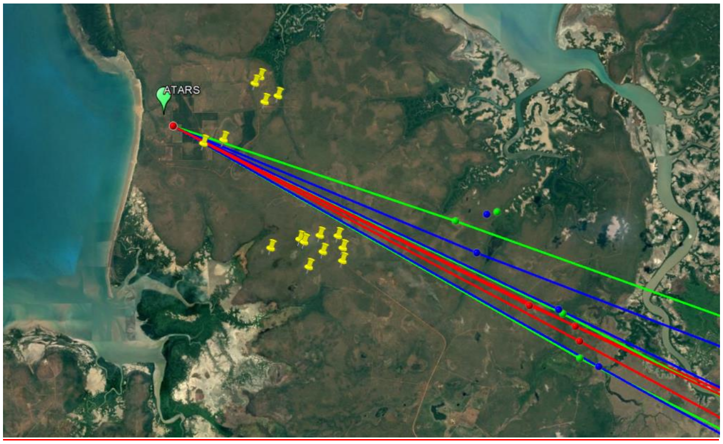
ATARS

(f)

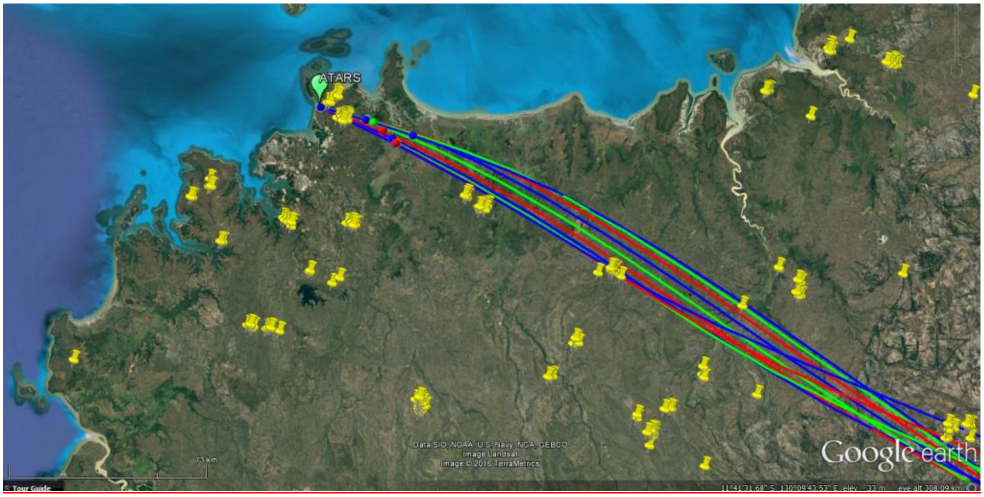
ATARS
73 km
Tour Guide
Data SIO, NOAA, U.S. Navy, NGA, GEBCO
Image Landsat
Image © 2016 TerraMetrics
Google earth
11°41'31.68" S 130°09'43.53" E elev 33 m eye alt 308.09 km

(g)

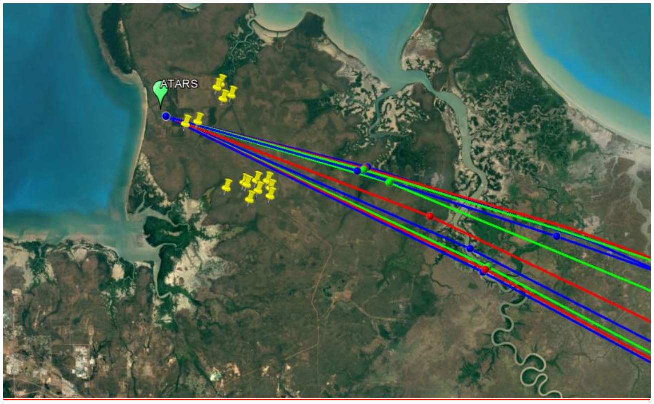
ATARS

(h)

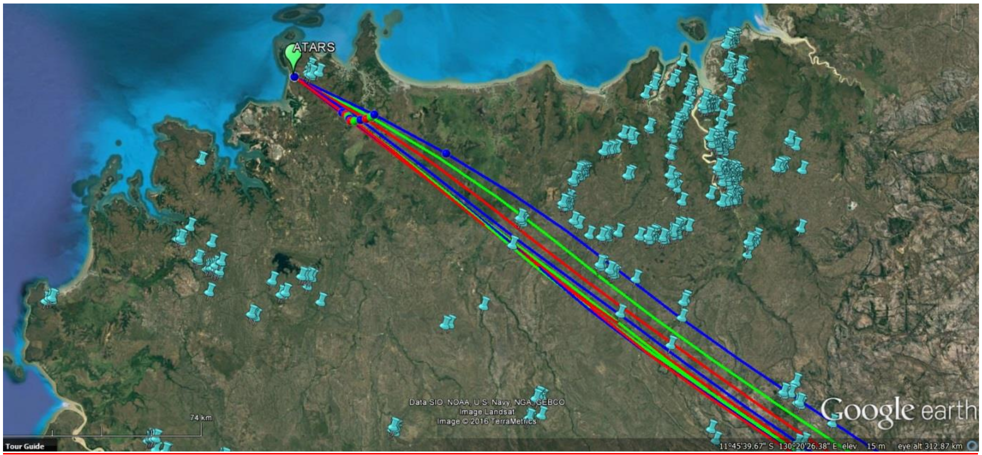

(i)

(j)

Figure S 7: Backtrajectories for event A, with close hot spots (a) and close and distant hot spots (b), for event C, with close hot spots (c) and close and distant hot spots (d), for event F, with close hot spots (e) and close and distant hot spots (f), for event G, with close hot spots (g) and close and distant hot spots (h) and for event E, with close hot spots (i) and close and distant hot spots (j). The backtrajectories were computed using the HYSPLIT (Hybrid Single-Particle Lagrangian Integrated Trajectory) model. All backtrajectories were run for 24h back in time. Different colours illustrate different starting time.

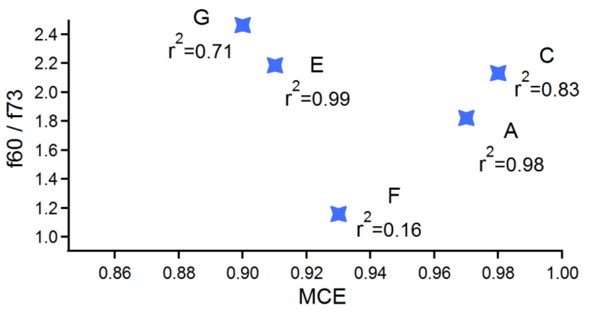

Figure S 8: f60/f73 ratio vs. modified combustion efficiency (MCE) for different events. Each point label indicates name of event and correlation value between f60 and f73.

S3 PMF performed on the whole dataset

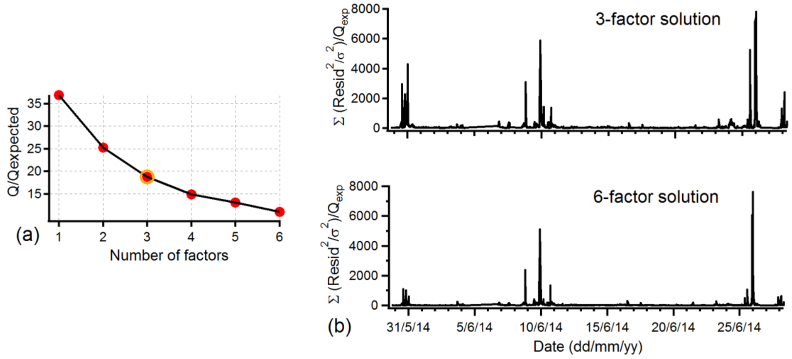

Figure S9: (a) Q/Qexpected (Q refers to the sum of squared scaled residuals over the whole dataset) vs. number of factors, illustrating high error and residual values. (b) Time series of Q/Q expected contribution for 3 and 6-factor solutions where it is clear that higher number of factors does not make the residual structure during BB events significantly lower.

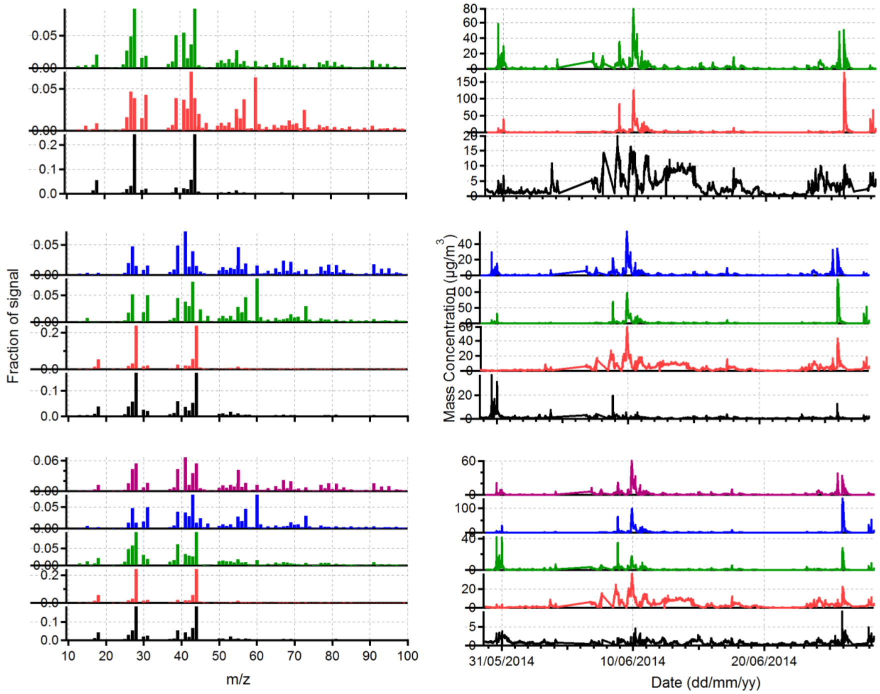

Figure S10: Factor profiles and time series for 3, 4 and 5-factor solutions showing BBOA factor splitting, suggesting that plumes are apportioned to different PMF factors.

S4 PMF performed on the background dataset

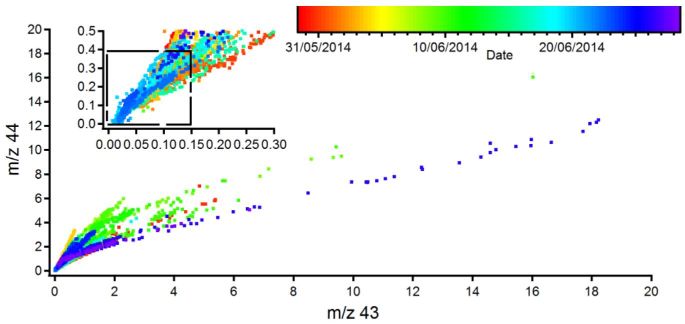

Figure S11: m/z 44 vs. m/z 43 coloured by date for the whole dataset and for background periods (inset). Black dashed box in inset graph illustrates cut-offs of 0.15 for m/z 43 and 0.4 for m/z 44 chosen for background data.

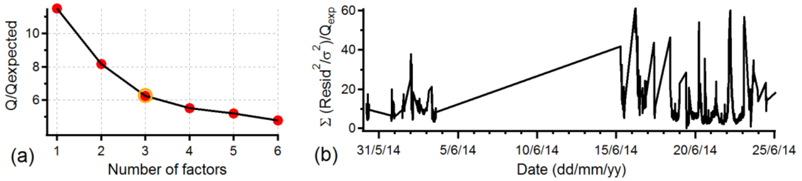

Figure S12: (a) Q/Qexpected vs. number of factors and (b) time series of Q/Q expected contribution for the 3-factor solution illustrating significantly smaller residuals in the case of the background dataset, compared to the whole dataset.

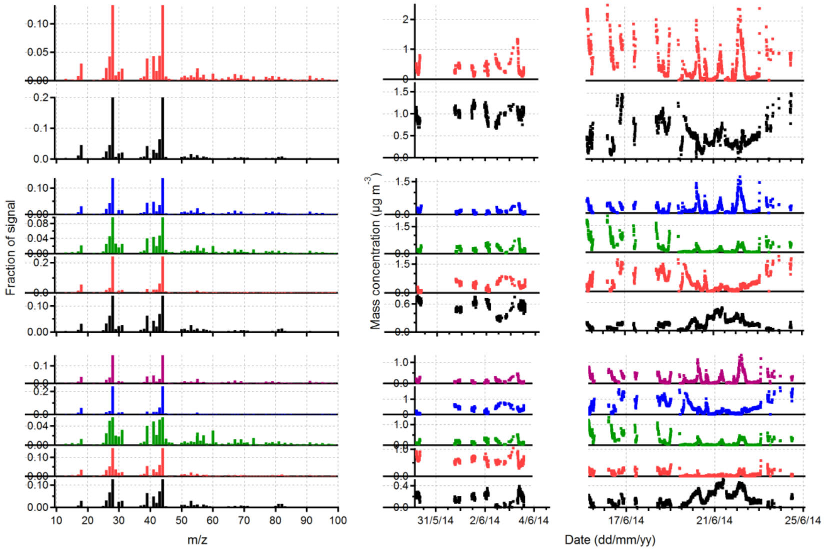

Figure S13: Factor profiles and time series for 2, 4 and 5-factor solutions for the background dataset.

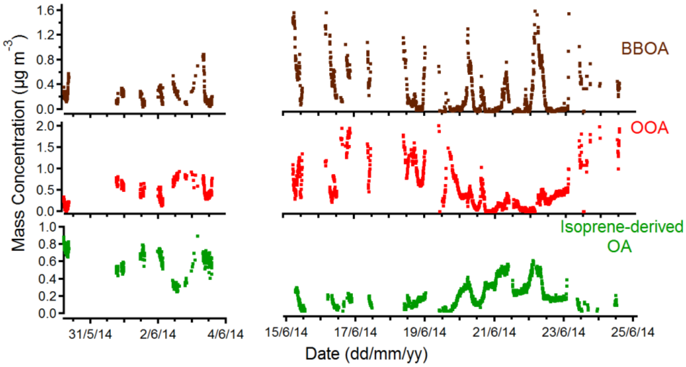

Figure S14: Time series for 3-factor solution for the background dataset.

S4.1 Isoprene-derived- organic aerosol

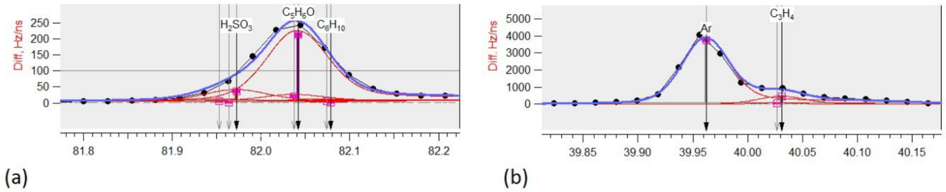

5 **Figure S15: HR peak fitting at (a) m/z 82 showing the dominance of the $C_5H_6O^+$ fragment and (b) m/z 40 demonstrating good m/z calibration.**

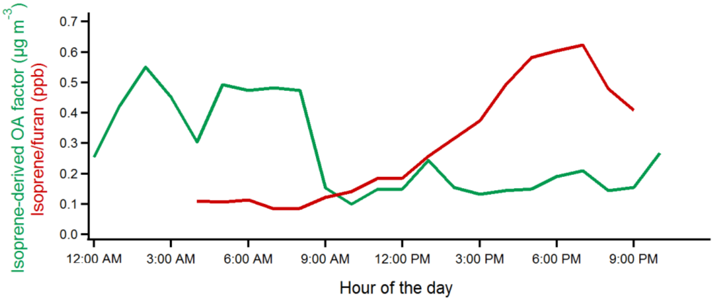

Figure S16: Diurnal trend of PMF IEPOX-SOA factor and isoprene/furan concentration measured by PTR-MS.

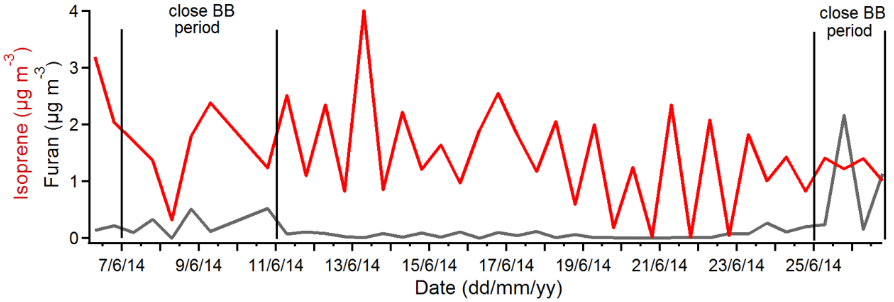

Figure S 17: Time series of isoprene and furan concentrations analysed by the gas chromatography-mass spectrometry. Black lines illustrate close BB periods.

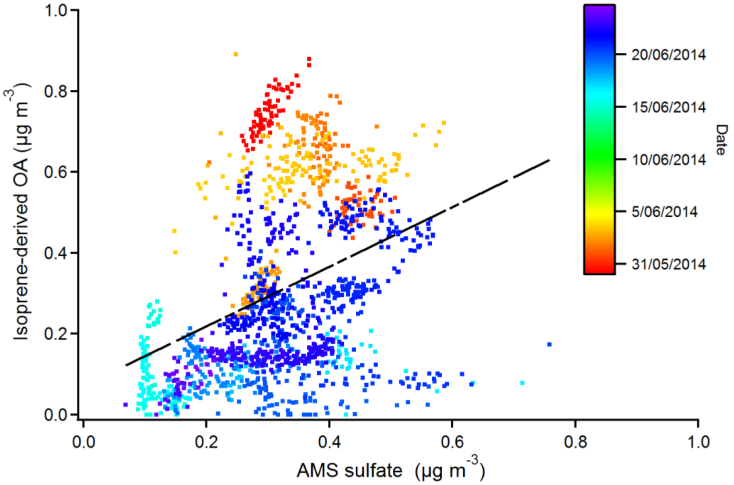

Figure S 18: Correlation between of AMS sulfate with the isoprene-derived OA PMF factor.